The custodially protected Randall-Sundrum model: theoretical aspects and flavour phenomenology

Dissertation von

Monika Blanke

Juli 2009

Lehrstuhl T31 Prof. A. J. Buras
Physik Department
Technische Universität München
James-Franck-Straße 2
85748 Garching

Max-Planck-Institut für Physik
Werner-Heisenberg-Institut
Föhringer Ring 6
80805 München

TECHNISCHE UNIVERSITÄT MÜNCHEN

Lehrstuhl T31 Prof. A. J. Buras
Physik Department
James-Franck-Straße 2
85748 Garching

Max-Planck-Institut für Physik
Werner-Heisenberg-Institut
Föhringer Ring 6
80805 München

The custodially protected Randall-Sundrum model: theoretical aspects and flavour phenomenology

Monika Blanke

Vollständiger Abdruck der von der Fakultät für Physik der Technischen Universität München zur Erlangung des akademischen Grades eines

Doktors der Naturwissenschaften (Dr. rer. nat.)

genehmigten Dissertation.

Vorsitzender:	Univ.-Prof. Dr. L. Oberauer
Prüfer der Dissertation:	1. Univ.-Prof. Dr. A. J. Buras
	2. Hon.-Prof. Dr. W. F. L. Hollik

Die Dissertation wurde am 01.07.2009 bei der Technischen Universität München eingereicht und durch die Fakultät für Physik am 24.07.2009 angenommen.

"Man kann also sagen, daß ein mathematisches Weib wider die Natur sei, in gewissem Sinne ein Zwitter. Es ist hier nicht anders als bei anderen Talenten. Gelehrte und künstlerische Frauen sind Ergebnisse der Entartung. Nur durch Abweichung von der Art, durch krankhafte Veränderungen kann das Weib andere Talente als die zur Geliebten und Mutter befähigenden, erwerben. Es ist daher zu erwarten, daß bei den talentierten Weibern auch andere Abweichungen zu finden seien."

P. J. Möbius, *Über die Anlage zur Mathematik* (1900)

Preface

P.1 Abstract

Models with a warped extra dimension, so-called Randall-Sundrum models, provide an appealing solution to the gauge and flavour hierarchy problems of the Standard Model. After introducing the theoretical basics of such models, we concentrate on a specific model whose symmetry structure is extended to protect the T parameter and the $Zb_L\bar{b}_L$ coupling from large corrections. We introduce the basic action and discuss in detail effects of electroweak symmetry breaking and the flavour structure of the model. Then we analyse meson-antimeson mixing and rare decays that are affected by new tree level contributions from the Kaluza-Klein modes of the gauge bosons and from the Z boson in an important manner. After deriving analytic expressions for the most important K and B physics observables, we perform a global numerical analysis of the new effects in the model in question. We confirm the recent findings that a stringent constraint on the model is placed by CP-violation in $K^0 - \bar{K}^0$ mixing. However, even for Kaluza-Klein particles in the reach of the LHC an agreement with all available data can be obtained without significant fine-tuning. We find possible large effects in either CP-violating effects in the $B_s - \bar{B}_s$ system or in the rare K decays, but not simultaneously. In any case the deviations from the Standard Model predictions in the rare B decays are small and difficult to measure. The specific pattern of new flavour effects allows to distinguish this model from other New Physics frameworks, which we demonstrate explicitly for the case of models with Minimal Flavour Violation and for the Littlest Higgs model with T-parity.

P.2 Zusammenfassung

Modelle mit einer gekrümmten Extradimension, sog. Randall-Sundrum Modelle, bieten eine ansprechende Lösung zum Hierarchieproblem und zum Flavour-Problem des Standardmodells. Nach einer Einführung in die theoretischen Grundlagen dieser Modelle konzentrieren wir uns auf ein spezifisches Modell mit erweiterter Symmetriestruktur, in dem der T Parameter und die $Zb_L\bar{b}_L$ Kopplung vor großen

Korrekturen geschützt sind. Wir führen die zugrundeliegende Wirkung ein und diskutieren detailliert die Effekte der elektroschwachen Symmetriebrechung und die Flavour-Struktur des Modells. Dann analysieren wir die Meson-Antimeson-Mischung sowie seltene Zerfälle, die wichtige neue Beiträge auf dem Tree-Niveau, generiert durch die Kalzua-Klein-Moden der Eichbosonen und durch das Z Boson, erhalten. Nach der Ableitung analytischer Formeln für die wichtigsten Observablen der K und B Physik führen wir eine globale numerische Analyse der neuen Effekte in diesem Modell durch. Wir bestätigen, dass CP-Verletzung in der $K^0 - \bar{K}^0$ Mischung eine besonders strikte Einschränkung des Modells liefert. Dennoch ist es selbst mit Kaluza-Klein-Teilchen, die am LHC beobachtet werden können, möglich, ohne relevantes Fine-Tuning Übereinstimming mit allen verfügbaren Daten zu bekommen. Wir finden mögliche große CP-verletzende Effekte im $B_s - \bar{B}_s$ System sowie in den seltenen K Zerfällen; diese sind aber nicht gleichzeitig möglich. Die Abweichungen von den Standardmodellvorhersagen bei seltenen B Zerfällen sind in jedem Fall klein und schwierig zu messen. Das spezifische Muster der neuen Flavour-Effekte erlaubt, dieses Modell von anderen Neue Physik Szenarien zu unterscheiden. Dies demonstrieren wir explizit am Beispiel von Modellen mit minimaler Flavourverletzung und am Littlest Higgs Modell mit T-Parität.

P.3 Danksagung

An dieser Stelle sei all jenen herzlich gedankt, die maßgeblich zum Gelingen dieser Arbeit beigetragen haben.

Zuallererst möchte ich meinem Betreuer und Doktorvater Andrzej Buras für die Möglichkeit danken, bei ihm über ein so interessantes und aktuelles Thema zu promovieren, für die exzellente Betreuung und Korrektur dieser Arbeit, sowie unzählige fruchtbare Diskussionen und entspannende Cappuccino-Pausen. Seine fachlichen und menschlichen Qualitäten tragen entscheidend dazu bei, dass in seiner Gruppe so ein angenehmes Arbeitsklima herrscht und ich mich stets sehr wohl gefühlt habe. Ich hoffe, dass der gute Kontakt nach der Beendigung meiner Promotion aufrecht erhalten bleibt und wir auch in Zukunft erfolgreich zusammenarbeiten. Nicht zuletzt danke ich für die entscheidende Unterstützung meiner PostDoc-Bewerbungen.

Des weiteren gilt mein besonderer Dank Wolfgang Hollik und dem Max-Planck-Institut für Physik in München für die Finanzierung meines Promotionsvorhabens sowie die wohlwollend bewilligte finanzielle Unterstützung meiner Dienstreisen zu Konferenzen und Workshops sowie zu meinen Gast-Aufenthalten an der Università di Roma Tre und an der Cornell University. Letzterer Aufenthalt hat sicher

entscheidend dazu beigetragen, dass ich ab Oktober diesen Jahres an der Cornell University als PostDoc tätig sein werde. Schließlich möchte ich Herrn Hollik für die Zweitkorrektur dieser Arbeit danken.

Gedankt sei auch der Technischen Universität München und dem DFG Cluster of Excellence "Origin and Structure of the Universe" für die finanzielle Unterstützng einiger Dienstreisen sowie die unentgeltliche Bereitstellung der benötigten Arbeitsmittel.

Ein ganz herzliches Dankeschön geht an Katrin Gemmler für die erfolgreiche Zusammenarbeit, die kritische Durchsicht dieser Arbeit und die freundliche Erlaubnis, zwei Abbildungen aus ihrer Diplomarbeit zu verwenden. Am meisten dankbar bin ich aber dafür, dass ich in ihr eine tolle Freundin gefunden habe, auf die ich mich hundertprozentig verlassen kann und die immer für mich da ist, mit der man aber auch einfach wunderbar Spaß haben kann.

Weiter gilt mein Dank Björn Duling für die jahrelange effektive Zusammenarbeit und für die sehr gute Büroatmosphäre, ganz zu schweigen von der freundlichen Bereitstellung des Wasserkochers, ohne den ich sicherlich schon längst verdurstet wäre.

Ebenfalls bedanken möchte ich mich bei Stefania Gori für die stets gute Zusammenarbeit und für das angenehme Arbeitsklima.

Auch bei Andreas Weiler möchte ich mich für die gute Zusammenarbeit bedanken, sowie für die guten Ratschläge bezüglich der PostDoc-Stellensuche und des Lebens in Ithaca.

Danke an Michaela Albrecht für die Zusammenarbeit bei der theoretischen Ausarbeitung des hier vorgestellten Modells.

Ganz besonders danken möchte ich Stefan Recksiegel für die hervorragende Administration des Rechnersystems am Physikdepartment, der wenn nötig sogar seine wohlverdiente Urlaubszeit dafür opfert, Probleme zu beheben und das System wieder zum Laufen zu bringen. Ebenfalls Danke für die stets freundliche und kompetente Hilfe bei computertechnischen Fragen, ohne die ich schon oft verzweifelt wäre. Vielen Dank auch für die gute Zusammenarbeit im Zusammenhang mit dem Little Higgs Projekt!

Mein Dank gilt auch Tillmann Heidsieck, der sich ebenfalls häufig um meine Computerprobleme gekümmert hat. Außerdem bedanke ich mich für viele anregende Diskussionen über Themen in und jenseits der Physik.

Ein dickes Dankeschön geht an Cecilia Tarantino für die stets effektive und erfolgreiche Zusammenarbeit, sowie für die Einladung, zwei tolle Wochen in Rom

an der Università di Roma Tre zu verbringen, sowie für die Unterstützung meiner PostDoc-Bewerbungen. Grazie mille!

Genauso danke ich Gino Isidori für die stets guten Kontakte sowie die Unterstützung meiner Bewerbungen.

Danken möchte ich des weiteren Selma Uhlig für die Zusammenarbeit im Little Higgs Projekt sowie die angenehm ruhige Atmosphäre im gemeinsamen Büro in der Anfangszeit dieser Arbeit.

Mein ganz spezieller Dank gilt Anton Poschenrieder für die Kollaboration beim Little Higgs Projekt.

Danken möchte ich auch Ikaros Bigi für die fruchtbare Zusammenheit zu CP-Verletzung im D System, im Laufe derer ich viel über diesen Bereich der Teilchenphysik sowie den besonderen bayerischen Humor erfahren durfte.

Ebenfalls Danke an Paride Paradisi für die vielen inspirierenden Diskussionen. Ich hoffe, dass eines Tages auch mal eine konkrete Zusammenarbeit daraus erwächst.

Selbstverständlich bedanke ich mich genauso bei allen Mitgliedern und Gästen am Lehrstuhl T31, die bisher unerwähnt geblieben sind, für interessante Diskussionen und ihren Beitrag zur tollen Lehrstuhl-Atmosphäre, sowie für die regelmäßig sehr leckeren Geburtstagskuchen. Dies gilt ebenso natürlich für Thorsten Feldmann, Michael Ratz und die Mitglieder seiner Gruppe, sowie Alejandro Ibarra, Martin Gorbahn und Sebastian Jäger.

Insbesondere danke ich Elke Krüger, der Sekretärin und Guten Fee am Lehrstuhl T31, durch deren tatkräftigen Einsatz unser Unialltag enorm erleichtert wird.

Genauso gilt mein Dank den MPI-Sekretärinnen Carola Reinke, Rosita Jurgeleit und Monika Goldammer, für die stets schnelle und kompetente Bearbeitung meiner Anliegen. Ebenso gilt mein Dank Frank Steffen für die engagierte Betreuung des IMPRS-Programms.

Ein besonderes Anliegen ist es mir, Matthias Neubert, Fulvia de Fazio und Yuval Grossman zu danken, die mir die Möglichkeit gegeben haben, in ihren Gruppen in Mainz, Bari und Cornell Seminarvorträge zu halten, die zu anregenden Diskussionen mit den Gruppenmitgliedern geführt haben.

Ein dickes Danke geht an Debora Mainardi, Monica Togni, Rosa Errico-Reiter und Guglielmo Fittante für die hervorragenden Italienischkurse am Sprachenzentrum der TU München, sowie an die Kursteilnehmer für die tolle Atmosphäre. Ganz besonders seien hierbei die Bemühungen von Stefan Schallinger um ein verbessertes Kursangebot gewürdigt.

Unerwähnt bleiben soll auch nicht die Leistung der Garchinger Mensa und ihres Personals, die nicht nur meine tägliche Energiezufuhr sichergestellt haben, sondern auch immer wieder für interessanten Diskussionsstoff gesorgt haben.

Mit am wichtigsten für das Gelingen dieser Arbeit war aber mein privates Umfeld, das besondere Würdigung verdient. Vielen Dank an meine Eltern für die großartige Unterstützung, ohne die ich es nie so weit gebracht hätte. Vielen Dank auch an meine Schwester Cornelia für den vielen Spaß, den wir zusammen haben, sowie die oft kritische Hinterfragung meiner Arbeit. Vielen Dank an meinen gesamten Freundeskreis für die schöne Zeit mit Euch, und dass Ihr immer für mich da seid, wenn ich Euch brauche. Und nicht zuletzt vielen Dank an meinen Freund Moritz: Schön, dass es Dich gibt!

Contents

1 Introduction

Although the Standard Model (SM) of elementary particle physics is so far in intriguing agreement with essentially all available data, it leaves several important questions of today's particle physics unanswered.

First of all, while strong and electroweak interactions are included in the SM, gravity, described by Einstein's theory of general relativity, remains external to this theory. One of the consequences of this lack of a complete theory of all fundamental forces is the emergence of the so-called *gauge-hierarchy problem*. While electroweak symmetry breaking (EWSB), described by the Higgs mechanism in the SM, takes place at the scale $v = 246\,\text{GeV}$, the fundamental Planck scale of gravity is by 16 orders of magnitude larger, $M_{\text{Pl}} \simeq 10^{19}\,\text{GeV}$. One may assume then that the SM is valid below that scale and must be extended only to include a quantum theory of gravity above M_{Pl}. However, as the Higgs potential in the SM is not protected by any symmetry principle, it receives quadratically divergent contributions at the loop level that would naturally lead to a Higgs mass of the order of the Planck scale, and EWSB would be associated to this scale. Barring the possibility of a tremendous fine-tuning required to keep the EWSB scale in the sub-TeV range, this observation leads to the immediate conclusion that at least the Higgs sector of the SM is incomplete and needs to be extended at the TeV scale. In fact this reasoning underlies our hopes to observe New Physics (NP) phenomena at future facilities such as the LHC.

The vast hierarchy between the electroweak and the Planck scale is however not the only hierarchy that remains unexplained in the SM. A very hierarchical pattern, often referred to as the *flavour hierarchy problem*, appears also in the flavour sector of the SM, where the charged fermion masses range from $\sim 0.5\,\text{MeV}$ for the electron to $\sim 170\,\text{GeV}$ for the top quark [1]. Similarly, also flavour violating effects in the quark sector exhibit a very hierarchical pattern, with the off-diagonal CKM elements describing the interactions between the various generations given by [2]

$$|V_{us}| \simeq 0.226\,, \qquad |V_{cb}| \simeq 0.041\,, \qquad |V_{ub}| \simeq 0.0038\,. \tag{1.1}$$

While also these hierarchies have to be put by hand in the SM Lagrangian, in contrast to the gauge hierarchy, the flavour hierarchies are protected by the approximate chiral symmetry of the model and therefore stable against radiative

corrections[1]. Consequently one might consider the flavour hierarchy problem as less severe than the gauge hierarchy problem; still however it contradicts the naturalness hypothesis that all parameters of a fundamental theory should be of $\mathcal{O}(1)$.

Many attempts have been undertaken to provide solutions to these two problems. While the most famous approach to address the gauge hierarchy problem is supersymmetry [3–5], other interesting NP models exist providing alternative solutions. For instance in Technicolour models [6] EWSB is achieved by the condensate of a strongly coupled sector. The large hierarchy of scales is then traced back to the logarithmic running of the new strong coupling constant. In models with large extra dimensions [7] on the other hand, gravity is allowed to propagate in one or more extra dimensions of TeV^{-1} size, while gauge and matter fields are confined to the usual 4dimensional (4D) world. A large effective 4D scale of gravity then arises naturally, being enhanced with respect to the fundamental scale of gravity by the large volume of the extra dimensions.

In order to solve the flavour hierarchy problem usually some kind of flavour symmetry is imposed. While the concept of Minimal Flavour Violation [8–12], in which the $U(3)^3$ flavour symmetry is exclusively broken by the SM Yukawa couplings, can only explain the smallness of NP effects in flavour changing neutral current (FCNC) processes, models based on the Froggatt-Nielsen [13] mechanism that interpret flavour as a spontaneously broken symmetry, can also explain the hierarchies in the SM Yukawa couplings. Other kinds of flavour symmetries have been proposed e. g. in [14–18]. In any case it must be realised that flavour cannot be an exact symmetry, as it is broken already in the SM.

While either of the two hierarchy problems in the SM can quite straightforwardly be addressed in the presence of NP, a *simultaneous* solution appears to be more involved. Efforts in this direction have been made e. g. by extensive studies of supersymmetric flavour models (see e. g. [19–22]). However bringing such models in simultaneous agreement with all available flavour physics data turns out to be a highly non-trivial task [23, 24].

Over the last decade a very appealing alternative solution to the gauge and flavour hierarchy problems has been developed. It is based on the observation by Randall and Sundrum [25] that by introducing a warped spatial extra dimension that is confined between two branes, the gauge hierarchy problem can be solved. To this end they placed the SM matter fields on the 4D brane called IR or TeV brane on which the effective energy scale is not M_{Pl}, but $\mathcal{O}(1\,\mathrm{TeV})$ thus protecting the scale of EWSB. Soon it has been realised however that this simple setup is in conflict with electroweak precision data. In addition the flavour problem can not

[1] The residual logarithmic cut-off dependence does not introduce a fine-tuning problem even for $\Lambda \sim \mathcal{O}(M_{\mathrm{Pl}})$, being suppressed by the loop factor $1/16\pi^2$.

be addressed.

Interestingly the above drawbacks can be circumvented by allowing the gauge and matter fields to propagate in the 5D bulk [26–30], while only the Higgs sector has to be confined to the IR brane. Then not only the stringent constraints from higher-dimensional operators can be avoided, but also the T parameter [31–33] and the $Zb_L\bar{b}_L$ coupling [34] can be protected by a slightly extended bulk symmetry group. Together with the latter coupling, at the same time all $Zd^i_L\bar{d}^j_L$ couplings turn out to be protected from large anomalous contributions [35–37], with important implications for flavour phenomenology [36].

In addition, the exponential localisation of fermion zero modes along the 5D bulk, depending on their bulk mass, provides a neat explanation of the hierarchies in the flavour sector [29, 30, 38, 39]. As the overlap of the fermion shape functions with the Higgs on the IR brane depends exponentially on the bulk mass parameters, choosing them to be $\mathcal{O}(1)$ numbers but slightly different from each other, the observed hierarchical Yukawa couplings can be generated without introducing unnaturally small parameters. In this manner the flavour hierarchy problem can be traced back to a geometric origin of flavour; however in order to obtain a theory predicting the observed masses and flavour mixings, a model explaining the 5D bulk masses is still missing. Consequently in the present versions of RS models with bulk fermions flavour hierarchies appear natural, but the actual values of parameters can not be explained – rather the number of parameters in the flavour sector is significantly increased.

In this thesis we present one of the simplest realisations of RS models with custodial protection of the T parameter and the $Zd^i_L\bar{d}^j_L$ couplings, whose details have been worked out in [40]. Subsequently, we perform an extensive phenomenological analysis of meson-antimeson mixing in the neutral K and $B_{d,s}$ meson sectors and of rare K and B decays in the model in question. These studies have also been published in [35, 36].

The remainder of this work is organised as follows. In **chapter 2** we introduce the basic Randall-Sundrum framework and show that the underlying metric is a solution to the 5D Einstein equations. We demonstrate explicitly how the gauge hierarchy problem can be solved in this framework. Due to the tension of the original RS1 framework with electroweak precision data, we then work out the formalism to describe bulk fields in a warped background, based on the Kaluza-Klein (KK) expansion of the 5D fields. We briefly review the constraints on the RS model with the SM gauge group in the bulk and show how they can be avoided by enlarging the bulk symmetry by an additional factor $SU(2)_R$ and a discrete $SU(2)_L \leftrightarrow SU(2)_R$ symmetry. Based on these observations, in **chapter 3** we introduce a fully realistic RS model in the reach of the LHC. After presenting

the full 5D action of this custodially protected RS model, we analyse its gauge symmetry breaking pattern, putting particular emphasis of the effects of EWSB. Subsequently we turn to the flavour sector of the model, showing how the observed hierarchies in fermion masses and CKM mixings can naturally be explained in this model by different localisations of the fermion zero modes along the 5D bulk. Simultaneously to the quark masses, all flavour violating effects are suppressed by the same exponential hierarchies, giving rise to the so-called RS-GIM mechanism [39]. **Chapter 4** is devoted to the study of the implications of this model on flavour physics observables in the K and B meson systems. To this end we work out all flavour violating couplings of neutral gauge bosons that appear already at the tree level in the model in question. We also discuss tree level flavour violating Higgs couplings that turn out to be strongly chirally suppressed and therefore negligible. Then we study the impact of the new tree level FCNCs on observables related to $K^0-\bar{K}^0$ and $B_{d,s}-\bar{B}_{d,s}$ mixings and to rare K and B decays. After calculating the relevant effective Hamiltonians describing $\Delta F = 2$ and $\Delta F = 1$ processes we provide analytic formulae for the most interesting observables related to these sectors. An extensive numerical analysis of all these observables is presented in **chapter 5**. After analysing the pattern of NP contributions to $\Delta F = 2$ processes, we focus on the CP-violating observable ε_K which yields the most stringent constraint on the RS parameter space. We show that even for low KK masses $M \simeq (2-3)\,\text{TeV}$ an agreement with the data can be obtained without significant fine-tuning in the 5D Yukawa couplings. The other $\Delta F = 2$ constraints are naturally fulfilled in the model in question, so that a simultaneous agreement with all available data is possible. At the same time large new CP-violating effects can be present in $B_s - \bar{B}_s$ mixing. We then extend our analysis to include the most interesting rare K and B decay branching ratios. Also here we start by analysing the pattern of NP effects, thus obtaining a feeling for the expected relative size of effects. Subsequently we determine the possible deviations from the SM in the various branching ratios and analyse possible correlations between the observables in question. We show how the specific pattern of new flavour violating effects encountered in the custodially protected RS model can help to distinguish this model from other NP scenarios, such as models with Minimal Flavour Violation or the Littlest Higgs model with T-parity [41–48]. In **chapter 6** we summarise our results and give a brief outlook. Some technical details are relegated to an **appendix**.

2 Warped extra dimensions

2.1 The original RS1 model

2.1.1 The RS metric

During the last decade, models with a warped extra dimension have attracted a lot of attention, both theoretically and phenomenologically. While it is possible to deduce the Randall-Sundrum (RS) [25] geometry from a stringy origin, see e. g. [49–51], we do not follow this route here, but merely sketch how the RS metric can be obtained from the 5dimensional (5D) Einstein equations, following the original derivation in [25].

We start by considering a 5D space-time, where the usual infinite 4D space-time is extended by a finite interval $0 \leq y \leq L$. The endpoints of this interval are so-called 3-branes, that we call *ultraviolet (UV) brane* for $y = 0$ and *infrared (IR) brane* for $y = L$, for reasons that will become clear later on.[1] The 5D space-time between the two branes ($0 < y < L$) is also referred to as the 5D *bulk*. The classical action for this set-up is given by

$$S = S_{\text{bulk}} + S_{\text{UV}} + S_{\text{IR}}\,, \tag{2.1}$$

where the three addends generally read

$$S_{\text{bulk}} = \int d^4x \int_0^L dy \, \left(\mathcal{L}_{\text{bulk}} + \sqrt{G}(2M^3R - \Lambda)\right)\,, \tag{2.2}$$

$$S_{\text{UV}} = \int d^4x \, \left(\mathcal{L}_{\text{UV}} - \sqrt{G}V_{\text{UV}}\right)\delta(y)\,, \tag{2.3}$$

$$S_{\text{IR}} = \int d^4x \, \left(\mathcal{L}_{\text{IR}} - \sqrt{G}V_{\text{IR}}\right)\delta(y-L)\,. \tag{2.4}$$

For the moment we set $\mathcal{L}_{\text{bulk}}, \mathcal{L}_{\text{UV}}, \mathcal{L}_{\text{IR}} = 0$, i. e. we neglect the back-reaction of the actual theory on the geometrical background. Λ is the 5D cosmological constant and M the fundamental 5D scale of gravity. R is the curvature or Ricci

[1] Sometimes they are also referred to as Planck and TeV brane, respectively.

scalar, being a complicated function of the metric g_{MN} ($M, N = 0, 1, 2, 3, 5$), and $G = \det(g_{MN})$ is introduced in order to obtain an invariant integration measure. For details of calculating in a warped space-time geometry, see Appendix A.1. Further, $V_{\rm UV}$ and $V_{\rm IR}$ are the 4D cosmological constants, also referred to as the *brane tensions* on the UV and IR branes, respectively.

Solving the 5D Einstein's equations for the above action, we find [25]

$$ds^2 = g_{MN}dx^M dx^N = e^{-2ky}\eta_{\mu\nu}dx^\mu dx^\nu - dy^2\,, \tag{2.5}$$

where $\eta_{\mu\nu} = \mathrm{diag}(1, -1, -1, -1)$ is the 4D Lorentz metric, and

$$k = \sqrt{\frac{-\Lambda}{24M^3}} \tag{2.6}$$

is the curvature scale of the extra dimension. This solution holds only if the additional condition

$$V_{\rm UV} = -V_{\rm IR} = 24M^3k \tag{2.7}$$

is satisfied.

Clearly the above solution is meaningful only in the case $\Lambda \leq 0$. While in the case $\Lambda = 0$ a flat extra dimension is recovered, in the case $\Lambda < 0$ the 5D bulk $0 < y < L$ is a slice of 5D Anti-de-Sitter space (AdS_5). Note that for fixed y the metric (2.5) respects 4D Poincaré invariance.

As a side-remark let us mention that it is also possible to consider the RS warp mechanism as an alternative to compactification [52]. In that scenario, the IR brane is absent ($L \to \infty$), so that the extra dimension is restricted to the half-line $0 \leq y < \infty$ rather than to a compact interval $0 \leq y \leq L$. Contrary to the naïve expectation, this non-compact 5D space-time turns out to be in accordance with present experimental tests of Newton's and Einstein's gravity. In the remainder of this thesis we will however not pursue this interesting route any further, but restrict ourselves to the RS1 geometry, with the space-time metric in (2.5) restricted to the interval $0 \leq y \leq L$.

2.1.2 Effective energy scales and the hierarchy problem

At low energy scales μ corresponding to length scales much larger than the size of the extra dimension, $1/\mu \gg L$, we can obtain an effective 4D theory by integrating over the extra dimension. To this end we insert the solution (2.5) into the fundamental 5D action (2.1), obtaining for the curvature term

$$S_{\rm 4D} \supset \int d^4x \int_0^L dy\, 2M^3 e^{-2ky}\sqrt{-\bar{G}}\bar{R}\,, \tag{2.8}$$

where $\bar{G} = \det \bar{g}_{\mu\nu}$, and $\bar{R}$ denotes the 4D Ricci scalar constructed out of $\bar{g}_{\mu\nu}$. Here

$$\bar{g}_{\mu\nu}(x) = \eta_{\mu\nu} + h_{\mu\nu}(x) \tag{2.9}$$

is the four-dimensional metric describing local gravitational fluctuations $h_{\mu\nu}(x)$ around the vacuum $\eta_{\mu\nu}$. In other words $h_{\mu\nu}(x)$ is the physical 4D graviton field. As this low energy effective field is independent of y, we can perform the integration over y explicitly and obtain for the effective 4D Planck scale of gravity

$$M_{\rm Pl}^2 = \frac{M^3}{k}\left(1 - e^{-2kL}\right) \simeq \frac{M^3}{k}\,. \tag{2.10}$$

We see immediately that $M_{\rm Pl}$ depends only very weakly on the actual size of the extra dimension L, so that in the limit $kL \gg 1$ the effective scale of gravity is solely determined by M and k.

Let us now determine what happens to energy scales in the matter Langrangian $\mathcal{L}_{\rm IR}$ on the IR brane. To this end we consider the case of a fundamental scalar H (that will be identified with the Higgs boson) living on the IR brane and developping a vacuum expectation value (VEV) $\langle H \rangle = v_0$. Its effective 4D action is given by

$$S_{4D} \supset \int d^4x\, \sqrt{-G_{\rm IR}}\left(g_{\rm IR}^{\mu\nu}\partial_\mu H^\dagger \partial_\nu H - \lambda(H^\dagger H - v_0^2)^2\right)\,, \tag{2.11}$$

with $g_{\rm IR}^{\mu\nu} = g^{\mu\nu}(y = L) = e^{2kL}\eta^{\mu\nu}$, and $G_{\rm IR} = \det(g_{\rm IR})_{\mu\nu} = -e^{-8kL}$. In order to canonically normalise H, we absorb a factor e^{-kL} into its definition, $H \to e^{kL}H$, and thus obtain

$$S_{4D} \supset \int d^4x\, \left(\eta^{\mu\nu}\partial_\mu H^\dagger \partial_\nu H - \lambda(H^\dagger H - e^{-2kL}v_0^2)^2\right)\,. \tag{2.12}$$

We observe that interestingly the effective symmetry breaking scale is *not* given by v_0, but instead by

$$v \equiv e^{-kL}v_0\,. \tag{2.13}$$

These findings have profound implications: While the effective gravity scale $M_{\rm Pl}$ is determined by M and k irrespective of the length of the interval L, the symmetry breaking scale v is exponentially suppressed by a factor e^{-kL} with respect to the fundamental scale v_0. If we now assume $M, k, v_0 \sim \mathcal{O}(M_{\rm Pl})$, i. e. avoiding large hierarchies in the fundamental parameters, we deduce that a fairly moderate hierarchy $kL \sim 35$ is enough to obtain

$$v \sim 10^{-16}v_0 \sim \mathcal{O}(1\,\text{TeV})\,, \tag{2.14}$$

the scale of electroweak symmetry breaking.

The RS geometric background thus offers an intriguing solution to the gauge hierarchy problem – the vast hierarchy of 16 orders of magnitude between the Planck scale $M_{\rm Pl}$ and the electroweak symmetry breaking scale v is traced back to a small hierarchy of ~ 35 between the curvature k of the extra dimension and its length L. We stress that the metric in (2.5) has not been merely "invented" for this purpose, but as we have seen is a solution to 5D Einstein's equations with negative bulk cosmological constant $\Lambda < 0$ and properly adjusted brane tensions $V_{\rm UV}$ and $V_{\rm IR}$.

Clearly in order to complete this theoretical framework, the following issues need to be addressed successfully:

1. Can one ensure the required relation between Λ, $V_{\rm UV}$ and $V_{\rm IR}$?
2. Can the length of the interval L be stabilised in spite of gravitational fluctuations, i. e. is the hierarchy $kL \sim 35$ stable?

Obviously in order to address these questions it is not sufficient to treat the RS space-time as a static geometrical background, but its dynamical origin has to be investigated. Therefore in what follows we will not pursue these issues any further; instead we will assume the presence of a static RS background with $0 \leq y \leq L \sim 35/k$ and the metric given in (2.5). In particular we will neglect possible back-reactions of the dynamical field content in the model on the 5D space-time via gravitational effects. As gravity is fully negligible compared to the other fundamental forces at low energy scales, this assumption is generally well justified.

2.1.3 The SM on the IR brane: phenomenological constraints

We have seen that by placing the Higgs sector of the SM on the IR brane of an RS background, the gauge hierarchy problem can be reduced to a quite moderate hierarchy between the curvature k and the length L of the extra dimension. The most straightforward extension of the SM making use of this concept is certainly to confine *all* SM fields to the IR brane and let only gravity propagate in the 5D warped bulk. Then the effective cut-off scale of the SM is not given by $\Lambda_0 \sim M_{\rm Pl}$, but by the effective "warped-down" cut-off

$$\Lambda_{\rm eff}(y = L) = e^{-kL}\Lambda_0 \,. \tag{2.15}$$

so that the scale of EWSB appears to be natural provided $\Lambda_{\rm eff}(y = L) \sim 1\,\text{TeV}$.

On the other hand, not only the quadratically divergent contributions to the Higgs potential depend on the cut-off scale of the theory, but also the size of non-renormalisable operators, that are suppressed by powers of the cut-off scale $\Lambda_{\rm eff}$ according to their dimension. Experimentally such higher-dimensional operators

are strongly constrained by EW precision data and FCNC processes. Generically EW precision constraints imply a lower bound

$$\Lambda_{\text{eff}} \gtrsim (5 - 10)\,\text{TeV} \tag{2.16}$$

on the NP scale, giving rise to the so-called *little hierarchy problem* that is common to most extensions of the SM.

While such a hierarchy of one order of magnitude, albeit not perfectly natural, is still acceptable, the flavour physics constraints in particular from the neutral K meson sector are much more severe. Flavour and CP-violating effects in the $K^0 - \bar{K}^0$ mixing are found to be in astonishing accordance with the SM predictions[2], so that generic new flavour violating operators have to be suppressed by [56]

$$\Lambda_{\text{eff}} \gtrsim (10^4 - 10^5)\,\text{TeV}\,, \tag{2.17}$$

where the strongest constraint arises from CP-violating left-right operators contributing to the ε_K observable. Barring the possibility of strong accidental cancellations between various contributions, some non-trivial flavour structure is required to cope with such stringent experimental FCNC constraints.

There is however a way to avoid this tension between the naturalness constraint from EWSB and the lower bounds from precision and flavour data. Note that the latter put constraints only on the fermion and gauge boson fields in the SM, while the Higgs due to its non-observation is fairly unconstrained. On the other hand, a low cut-off scale is required only for the Higgs sector in order to maintain naturalness. Thus if it is possible to construct a model in such a way that the effective cut-off scales for the Higgs sector and the matter sector of the SM differ from each other, the problem of dangerously large contributions from higher-dimensional operators can be bypassed.

Indeed, models with a warped extra dimension offer a neat tool to explain the presence of different cut-off scales in the theory. To this end we recall that effective energy scales depend exponentially on the localisation along the extra dimension,

$$\Lambda_{\text{eff}}(y) = e^{-ky}\Lambda_0\,. \tag{2.18}$$

By placing the SM matter fields in the 5D bulk ($y < L$), the effective cut-off scale suppressing their higher-dimensional interactions can be significantly larger than the one regularising the Higgs sector. Therefore in what follows we will consider RS models in which only the Higgs boson is confined to the IR brane, while the fermion and gauge fields are 5D fields that propagate along the extra dimension.

[2] Recent hints for a possible non-negligible NP contribution to the CP-violating parameter ε_K [53–55] do not qualitatively change this picture.

2.2 Bulk fields in RS and KK decomposition

The first steps to consider bulk fields in the RS background have been undertaken in [26–30]. While in [26, 27] only gauge fields were allowed to propagate in the bulk with the fermion fields still confined to the IR brane, the model considered in [28] went one step further and included also 5D fermion fields. There it was shown that in the absence of a 5D bulk mass term, the zero modes are localised exponentially towards the IR brane. Subsequently the impact of non-zero bulk masses on the fermion zero mode localisation has been investigated in [29]. The authors observed that depending on the value of the bulk mass, the fermion zero modes can be localised at very different places along the 5D bulk, either close to the IR or to the UV brane, and exponentially suppressed on the other. These findings have an important impact on the description of flavour in RS models, as we will see later on, and provide a natural origin of the split fermion scenario [57]. Finally a very detailed study of the different types of RS bulk fields has been presented in [30].

2.2.1 Equation of motion

While the full 5D action of the model under consideration will be presented in chapter 3, for the derivation of the 5D bulk equations of motion (EOMs) it is sufficient to consider the free field action S_{free} of a gauge and a fermion field, that is given by

$$S_{\text{free}} = \int d^4x \int_0^L dy\, \sqrt{G}\Big[-\frac{1}{4}F_{MN}F^{MN} + \frac{1}{2}\bar{\psi}\left(i\Gamma^M(\partial_M + \omega_M) - ck\right)\psi\Big] + h.c.\,, \tag{2.19}$$

where $F_{MN} = \partial_M A_N - \partial_N A_M$ and $m = ck$ is the fermion bulk mass. Γ^M and ω_M are the Dirac matrices and spin connection in curved space-time, respectively, as described in appendix A.1.2. As usual the interaction terms present in a realistic weakly coupled model will be treated perturbatively.

Following [30] the bulk EOMs can now straightforwardly be obtained from the variation principle $\delta S_{\text{free}} = 0$, which yields generally

$$\left[-e^{2ky}\eta^{\mu\nu}\partial_\mu\partial_\nu + e^{sky}\partial_5(e^{-sky}\partial_5) - M_\Phi^2\right]\Phi(x^\mu, y) = 0\,. \tag{2.20}$$

In the case of gauge fields, $\Phi \equiv A_\mu$, $s = 2$ and $M_\Phi^2 = 0$, and we chose to work in the gauge $\partial_\mu A^\mu = 0$, $A_5 = 0$. In the case of fermions, $\psi_{L,R}$ has to be rescaled by $\Phi \equiv e^{-2ky}\psi_{L,R}$, $s = 1$, and $M_\Phi^2 = c(c \pm 1)k^2$ for left-/right-handed modes.

Eq. (2.20) can be solved by making the ansatz[3]

$$\Phi(x^\mu, y) = \frac{1}{\sqrt{L}} \sum_{n=0}^{\infty} \phi^{(n)}(x^\mu) f^{(n)}(y)\,, \tag{2.21}$$

which is called the *Kaluza-Klein (KK) decomposition* of $\Phi(x^\mu, y)$. From the 4D point of view this infinite sum corresponds to a *tower* of 4D KK states $\phi^{(n)}(x^\mu)$, each being multiplied by the corresponding function $f^{(n)}(y)$ that can be interpreted as its *bulk profile* or *shape function* along the 5th dimension. Denoting the mass of the n-th KK mode by m_n, we have

$$\eta^{\mu\nu}\partial_\mu\partial_\nu\phi^{(n)}(x^\mu) = -m_n^2\phi^{(n)}(x^\mu)\,. \tag{2.22}$$

Consequently the shape function $f^{(n)}(y)$ has to obey

$$\left[\partial_y^2 - sk\partial_y - \left(M_\Phi^2 - e^{2ky}m_n^2\right)\right] f^{(n)}(y) = 0\,. \tag{2.23}$$

Like every second order differential equation, a solution to (2.23) is unambiguously determined only after specifying two additional conditions, that we choose to be the boundary conditions (BCs) at the endpoints $y = 0$ and $y = L$ of the interval. While more general BCs are possible [58–60], in the present thesis we concentrate on the two most simple and straightforward cases:

- *Dirichlet* $(-)$ *BC*: The first obvious possibility is to demand that $\Phi(x^\mu, y)$, or equivalently $f^{(n)}(y)$ for all n, vanishes on the respective brane.
- *Neumann* $(+)$ *BC*: Alternatively we can also require the derivative $\partial_5\Phi(x^\mu, y)$ to vanish on the brane.

Indeed it turns out that by appropriately choosing $+$ and $-$ BCs for the field content of the model, realistic scenarios in agreement with the currently available data can be constructed. One of the most famous examples, the RS model with implemented custodial protection of the T parameter and the flavour diagonal and non-diagonal $Zd_L^i\bar{d}_L^j$ couplings is presented in chapter 3, and its flavour phenomenology is studied subsequently (see also [35, 36, 40]).

As (2.23), together with the specified BCs, is a so-called *linear boundary value problem*, its solutions $f^{(n)}(y)$ form a complete set of orthogonal functions. This orthogonality is an important feature of the KK decomposition (2.21) and will turn out to be relevant for phenomenology.

We will now discuss the solution of (2.23) separately for the cases of gauge and fermion fields living in the RS bulk.

[3] Due to the rescaling $\Phi \equiv e^{-2ky}\psi_{L,R}$ the fermionic KK decomposition contains an additional factor e^{2ky}, see (2.35).

2.2.2 Gauge fields

Solving (2.23) for the case of gauge fields, i. e. $s = 2$ and $M_\Phi^2 = 0$, we obtain for the gauge KK modes [30]

$$f^{(0)}_{\text{gauge}}(y) = 1\,, \tag{2.24}$$

$$f^{(n)}_{\text{gauge}}(y) = \frac{e^{ky}}{N_n}\left[J_1\left(\frac{m_n}{k}e^{ky}\right) + b_1(m_n)Y_1\left(\frac{m_n}{k}e^{ky}\right)\right] \qquad (n = 1, 2, \dots)\,, \tag{2.25}$$

where $J_\alpha(x)$ and $Y_\alpha(x)$ are the Bessel functions of first and second kind. Note that $f^{(0)}_{\text{gauge}}(y)$ exists only for $(++)$ BCs, i. e. Neumann BCs on both branes (see (2.27)). The resulting gauge boson zero mode is massless, $m_0 = 0$. The shape functions $f^{(n)}_{\text{gauge}}(y)$ satisfy the orthonormality condition

$$\frac{1}{L}\int_0^L dy\, f^{(n)}_{\text{gauge}}(y) f^{(m)}_{\text{gauge}}(y) = \delta_{nm}\,. \tag{2.26}$$

$b_1(m_n)$ and m_n are then determined through the choice of BCs on the branes.

We observe that while the zero mode profile $f^{(0)}_{\text{gauge}}(y)$ is flat along the extra dimension, this is not the case for the KK profiles $f^{(n)}_{\text{gauge}}(y)$ $(n = 1, 2, \dots)$ that are exponentially peaked at the IR brane.

For fields obeying $(++)$ BCs, which means

$$\partial_y f^{(n)}_{\text{gauge}}(y)\Big|_{y=0,L} = 0\,, \tag{2.27}$$

one obtains [30]

$$b_1(m_n) = -\frac{J_1(m_n/k) + m_n/k\, J_1'(m_n/k)}{Y_1(m_n/k) + m_n/k\, Y_1'(m_n/k)} = b_1(m_n e^{kL})\,. \tag{2.28}$$

This condition can only be solved numerically for m_n and $b_1(m_n)$. For large values of n, the result can be well approximated by [30]

$$b_1(m_n) = 0\,, \qquad m_n^{\text{gauge}} \simeq \left(n - \frac{1}{4}\right)\pi k e^{-kL} \qquad (n = 1, 2, \dots)\,, \tag{2.29}$$

however, for small values of n it is safer to use the exact numerical result. Numerically one finds

$$m_1^{\text{gauge}}(++) \equiv M_{++} \simeq 2.45 f\,, \tag{2.30}$$

with $f = ke^{-kL}$.

For fields obeying $(-+)$ BCs, meaning

$$f^{(n)}_{\text{gauge}}(y)\Big|_{y=0} = \partial_y f^{(n)}_{\text{gauge}}(y)\Big|_{y=L} = 0\,, \tag{2.31}$$

one finds instead

$$b_1(m_n) = -\frac{J_1(m_n/k)}{Y_1(m_n/k)} = -\frac{J_1(m_n e^{kL}/k) + m_n e^{kL}/k\, J_1'(m_n e^{kL}/k)}{Y_1(m_n e^{kL}/k) + m_n e^{kL}/k\, Y_1'(m_n e^{kL}/k)}\,. \tag{2.32}$$

The numerical solution yields a $\sim 2\%$ suppression of m_1^{gauge} in that case, with respect to the $(++)$ one:

$$m_1^{\text{gauge}}(-+) \equiv M_{-+} \simeq 2.40 f\,. \tag{2.33}$$

We do not consider gauge fields with a Dirichlet BC on the IR brane here, as this choice of BCs does not appear in our model and is therefore irrelevant for the subsequent analysis. Note that the BCs for a gauge field V_μ imply automatically opposite BCs for its 5th component V_5. Throughout this analysis we choose to work in the gauge $V_5 = 0$ and $\partial_\mu V^\mu = 0$. This is generally possible as long as no gauge field V_μ is assigned $(--)$ BCs. In this latter case a physical massless zero mode V_5 would exist that can not be gauged away. The V_5 KK modes, on the other hand, serve as the Goldstone bosons eaten by the corresponding KK modes of V_μ and can therefore be gauged away.

Finally, N_n has to be determined from the normalisation condition (2.26). For fields (also fermions) with a Neumann BC the IR brane, N_n is approximately given by [30]

$$N_n \simeq \frac{e^{kL/2}}{\sqrt{\pi L m_n}}\,. \tag{2.34}$$

Note that this approximation is however *not* valid in case of a Dirichlet $(-)$ BC on the IR brane.

2.2.3 Fermion fields

Due to the rescaling of $\psi_{L,R}$, by a factor e^{-2ky}, the KK decomposition reads in this case

$$\psi_{L,R}(x^\mu, y) = \frac{e^{2ky}}{\sqrt{L}} \sum_{n=0}^{\infty} \psi_{L,R}^{(n)}(x^\mu) f_{L,R}^{(n)}(y)\,. \tag{2.35}$$

Inserting this into (2.23) and using $s = 1$ and $M_\Phi^2 = c(c \pm 1)k^2$, we find for the left-handed fermionic KK modes [30]

$$f_L^{(0)}(y, c) = \sqrt{\frac{(1-2c)kL}{e^{(1-2c)kL} - 1}} e^{-cky}\,, \tag{2.36}$$

$$f_L^{(n)}(y, c) = \frac{e^{ky/2}}{N_n}\left[J_\alpha\left(\frac{m_n}{k}e^{ky}\right) + b_\alpha(m_n) Y_\alpha\left(\frac{m_n}{k}e^{ky}\right)\right] \qquad (n = 1, 2, \dots)\,, \tag{2.37}$$

where $\alpha = |c+1/2|$. Again a massless zero mode $f_L^{(0)}(y,c) \neq 0$ exists only for $(++)$ BCs for the left-handed mode. The shape functions $f_R^{(n)}(y,c)$ for the right-handed modes can be obtained by replacing c by $-c$ in the above formulae,

$$f_R^{(n)}(y,c) = f_L^{(n)}(y,-c)\,. \tag{2.38}$$

Consequently a right-handed massless zero mode is present in the spectrum if the corresponding BCs are $(++)$.

The $f_{L,R}^{(n)}(y,c)$ satisfy the orthonormality condition

$$\frac{1}{L}\int_0^L dy\, e^{ky} f_{L,R}^{(n)}(y,c) f_{L,R}^{(m)}(y,c) = \delta_{nm}\,, \tag{2.39}$$

determining the normalisation constant N_n.

Again $b_\alpha(m_n)$ and m_n are determined through the BCs on the branes. In the case of left-handed fermions, a $-$ BC means

$$f_L^{(n)}(y,c)\Big|_{\text{brane}} = 0\,, \tag{2.40}$$

while the $+$ BC is modified with respect to the gauge fields and reads

$$(\partial_y + ck) f_L^{(n)}(y,c)\Big|_{\text{brane}} = 0\,. \tag{2.41}$$

For right-handed fields, the replacement $c \to -c$ has to be made.

$b_\alpha(m_n)$ and m_n are then derived in a completely analogous manner with respect to the gauge case. Also here the resulting equations can only be solved numerically.

As left- and right-handed modes are coupled by the massive Dirac equation, the BCs for the right-handed modes are not independent of the left-handed ones. In fact it is straightforward to see that the right-handed mode has to obey automatically opposite BCs. Consequently three scenarios with fundamentally different phenomenological implications arise:

1. The left-handed modes obey $(++)$ BCs, so that the spectrum contains a massless *left-handed zero mode*. As the right-handed modes then have to obey $(--)$ BCs, no right-handed zero mode is present.
2. The left-handed modes obey $(--)$ BCs. While in that case no left-handed zero mode arises, the right-handed modes have to obey $(++)$ BCs and a massless *right-handed zero mode* is present.
3. Mixed BCs, i. e. $(-+)$ or $(+-)$, are chosen for the left-handed modes. Then also the right-handed modes obey mixed BCs, and consequently the spectrum contains *no zero mode*.

While the precise values of the KK masses m_n also depend on the choice of BCs, it is common to all three cases that in addition to the possible chiral zero mode an infinite tower of massive KK modes with approximately vectorlike couplings exists. Like in the case of KK gauge bosons, also the bulk profiles of KK fermions are exponentially localised towards the IR brane.

A comment on the zero mode bulk profile is in order. While we have seen in (2.24) that the gauge boson zero mode profile is flat along the extra dimension, this is not the case for fermionic zero modes. Instead from (2.36) we observe that the latter bulk profile depends exponentially on the bulk mass parameter c. By performing some trivial field redefinitions it is possible to re-write the fermionic action with respect to the flat tangent space metric $\eta_{AB} = \mathrm{diag}(1, -1, -1, -1, -1)$. The resulting left-handed fermionic zero mode profile reads [29, 30]

$$f^{(0)}_{\mathrm{flat},L}(y, c) = \sqrt{\frac{(1-2c)kL}{e^{(1-2c)kL} - 1}}\, e^{(\frac{1}{2}-c)ky} \,. \tag{2.42}$$

Having at hand $f^{(0)}_{\mathrm{flat},L}(y, c)$ it is easy to deduce how the localisation of fermion zero modes along the 5D bulk depends on the bulk mass parameter c. We distinguish the following cases:

- For $c > 1/2$ the normalisation factor in (2.42) is $\mathcal{O}(1)$ and $f^{(0)}_{L}(y, c)$ is peaked around $y = 0$, i. e. fermions with bulk mass parameter $c > 1/2$ are placed close to the UV brane. At the same time their overlap with fields on or near the IR brane is exponentially suppressed.

- For $c < 1/2$ the second term in the denominator of (2.42) can be neglected and we obtain

$$f^{(0)}_{\mathrm{flat},L}(y, c) \simeq \sqrt{(1-2c)kL}\, e^{(\frac{1}{2}-c)k(y-L)} \,. \tag{2.43}$$

  Thus the shape function is strongly peaked towards $y = L$, i. e. the IR brane. Consequently the overlap with fields on or near the IR brane is $\mathcal{O}(1)$.

- In the limiting case $c = 1/2$ the shape function is flat, so that the zero mode fermion is delocalised in the 5D bulk. Interestingly, due to the orthonormality condition for gauge fields (2.26) this mode does not couple to the heavy KK gauge bosons.

In case of a right-handed zero mode $f^{(0)}_{\mathrm{flat},R}(y, c)$ analogous comments apply, with c replaced by $-c$.

2.3 Electroweak constraints on the RS bulk standard model

2.3.1 General remarks

We are now prepared to consider the most straightforward extension of the SM in terms of RS bulk fields. Consider a warped extra dimension with the SM gauge symmetry $SU(3)_c \times SU(2)_L \times U(1)_Y$ in the bulk. A Higgs doublet H is introduced on the IR brane that develops a VEV v_0 and therefore leads to electroweak symmetry breaking. In order to reproduce the SM field content in the low-energy limit we introduce the following 5D quark fields:

$$Q^i(++) = \begin{pmatrix} u^i \\ d^i \end{pmatrix}(++)\,, \qquad U^i(--)\,, \qquad D^i(--)\,, \tag{2.44}$$

where the BCs are those for the left-handed modes, and $i = 1, 2, 3$ is the flavour index. Consequently, the spectrum contains a left-handed zero mode doublet and two right-handed zero mode singlets per generation, in agreement with observation.

Following the strategy outlined in section 2.2, it is possible to obtain a purely 4D theory by performing the KK decomposition of the fundamental 5D action. In particular Feynman rules can be derived and corrections to low-energy observables can be evaluated.

Particularly stringent constraints arise from the measurements of electroweak precision observables that show the SM in surprisingly good agreement with the data. While a complete analysis of all these constraints requires a simultaneous fit of all oblique and non-oblique corrections, see e. g. [1, 61–70], such an analysis is clearly beyond the scope of this work. Rather we focus here on the most stringent constraints, coming from the Peskin-Takeuchi parameters S and T [61] and the anomalous $Zb_L\bar{b}_L$ coupling. Electroweak precision constraints on the RS bulk SM have been studied extensively in the literature [31, 71–75], most recently in [76]. In what follows we will briefly review these results.

2.3.2 The S parameter

We start by considering the S parameter, defined as [1]

$$\frac{\alpha(M_Z)}{4\sin^2\theta_W\cos^2\theta_W} S = \frac{\Pi^{\text{new}}_{ZZ}(M_Z^2) - \Pi^{\text{new}}_{ZZ}(0)}{M_Z^2} - \frac{cos^2\theta_W - \sin^2\theta_W}{\cos\theta_W \sin\theta_W}\frac{\Pi^{\text{new}}_{Z\gamma}(M_Z^2)}{M_Z^2} - \frac{\Pi^{\text{new}}_{\gamma\gamma}(M_Z^2)}{M_Z^2}\,, \tag{2.45}$$

where $\alpha(M_Z)$ and θ_W are the corresponding $\overline{\text{MS}}$ values at the scale M_Z. Here $\Pi_{ij}^{\text{new}}(q^2)$ denotes the NP contribution to the self-energy of the gauge bosons $i, j = W, Z, \gamma$ at the scale q^2. Thus S is associated to the difference of the Z boson self-energies at $q^2 = M_Z^2$ and $q^2 = 0$.

Assuming $m_H = 117\,\text{GeV}$ and $U = 0$, a combined analysis of electroweak precision measurements leads to the constraint [1]

$$S = -0.04 \pm 0.09\,, \tag{2.46}$$

which induces severe constraints on the parameter space of many NP models. For instance, new strong dynamics at the TeV scale generically induces a positive $\mathcal{O}(1)$ correction (for a recent analysis, see [77]) to S, in vast disagreement with the data. One should however keep in mind that the corrections to S are not calculable in such kinds of models, being non-perturbative, and therefore can only be estimated.

With the help of the AdS/CFT correspondence [78] certain strongly coupled 4D theories can be interpreted as weakly coupled 5D models in the RS background. Then it is possible to perturbatively calculate the corrections to the S parameter. In case of the RS bulk SM, such calculations yield [31]

$$S \simeq \frac{12\pi v^2}{M^2}\,, \tag{2.47}$$

which, together with (2.46), yields the lower bound

$$M \gtrsim (2-3)\,\text{TeV}\,, \tag{2.48}$$

with M being the mass of the first gauge KK modes.

We note that the bound (2.48) depends only weakly on the detailed structure of the RS model under consideration and is also valid in case of the RS model with custodial protection discussed later on.

2.3.3 The T parameter

Another powerful constraint is given by the T parameter, conveniently defined as [1]

$$\alpha(M_Z)T = \frac{\Pi_{WW}^{\text{new}}(0)}{M_W^2} - \frac{\Pi_{ZZ}^{\text{new}}(0)}{M_Z^2}\,, \tag{2.49}$$

measuring the violation of custodial symmetry in the electroweak sector. In this case the LEP data yield [1]

$$T = 0.02 \pm 0.09\,, \tag{2.50}$$

again determined for $m_H = 117\,\text{GeV}$ and $U = 0$.

In the RS bulk SM custodial symmetry is violated already at the tree level by the presence of the heavy gauge KK modes and their mixing with the respective zero modes. It then turns out that the constraint (2.50) is even more severe than the one from the S parameter (2.46) and yields the constraint [31]

$$M \gtrsim 10\,\text{TeV}\,. \tag{2.51}$$

Consequently electroweak precision constraints push this simple extension of the SM to the RS bulk far beyond the reach of the LHC.

Fortunately the situation can be significantly ameliorated by extending the symmetry structure of the model to include an intrinsic custodial symmetry in the Higgs sector of the model. To this end, the bulk gauge symmetry needs to be enlarged to [31–33]

$$SU(3)_c \times SU(2)_L \times SU(2)_R \times U(1)_X\,. \tag{2.52}$$

In order to maintain the correct low-energy limit of the theory, on the UV brane the breaking

$$SU(2)_R \times U(1)_X \to U(1)_Y \tag{2.53}$$

has to be achieved by appropriately chosen BCs. As the Higgs field lives on the IR brane and does not feel this breaking directly, the custodial symmetry in the Higgs sector is approximately preserved. Therefore the corrections to the T parameter turn out to be safely small even for KK gauge bosons at the $(2-3)\,\text{TeV}$ scale [31–33, 75, 79–81].

2.3.4 The anomalous $Zb_L\bar{b}_L$ coupling

Finally let us consider the RS contributions to the anomalous $Zb_L\bar{b}_L$ coupling. Experimentally, such flavour non-universal contributions are bounded by [1]

$$-2\cdot 10^{-3} \lesssim \delta g_{Zb_L\bar{b}_L} \lesssim 6\cdot 10^{-3} \qquad (95\%\ \text{C.L.})\,. \tag{2.54}$$

In order to understand the importance of this constraint for RS scenarios with bulk fermions as considered here, let us briefly anticipate the flavour structure of such models, discussed in detail in section 3.4. We have seen in section 2.2.3 that the localisation of a fermionic zero mode depends exponentially on its bulk mass parameter c. Consequently, for $c > 1/2$ ($c < -1/2$ for right-handed modes) the overlap of the fermion shape function with the Higgs boson living on the IR brane is exponentially suppressed, while it is $\mathcal{O}(1)$ else. As the strength of the effective

fermionic Yukawa couplings to the Higgs depend on this overlap, the hierarchical pattern of the SM Yukawa couplings can be reduced to appropriately chosen $\mathcal{O}(1)$ values for the respective bulk mass parameters. Clearly, in order to account for its large mass, the top quark has to be localised close to the IR brane. However, as the left-handed top quark t_L resides in an $SU(2)_L$ doublet together with the left-handed bottom quark b_L, also the latter one is necessarily localised close to the IR brane.

Since the KK gauge bosons, similar to all KK modes, are strongly localised towards the IR brane (see section 2.2.2), they couple much more strongly to b_L than to the other down-type quarks. As in the process of EWSB discussed in detail in section 3.3 the Z boson zero mode mixes with its heavy KK excitations, this non-universality in the gauge couplings is transmitted also to the SM Z boson. Similarly, mixing between fermionic zero and KK modes generates non-universalities in the Z couplings, with the latter effect being however subleading [35–37]. Typically for low KK scales $M \simeq (2-3)\,\text{TeV}$ then a correction to $\delta g_{Zb_L\bar{b}_L}$ at the percent level is obtained, in conflict with the data (2.54).

Interestingly, in [34] it has been pointed out that the custodial symmetry (2.52) can straightforwardly be used to protect not only the T parameter from unwantedly large corrections, but at the same time to keep also the corrections to $\delta g_{Zb_L\bar{b}_L}$ under control. To this end an additional discrete $\mathbb{Z}_2$ symmetry

$$P_{LR} : SU(2)_L \leftrightarrow SU(2)_R \tag{2.55}$$

needs to be introduced, that interchanges the two $SU(2)$ factors of the gauge group (2.52). Clearly, in order to construct a P_{LR}-symmetric theory the gauge couplings of $SU(2)_L$ and $SU(2)_R$ have to be equal,

$$g_L = g_R \equiv g\,, \tag{2.56}$$

and the fermion fields (2.44) have to be embedded into enlarged P_{LR}-symmetric representations, with b_L being an eigenstate of P_{LR}.

Before presenting in chapter 3 the details of such a P_{LR}-symmetric model, we show explicitly, following [34], how this simple symmetry can help to protect the $Zb_L\bar{b}_L$ coupling from large corrections. To this end we consider the general structure of the Z boson coupling:

$$g_Z = \frac{g}{\cos\theta_W}\left(Q_L^3 - Q_{\text{em}}\sin^2\theta_W\right)\,. \tag{2.57}$$

As $U(1)_{\text{em}}$ is an exact symmetry, corrections to g_Z can only arise from the first term in (2.57). While a priori $Q_L^3 = T_L^3$ holds, this equality can receive corrections in the process of EWSB,

$$Q_L^3 = T_L^3 + \delta Q_L^3\,. \tag{2.58}$$

On the other hand the diagonal subgroup $SU(2)_V$ of $SU(2)_L \times SU(2)_R$ is left unbroken even after EWSB, so that its isospin T_V^3 is conserved. Consequently we have

$$\delta Q_V^3 = \delta Q_L^3 + \delta Q_R^3 = 0\,. \tag{2.59}$$

Furthermore an unbroken P_{LR} symmetry ensures that for fermions embedded as P_{LR} eigenstates

$$\delta Q_L^3 = \delta Q_R^3\,. \tag{2.60}$$

This immediately yields

$$\delta Q_L^3 = 0\,, \tag{2.61}$$

so that the coupling of the respective fermion to the Z boson is protected from anomalous contributions.

By now we have collected all necessary ingredients to construct a realistic RS model in the reach of the LHC that passes electroweak precision tests. Alternative realisation of this type of models have been worked out and analysed in the literature [82–84]. In the next chapter we will present one of the simplest versions, based on [84], whose electroweak and flavour structure has been discussed in detail in [40], where also a complete set of Feynman rules has been derived. Subsequently in chapters 4 and 5 its phenomenological impact on K and B physics observables will be discussed in detail, based on the analyses presented in [35, 36].

3 The custodially protected model

3.1 Preliminaries

We have seen in the previous chapter that the simple RS model with bulk fields and only the SM gauge group in the bulk has severe problems to pass electroweak precision constraints unless the lowest lying KK modes are heavier than about 10 TeV. However KK modes in the reach of the LHC, i. e. $M \simeq (2-3)\,\text{TeV}$, are still possible if the bulk symmetry of the model is extended to

$$G_{\text{bulk}} = SU(3)_c \times SU(2)_L \times SU(2)_R \times P_{LR} \times U(1)_X \,. \tag{3.1}$$

In the present chapter we introduce one of the simplest realisations of this gauge group. To this end we follow the top-down approach and first give the complete 5D action of the model, and discuss its details and implications subsequently. An extensive theoretical description of the model considered has been presented by us in [40], to which we refer the reader for further details.

3.2 Fundamental 5D action

The fundamental 5D action of the custodially protected RS model under consideration can be decomposed as

$$S = \int d^4x \int_0^L dy \, \left(\mathcal{L}_{\text{gauge}} + \mathcal{L}_{\text{fermion}} + \mathcal{L}_{\text{Higgs}} + \mathcal{L}_{\text{Yuk}}\right) \,. \tag{3.2}$$

$\mathcal{L}_{\text{gauge}}$, describing the kinetic terms for the $SU(3)_c \times SU(2)_L \times SU(2)_R \times U(1)_X$ gauge fields, is discussed in section 3.2.1. The fermion representations present in the theory as well as their kinetic and bulk mass terms $\mathcal{L}_{\text{fermion}}$ are introduced in section 3.2.2. $\mathcal{L}_{\text{Higgs}}$ contains the Higgs kinetic term and its potential, leading to EWSB, see section 3.2.3. Finally the fermion Yukawa couplings to the Higgs boson are contained in $\mathcal{L}_{\text{Yuk}}$ and discussed in section 3.2.4.

3.2.1 Gauge sector

The kinetic terms for the gauge fields are given by

$$\mathcal{L}_{\text{gauge}} = \sqrt{G}\left[-\frac{1}{4}G^A_{MN}G^{MN,A} - \frac{1}{4}L^a_{MN}L^{MN,a} - \frac{1}{4}R^\alpha_{MN}R^{MN,\alpha} - \frac{1}{4}X_{MN}X^{MN}\right], \tag{3.3}$$

where the $SU(3)_c$ field strength tensor is given by

$$G^A_{MN} = \partial_M G^A_N - \partial_N G^A_M - g_s f^{ABC} G^B_M G^C_N \qquad (A = 1, \ldots, 8)\,. \tag{3.4}$$

g_s is the 5D strong coupling constant, and f^{ABC} are the $SU(3)$ structure constants. Note that due to the antisymmetric structure of G^A_{MN} the two terms involving the Christoffel symbols (A.3) cancel each other. Similarly the $SU(2)_L$ and $SU(2)_R$ field strength tensors read

$$L^a_{MN} = \partial_M W^a_{L,N} - \partial_N W^a_{L,M} - g\varepsilon^{abc} W^b_{L,M} W^c_{L,N} \qquad (a = 1, 2, 3)\,, \tag{3.5}$$

$$R^\alpha_{MN} = \partial_M W^\alpha_{R,N} - \partial_N W^\alpha_{R,M} - g\varepsilon^{\alpha\beta\gamma} W^\beta_{R,M} W^\gamma_{R,N} \qquad (\alpha = 1, 2, 3)\,. \tag{3.6}$$

Note that due to the P_{LR} symmetry the gauge couplings g of $SU(2)_L$ and $SU(2)_R$ are equal. Finally the field strength tensor of the Abelian gauge group factor $U(1)_X$ is

$$X_{MN} = \partial_M X_N - \partial_N X_M\,, \tag{3.7}$$

with the $U(1)_X$ gauge coupling constant denoted by g_X. Here and throughout this work the coupling constants g_s, g and g_X are understood to be the fundamental 5D ones that are not dimensionless. In the absence of brane kinetic terms (see e. g. [35, 85] and section 3.2.5 for details), the effective 4D coupling constants can then be determined via the simple tree level matching condition

$$g^{\text{4D}} = \frac{g}{\sqrt{L}}\,, \tag{3.8}$$

and analogous relations holding for g_s^{4D} and g_X^{4D}.

We denote $SU(2)_L$ indices by small Latin letters a, b, c and $SU(2)_R$ indices by small Greek letters α, β, γ. $SU(3)_c$ indices are denoted by capital Latin letters A, B, C, but are usually made implicit in order to simplify the notation.

In order to obtain the correct low energy spectrum, the gauge group (3.1) has to be broken by appropriate BCs on the UV brane ($y = 0$) to the SM gauge group, i. e.

$$SU(3)_c \times SU(2)_L \times SU(2)_R \times P_{LR} \times U(1)_X \xrightarrow{\text{UV brane}} SU(3)_c \times SU(2)_L \times U(1)_Y\,. \tag{3.9}$$

This breakdown is achieved by the following assignment of BCs[1]

$$G^A_{\mu\nu}(++)\,, \qquad W^a_{L\mu}(++)\,, \qquad B_\mu(++)\,, \tag{3.10}$$

$$W^\beta_{R\mu}(-+)\,, \qquad Z_{X\mu}(-+)\,, \tag{3.11}$$

where as usual the first (second) sign denotes the BC on the UV (IR) brane: $+$ stands for a Neumann BC while $-$ stands for a Dirichlet BC, see section 2.2.2. Furthermore $A = 1, \ldots, 8$, $a = 1, 2, 3$ and $\beta = 1, 2$. The fields B_μ and $Z_{X\mu}$ are orthogonal linear combinations of $W^3_{R\mu}$ and X_μ and given in terms of the original fields as follows:

$$Z_{X\mu} = \cos\phi\, W^3_{R\mu} - \sin\phi\, X_\mu\,, \tag{3.12}$$

$$B_\mu = \sin\phi\, W^3_{R\mu} + \cos\phi\, X_\mu\,, \tag{3.13}$$

where

$$\cos\phi = \frac{g}{\sqrt{g^2 + g_X^2}}\,, \qquad \sin\phi = \frac{g_X}{\sqrt{g^2 + g_X^2}}\,. \tag{3.14}$$

The 5D gauge coupling g_Y of the resulting gauge group $U(1)_Y$, corresponding to the gauge boson B_μ in (3.13), is then given by

$$g_Y = g \sin\phi = g_X \cos\phi\,. \tag{3.15}$$

3.2.2 Fermion Sector

Quarks

In the quark sector the following P_{LR}-symmetric fermion representations are introduced [84]

$$(\xi^i_1)_{a\alpha} = \begin{pmatrix} \chi^{u_i}(-+)_{5/3} & q^{u_i}(++)_{2/3} \\ \chi^{d_i}(-+)_{2/3} & q^{d_i}(++)_{-1/3} \end{pmatrix}_{2/3}\,, \tag{3.16}$$

$$\xi^i_2 = u^i(--)_{2/3}\,, \tag{3.17}$$

$$\xi^i_3 = (T^i_3)_a \oplus (T^i_4)_\alpha = \begin{pmatrix} \psi'^i(+-)_{5/3} \\ U'^i(+-)_{2/3} \\ D'^i(+-)_{-1/3} \end{pmatrix}_{2/3} \oplus \begin{pmatrix} \psi''^i(+-)_{5/3} \\ U''^i(+-)_{2/3} \\ D^i(--)_{-1/3} \end{pmatrix}_{2/3}\,. \tag{3.18}$$

They transform as $(\mathbf{2}, \mathbf{2})_{2/3}$, $(\mathbf{1}, \mathbf{1})_{2/3}$ and $(\mathbf{3}, \mathbf{1})_{2/3} \oplus (\mathbf{1}, \mathbf{3})_{2/3}$, respectively, under $SU(2)_L \times SU(2)_R \times U(1)_X$. Again $SU(2)_L$ indices are denoted by Latin letters

[1] These BCs can be naturally achieved by adding a scalar $SU(2)_R$ doublet with $Q_X = 1/2$ charge on the UV brane, that develops a VEV $v_{\mathrm{UV}} \to \infty$ (see [58, 60] for details).

while $SU(2)_R$ indices are denoted by Greek letters. Note that in the notation of (3.16), $SU(2)_L$ acts vertically while $SU(2)_R$ acts horizontally,

$$\xi_1^i \to U_L \xi_1^i U_R^T \qquad (U_L \in SU(2)_L, U_R \in SU(2)_R)\,. \tag{3.19}$$

The subscripts of the various components indicate their electric charge. All these multiplets transform as triplets under $SU(3)_c$. The signs in brackets indicate the boundary conditions (BCs) for the left-handed fermion mode on the UV and IR brane, respectively, where "+" denotes a modified Neumann BC and "−" stands for a Dirichlet BC, as discussed in section 2.2.3. The corresponding right-handed modes, that are necessarily present in a 5D theory, obey opposite BCs. As only fields with (++) BCs contain a massless zero mode, the low energy spectrum will contain a left-handed doublet $(q_L^{u_i(0)}, q_L^{d_i(0)})$ and two right-handed singlets $u_R^{i(0)}$ and $D_R^{i(0)}$ for each quark generation $i = 1, 2, 3$, reproducing precisely the field content of the SM.

In our phenomenological analysis we mostly neglect the impact of the fermionic KK modes, as their effect turns out to subleading and therefore negligible [35–38]. In order to keep the notation as transparent as possible, the zero modes are then simply denoted by $Q_L^i = (u_L^i, d_L^i)$ and u_R^i, d_R^i.

We note that χ^{u_i}, q^{d_i} and u^i are eigenstates of the P_{LR} transformation. Consequently, the couplings of the corresponding zero and KK modes to the Z boson are protected from EWSB corrections [34]. In particular this leads to the phenomenologically relevant protection of the anomalous $Zb_L\bar{b}_L$ coupling as well as of all flavour conserving and violating $Zd_L^i\bar{d}_L^j$ vertices [35–37].

The fermionic Lagrangian then reads

$$\begin{aligned}\mathcal{L}_{\text{fermion}} = \frac{1}{2}\sqrt{G}\sum_{i=1}^{3}\Big[&(\bar{\xi}_1^i)_{a\alpha} i\Gamma^M (D_M^1)_{ab,\alpha\beta}(\xi_1^i)_{b\beta} + (\bar{\xi}_1^i)_{a\alpha}(i\Gamma^M\omega_M - c_Q^i k)(\xi_1^i)_{a\alpha} \\ &+ \bar{\xi}_2^i(i\Gamma^M D_M^2 + i\Gamma^M\omega_M - c_u^i k)\xi_2^i \\ &+ (\bar{T}_3^i)_a i\Gamma^M (D_M^3)_{ab}(T_3^i)_b + (\bar{T}_3^i)_a(i\Gamma^M\omega_M - c_d^i k)(T_3^i)_a \\ &+ (\bar{T}_4^i)_\alpha i\Gamma^M (D_M^4)_{\alpha\beta}(T_4^i)_\beta + (\bar{T}_4^i)_\alpha(i\Gamma^M\omega_M - c_d^i k)(T_4^i)_\alpha\Big] + h.c.\,,\end{aligned} \tag{3.20}$$

where summation over repeated indices is understood. Details on the Dirac gamma matrices Γ^M and the spin connection ω_M in curved space-time are collected in Appendix A.1.2. Writing out the "$+h.c.$" term explicitly, one finds that the terms including the spin connection ω_M cancel each other [59]. Note that throughout this analysis we work in the special basis in which the bulk mass matrices $c_{Q,u,d}k$ are real and diagonal.

The covariant derivatives D_M^i in (3.20) are given by

$$\begin{aligned}(D_M^1)_{ab,\alpha\beta} &= (\partial_M + ig_s t^A G_M^A + ig_X Q_X X_M)\delta_{ab}\delta_{\alpha\beta} \\ &\quad + ig(\tau^c)_{ab} W_{L,M}^c \delta_{\alpha\beta} + ig(\tau^\gamma)_{\alpha\beta} W_{R,M}^\gamma \delta_{ab}\,, \qquad (3.21)\\ D_M^2 &= \partial_M + ig_s t^A G_M^A + ig_X Q_X X_M\,, \qquad (3.22)\\ (D_M^3)_{ab} &= (\partial_M + ig_s t^A G_M^A + ig_X Q_X X_M)\delta_{ab} + g\varepsilon^{abc} W_{L,M}^c\,, \qquad (3.23)\\ (D_M^4)_{\alpha\beta} &= (\partial_M + ig_s t^A G_M^A + ig_X Q_X X_M)\delta_{\alpha\beta} + g\varepsilon^{\alpha\beta\gamma} W_{R,M}^\gamma\,. \qquad (3.24)\end{aligned}$$

$t^A = \lambda^A/2$ $(A = 1, \ldots, 8)$ are the generators of the fundamental representation of $SU(3)_c$, where λ^A are the known Gell-Mann matrices. $\tau^a = \sigma^a/2$ $(\tau^\alpha = \sigma^\alpha/2)$ are the generators of the fundamental $SU(2)_L$ $(SU(2)_R)$ representations, respectively, where σ^a, σ^α are the Pauli matrices, and $-i\varepsilon^{abc}$ and $-i\varepsilon^{\alpha\beta\gamma}$ are the generators of the adjoint triplet representations of $SU(2)_L$ and $SU(2)_R$, respectively. Recall that despite having the same matrix structure, the $SU(2)_L$ and $SU(2)_R$ generators act on different internal spaces.

Finally we would like to caution the reader that the components of the $T_{3,4}^i$ triplets, as given in (3.18), are *not* those components associated to $a, \alpha = 1, 2, 3$. Instead

$$(T_3^i)_a = \begin{pmatrix} \frac{1}{\sqrt{2}}(\psi'^i + D'^i) \\ \frac{i}{\sqrt{2}}(\psi'^i - D'^i) \\ U'^i \end{pmatrix}\,, \qquad (T_4^i)_\alpha = \begin{pmatrix} \frac{1}{\sqrt{2}}(\psi''^i + D^i) \\ \frac{i}{\sqrt{2}}(\psi''^i - D^i) \\ U''^i \end{pmatrix}\,. \qquad (3.25)$$

Recall that the same structure appears also in the gauge sector, where $W_{L,R}^{1,2}$ are related to $W_{L,R}^\pm$ via

$$W_{L,R}^\pm = \frac{W_{L,R}^1 \mp iW_{L,R}^2}{\sqrt{2}}\,. \qquad (3.26)$$

Leptons

In order to preserve the minimality of the model, we take the lepton sector in complete analogy to the quark sector. The resulting lepton representations can be found in [40]. Basically the only necessary modifications are:

1. Leptons transform as singlets under $SU(3)_c$, i. e. the coupling to gluons, $+ ig_s t^A G_M^A$ in (3.21)–(3.24), has to be removed.
2. In order to obtain correct electric charges for the leptons, $Q_X = 0$ has to be imposed, so that leptons do not couple to the X_M gauge boson of $U(1)_X$. Effectively thus also the $+ ig_X Q_X X_M$ term in (3.21)–(3.24) is absent in the case of leptons.

An immediate consequence of this P_{LR}-symmetric realisation of the lepton sector is that also the couplings $Z\ell_L^i\bar{\ell}_L^j$ and $Z\nu_R^i\bar{\nu}_R^j$ are protected from large corrections, with possibly profound implications on lepton flavour violating observables.

For completeness sake we note that in principle other implementations of the lepton sector are possible and in agreement with the data. First of all, the lepton sector does not necessarily have to preserve the P_{LR} symmetry, as the leptons, due to their small masses, are localised far enough in the UV anyway to fulfil experimental constraints on their couplings. Therefore the left- and right-handed SM leptons may as well be embedded into $(\mathbf{2},\mathbf{1})$ and $(\mathbf{1},\mathbf{2})$ representations, respectively. Another possibility would be to implement the right-handed neutrinos as complete gauge singlets, $(\mathbf{1},\mathbf{1})_0$, and add Majorana mass terms in the bulk and/or on the branes.

3.2.3 Higgs Sector

The Lagrangian describing the Higgs dynamics reads

$$\mathcal{L}_{\text{Higgs}} = \delta(y-L)\sqrt{G}\left[(D_\mu H)^\dagger_{a\alpha}(D^\mu H)_{a\alpha} - V(H)\right] , \tag{3.27}$$

with the covariant derivative given by

$$(D_\mu H)_{a\alpha} = \partial_\mu H_{a\alpha} + ig(\tau^c)_{ab}W^c_{L,\mu}H_{b\alpha} + ig(\tau^\gamma)_{\alpha\beta}W^\gamma_{R,\mu}H_{a\beta}\,. \tag{3.28}$$

Furthermore

$$V(H) = -\mu^2 H^\dagger H + \lambda(H^\dagger H)^2 \tag{3.29}$$

is the Higgs potential that for $\mu^2 > 0$ leads to EWSB. The Higgs field transforms as a self-dual bidoublet $(\mathbf{2},\mathbf{2})_0$ under the electroweak gauge group. Its degrees of freedom can be parameterised as

$$H = \begin{pmatrix} \pi^+/\sqrt{2} & -(h^0 - i\pi^0)/2 \\ (h^0 + i\pi^0)/2 & \pi^-/\sqrt{2} \end{pmatrix} , \tag{3.30}$$

where again $SU(2)_L$ acts vertically and $SU(2)_R$ horizontally. The Goldstone bosons eaten by the gauge boson zero modes of $W_L^\pm$ and Z are denoted by $\pi^\pm$ and π^0, while h^0 is the physical Higgs boson whose VEV eventually leads to EWSB.

Although in [40] we considered the more general case of a bulk Higgs boson, in the present thesis we will restrict ourselves to the case of a 4D Higgs field confined to the IR brane. As in order to maintain the solution to the gauge hierarchy problem, the Higgs has to be localised close to the IR brane anyway, the phenomenology of the model depends only weakly on the actual form of the Higgs profile considered.

The kinetic term in $\mathcal{L}_{\text{Higgs}}$ is responsible for the effects of EWSB in the gauge sector. Those will be discussed in detail in section 3.3.

3.2.4 Yukawa Sector

The most general Yukawa coupling including the Higgs bidoublet H and the quark fields $\xi^i_{1,2,3}$ is given by

$$\mathcal{L}_{\text{Yuk}} = \delta(y-L)\sqrt{G}\sum_{i,j=1}^{3}\Big[\sqrt{2}\lambda^u_{ij}(\bar{\xi}^i_1)_{a\alpha}H_{a\alpha}\xi^j_2 - 2\lambda^d_{ij}\left[(\bar{\xi}^i_1)_{a\alpha}(\tau^c)_{ab}(T^j_3)^c H_{b\alpha} + (\bar{\xi}^i_1)_{a\alpha}(\tau^\gamma)_{\alpha\beta}(T^j_4)^\gamma H_{a\beta}\right] + h.c.\Big], \tag{3.31}$$

where again summation over repeated indices is understood. The normalisation factors and the overall signs of the two contributions are chosen for later convenience.

Interestingly, while the first coupling, proportional to λ^u_{ij}, contributes, after EWSB, only to the mass matrix of $+2/3$ charge quarks, the second term, proportional to λ^d_{ij}, contributes to all $+5/3$, $+2/3$ and $-1/3$ mass matrices. Explicit expressions for these matrices, including zero and first KK modes, can be found in [40].

We note that $\lambda^{u,d}_{ij}$, being 5D couplings, are not dimensionless, but carry mass dimension -1. In order to maintain perturbativity of the model at least up to the second KK level

$$\left|\lambda^{u,d}_{ij}\right| k \lesssim 3 \tag{3.32}$$

has to be fulfilled. See e. g. [39, 85] for an NDA estimate of this bound.

3.2.5 Additional brane terms

Sections 3.2.1 and 3.2.2 describe the most general bulk Lagrangian consistent with the symmetry (3.1) and including the fermion representations (3.16)–(3.18). However the presence of the two branes at $y = 0$ and $y = L$ would allow us to extend the theory by brane-localised Lagrangians including the fields with + BCs on the respective brane, and invariant under the symmetry that is unbroken on this brane, i. e.

$$\text{UV brane:} \qquad SU(3)_c \times SU(2)_L \times U(1)_Y\,, \tag{3.33}$$

$$\text{IR brane:} \qquad SU(3)_c \times SU(2)_L \times S(2)_R \times P_{LR} \times U(1)_X\,. \tag{3.34}$$

Herewith one should keep in mind that even if such terms are not introduced at tree level, they will be unavoidably generated by radiative corrections.

However in order to keep the presentation as simple as possible and to omit introducing additional sets of new parameters, in the present work we neglect such

brane localised Lagrangians. While the general picture of flavour violating effects in the RS model in question is independent of such additional terms, we note that quantitatively some of the results presented in chapter 5 depend on this assumption.

In particular the presence of brane kinetic terms for the gauge fields modifies the simple tree level matching relation (3.8). As the strengths of the zero mode couplings is determined experimentally, this in turn modifies the necessary 5D gauge coupling constants, and consequently also the coupling strength of the KK gauge bosons. This consequently affects the size of NP effects in flavour violating observables which are dominantly induced by the presence of the heavy KK gauge bosons. For further details we refer the reader to [35, 85].

3.3 Electroweak symmetry breaking

3.3.1 Symmetry breaking pattern

We have seen already in section 3.2.1 that the bulk gauge group G_{bulk} in (3.1) is broken to the SM gauge group by means of appropriately chosen BCs on the UV brane. Consequently the custodial symmetry $SU(2)_V$ and the discrete P_{LR} symmetry are broken on this brane, so that the protection of the T parameter and the $Zd_L^i\bar{d}_L^j$ couplings is no longer exact. On the other hand the Higgs sector, being localised on the IR brane, feels this symmetry breaking only indirectly. Therefore the tree and one-loop corrections to the T parameter and the $Zb_L\bar{b}_L$ coupling turn out to be consistent with electroweak precision data [80, 81, 86].

Now, due to the potential $V(H)$ given in (3.29) the Higgs boson develops a vacuum expectation value (VEV)

$$\langle H\rangle = \begin{pmatrix} 0 & -v_0/2 \\ v_0/2 & 0 \end{pmatrix}, \tag{3.35}$$

with $\langle h_0\rangle = v_0$ being the fundamental Planck scale Higgs VEV. The scale of EWSB is then given by (see section 2.1.2)

$$v = e^{-kL}v_0 \simeq 246\,\text{GeV}\,. \tag{3.36}$$

The Higgs VEV (3.35) induces the breakdown

$$SU(2)_L \times SU(2)_R \xrightarrow{v} SU(2)_V \tag{3.37}$$

on the IR brane. We notice that the custodial symmetry $SU(2)_V$ and consequently also the P_{LR} symmetry remains unbroken in the Higgs sector. Therefore the protection mechanism for the T parameter and the $Zd_L^i\bar{d}_L^j$ couplings is active.

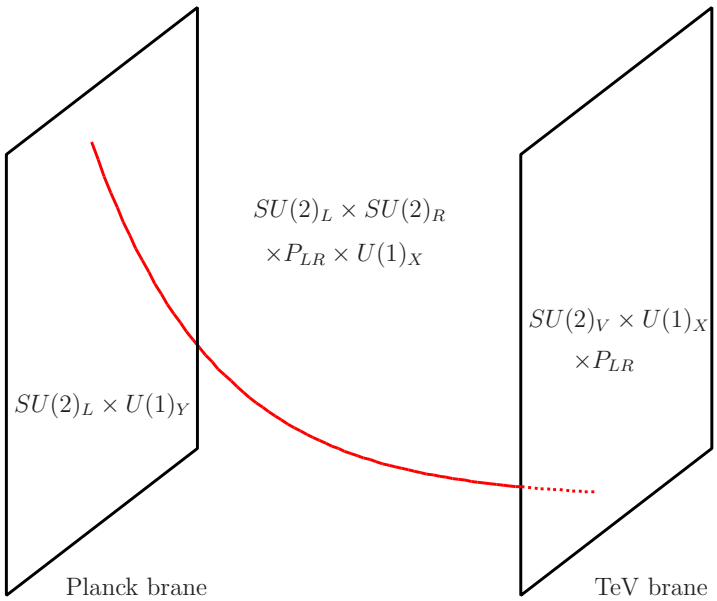

Figure 3.1: *EWSB pattern of the RS model with custodial protection (figure taken from [87]).*

Together with the symmetry breaking by BCs on the UV brane,

$$SU(2)_L \times SU(2)_R \times P_{LR} \times U(1)_X \xrightarrow{\text{UV brane}} SU(2)_L \times U(1)_Y \,, \tag{3.38}$$

in the low energy limit effectively the SM structure of EWSB

$$SU(2)_L \times U(1)_Y \to U(1)_{\text{em}} \tag{3.39}$$

is recovered. The symmetry breaking pattern in the RS model with custodial protection is schematically displayed in figure 3.1.

In order to discuss the impact of EWSB on the gauge boson masses and mixings in the next section, it will be useful to follow [88,89] and define the following fields

$$W^{\pm}_{L\mu} = \frac{W^1_{L\mu} \mp i W^2_{L\mu}}{\sqrt{2}} \,, \qquad W^{\pm}_{R\mu} = \frac{W^1_{R\mu} \mp i W^2_{R\mu}}{\sqrt{2}} \,, \tag{3.40}$$

and

$$Z_\mu = \cos\psi \, W^3_{L\mu} - \sin\psi \, B_\mu \,, \tag{3.41}$$

$$A_\mu = \sin\psi \, W^3_{L\mu} + \cos\psi \, B_\mu \,, \tag{3.42}$$

where again $\sin\psi$ is given in terms of gauge couplings (see (3.14) for the definition of ϕ)

$$\cos\psi = \frac{1}{\sqrt{1+\sin^2\phi}} \,, \qquad \sin\psi = \frac{\sin\phi}{\sqrt{1+\sin^2\phi}} \,. \tag{3.43}$$

It turns out that A_μ is unaffected by EWSB, so that its zero mode $A^{(0)}$ corresponds to the massles photon. On the other hand $W^\pm_{L\mu}$, $W^\pm_{R\mu}$ and Z_μ feel the effects of EWSB, so that the zero modes $W_L^{(0)}$ and $Z^{(0)}$ mix with the KK modes $W_L^{(n)}$, $W_R^{(n)}$ and $Z^{(n)}$, $Z_X^{(n)}$, with corrections appearing first at the level $\mathcal{O}(v^2/M^2)$. We will now analyse this mixing in more detail.

3.3.2 Impact on gauge boson masses and mixings

In the absence of EWSB the gauge boson mass matrices are diagonal with the only non-vanishing entries given by the gauge boson KK masses. Consequently the gauge boson zero modes $W_L^{(0)}$, $Z^{(0)}$, $A^{(0)}$ and $G^{(0)A}$ are exactly massless at this stage, and the several modes do not mix with each other.

After EWSB, however, the mass matrices for charged and neutral weak gauge bosons receive corrections to both their diagonal and off-diagonal entries at order $\mathcal{O}(v^2)$ [88]. Restricting ourselves to the zero modes and first KK level for simplicity[2], these matrices are defined by

$$\left(W_L^{(0)+} \quad W_L^{(1)+} \quad W_R^{(1)+}\right) \mathcal{M}^2_{\text{charged}} \begin{pmatrix} W_L^{(0)-} \\ W_L^{(1)-} \\ W_R^{(1)-} \end{pmatrix} , \tag{3.44}$$

$$\frac{1}{2}\left(Z^{(0)} \quad Z^{(1)} \quad Z_X^{(1)}\right) \mathcal{M}^2_{\text{neutral}} \begin{pmatrix} Z^{(0)} \\ Z^{(1)} \\ Z_X^{(1)} \end{pmatrix} . \tag{3.45}$$

Inserting the Higgs VEV (3.35) into the Higgs kinetic term (3.27), we find

$$\mathcal{M}^2_{\text{charged}} = \begin{pmatrix} \frac{g^2v^2}{4L} & \frac{g^2v^2}{4L}\mathcal{I}_1^+ & -\frac{g^2v^2}{4L}\mathcal{I}_1^- \\ \frac{g^2v^2}{4L}\mathcal{I}_1^+ & M^2_{++} + \frac{g^2v^2}{4L}\mathcal{I}_2^{++} & -\frac{g^2v^2}{4L}\mathcal{I}_2^{-+} \\ -\frac{g^2v^2}{4L}\mathcal{I}_1^- & -\frac{g^2v^2}{4L}\mathcal{I}_2^{-+} & M^2_{--} + \frac{g^2v^2}{4L}\mathcal{I}_2^{--} \end{pmatrix} , \tag{3.46}$$

$$\mathcal{M}^2_{\text{neutral}} = \begin{pmatrix} \frac{g^2v^2}{4L\cos^2\psi} & \frac{g^2v^2\mathcal{I}_1^+}{4L\cos^2\psi} & -\frac{g^2v^2\cos\phi\mathcal{I}_1^-}{4L\cos\psi} \\ \frac{g^2v^2\mathcal{I}_1^+}{4L\cos^2\psi} & M^2_{++} + \frac{g^2v^2\mathcal{I}_2^{++}}{4L\cos^2\psi} & -\frac{g^2v^2\cos\phi\mathcal{I}_2^{-+}}{4L\cos\psi} \\ -\frac{g^2v^2\cos\phi\mathcal{I}_1^+}{4L\cos\psi} & -\frac{g^2v^2\cos\phi\mathcal{I}_2^{-+}}{4L\cos\psi} & M^2_{--} + \frac{g^2v^2\cos^2\phi\mathcal{I}_2^{--}}{4L} \end{pmatrix} , \tag{3.47}$$

[2]The effects of higher KK levels are suppressed by their masses $m_n > M$ $(n > 1)$ and therefore have a subleading phenomenological impact. More explicitly, the results obtained taking into account only the first massive KK level deviates from the exact result at the 10% level [35, 40, 85, 90]. In view of other theoretical uncertainties it is thus well justified to neglect the higher KK modes.

where we defined M_{++} and M_{-+} in (2.30) and (2.33), respectively. The mixing angles ϕ and ψ in the neutral gauge boson sector are given in (3.14) and (3.43), respectively. Finally the gauge boson overlaps $\mathcal{I}_1^{\pm}$ and $\mathcal{I}_2^{ij}$ with the Higgs field are given by

$$\mathcal{I}_1^{+} = g(y=L)\,, \qquad \mathcal{I}_1^{-} = \tilde{g}(y=L)\,, \tag{3.48}$$

$$\mathcal{I}_2^{++} = g(y=L)^2\,, \qquad \mathcal{I}_2^{--} = \tilde{g}(y=L)^2\,, \qquad \mathcal{I}_2^{-+} = g(y=L)\tilde{g}(y=L)\,, \tag{3.49}$$

where we introduced the short-hand notation

$$g(y) = f^{(1)}_{\text{gauge}}(y,(++)) \tag{3.50}$$

for the bulk shape function of $Z^{(1)}$ and $W_L^{(1)}$, as well as for the KK gluons $G^{(1)A}$ and photon $A^{(1)}$, and

$$\tilde{g}(y) = f^{(1)}_{\text{gauge}}(y,(-+)) \tag{3.51}$$

for the bulk shape function of $Z_X^{(1)}$ and $W_R^{(1)}$.

The mass matrices $\mathcal{M}^2_{\text{charged}}$ and $\mathcal{M}^2_{\text{neutral}}$ in (3.46), (3.47) can be diagonalised by means of orthogonal transformations. In order to obtain transparent expressions for mass eigenvalues and mass eigenstates we introduce first the following parameterisation

$$M^2_{++} = M^2 + av^2\,, \qquad M^2_{--} = M^2 - av^2\,, \tag{3.52}$$

$$\mathcal{I}_2^{--} = \mathcal{I}_2\,, \qquad \mathcal{I}_2^{-+} = \mathcal{I}_2\left(1+\delta^{-+}\frac{v^2}{f^2}\right)\,, \qquad \mathcal{I}_2^{++} = \mathcal{I}_2\left(1+\delta^{++}\frac{v^2}{f^2}\right)\,, \tag{3.53}$$

where numerically the parameter $a = \mathcal{O}(1)$ for $f = \mathcal{O}(1\,\text{TeV})$, and the coefficients δ^{ij} turn out to be much smaller than unity.

Further we introduce the function

$$B(\zeta) = \sqrt{16a^2L^2\cos^2\zeta + 8aLg^2\mathcal{I}_2\sin^2\zeta + g^4\mathcal{I}_2^2\cos^2\zeta}\,. \tag{3.54}$$

In order to evaluate tree level contributions to FCNC processes discussed in chapter 4 to the level $\mathcal{O}(v^2/f^2)$, it is sufficient to evaluate $\mathcal{O}(v^2/f^2)$ corrections to the couplings of $W^{\pm}$ and Z but only $\mathcal{O}(1)$ couplings involving heavy gauge boson mass eigenstates. The latter contributions in Feynman diagrams will be suppressed by their large masses in the propagators. It turns out then that to this order in v^2/f^2 the coefficients δ^{-+} and δ^{++} can be set to zero so that only a universal $\mathcal{I}_2$ will enter the expressions below.

The resulting mass eigenstates in the charged gauge boson sector then read

$$W^{\pm} = W_L^{(0)\pm} - \frac{g^2v^2}{4LM^2}\mathcal{I}_1^+ W_L^{(1)\pm} + \frac{g^2v^2}{4LM^2}\mathcal{I}_1^- W_R^{(1)\pm}\,, \tag{3.55}$$

$$W_H^{\pm} = \frac{g^2v^2}{4LM^2}\left(\mathcal{I}_1^+\cos\chi - \mathcal{I}_1^-\sin\chi\right) W_L^{(0)\pm} + \cos\chi W_L^{(1)\pm} + \sin\chi W_R^{(1)\pm}\,, \tag{3.56}$$

$$W'^{\pm} = -\frac{g^2v^2}{4LM^2}\left(\mathcal{I}_1^+\sin\chi + \mathcal{I}_1^-\cos\chi\right) W_L^{(0)\pm} - \sin\chi W_L^{(1)\pm} + \cos\chi W_R^{(1)\pm}\,, \tag{3.57}$$

where the $\mathcal{O}(1)$ mixing between the heavy KK modes $W_L^{(1)}$ and $W_R^{(1)}$ is parameterised by the mixing angle

$$\cos\chi = \sqrt{\frac{1}{2} - \frac{2aL}{B(0)}}\,, \qquad \sin\chi = \sqrt{\frac{1}{2} + \frac{2aL}{B(0)}}\,. \tag{3.58}$$

Note that in the limit of exact P_{LR} symmetry $a \to 0$, so that maximal mixing $\chi = 45°$ between the two KK states appears. As however P_{LR} is violated by the different BCs for $W_L^{(1)}$ and $W_R^{(1)}$ on the UV brane, χ deviates from this limit by roughly 10%.

The masses of $W^{\pm}$, $W_H^{\pm}$ and $W'^{\pm}$ are given by

$$M_W^2 = \frac{g^2v^2}{4L} - \frac{g^4v^4}{16L^2M^2}\left((\mathcal{I}_1^+)^2 + (\mathcal{I}_1^-)^2\right)\,, \tag{3.59}$$

$$M_{W_H}^2 = M^2 + \frac{v^2}{4L}\left(g^2\mathcal{I}_2 - B(0)\right)\,, \tag{3.60}$$

$$M_{W'}^2 = M^2 + \frac{v^2}{4L}\left(g^2\mathcal{I}_2 + B(0)\right)\,. \tag{3.61}$$

Similarly the neutral electroweak gauge bosons in the mass eigenbasis are

$$Z = Z^{(0)} - \frac{g^2v^2\mathcal{I}_1^+}{4LM^2\cos^2\psi}Z^{(1)} + \frac{g^2v^2\mathcal{I}_1^-\cos\phi}{4LM^2\cos\psi}Z_X^{(1)}\,, \tag{3.62}$$

$$Z_H = \frac{g^2v^2}{4LM^2\cos^2\psi}\left(\mathcal{I}_1^+\cos\xi - \cos\phi\cos\psi\,\mathcal{I}_1^-\sin\xi\right) Z^{(0)} + \cos\xi Z^{(1)} + \sin\xi Z_X^{(1)}\,, \tag{3.63}$$

$$Z' = -\frac{g^2v^2}{4LM^2\cos^2\psi}\left(\mathcal{I}_1^+\sin\xi + \cos\phi\cos\psi\,\mathcal{I}_1^-\cos\xi\right) Z^{(0)} - \sin\xi Z^{(1)} + \cos\xi Z_X^{(1)}\,. \tag{3.64}$$

Here the mixing between $Z^{(1)}$ and $Z_X^{(1)}$ is parameterised by the angle ξ, defined

through

$$\cos\xi = \sqrt{\frac{B(\psi)\cos\psi - 4aL\cos^2\psi - \sin^2\psi g^2\mathcal{I}_2}{2B(\psi)\cos\psi}}\,, \tag{3.65}$$

$$\sin\xi = \sqrt{\frac{B(\psi)\cos\psi + 4aL\cos^2\psi + \sin^2\psi g^2\mathcal{I}_2}{2B(\psi)\cos\psi}}\,. \tag{3.66}$$

These expressions deviate from the result obtained in the limit of exact P_{LR} symmetry,

$$\cos\xi = \frac{\cos\phi}{\sqrt{2}}\,, \qquad \sin\xi = \frac{1}{\sqrt{2}\cos\psi}\,, \tag{3.67}$$

again by roughly 10%.

The corresponding masses read

$$M_Z^2 = \frac{g^2v^2}{4L\cos^2\psi} - \frac{g^4v^4}{16L^2M^2\cos^2\psi}\left(\frac{(\mathcal{I}_1^+)^2}{\cos^2\psi} + (\mathcal{I}_1^-)^2\cos^2\phi\right)\,, \tag{3.68}$$

$$M_{Z_H}^2 = M^2 + \frac{v^2}{4L}\left(g^2\mathcal{I}_2 - \frac{B(\psi)}{\cos\phi}\right)\,, \tag{3.69}$$

$$M_{Z'}^2 = M^2 + \frac{v^2}{4L}\left(g^2\mathcal{I}_2 + \frac{B(\psi)}{\cos\phi}\right)\,. \tag{3.70}$$

3.3.3 Comment on the perturbative approach

Throughout this work, we follow the perturbative approach to treat the effects of EWSB, i. e. we first solve the bulk EOMs in the absence of the Higgs VEV, as discussed in detail in section 2.2. The effects of EWSB, due to the presence of the Higgs VEV v, are then treated as a small perturbation of the previously obtained KK mass matrices. Consequently the zero modes corresponding to the broken symmetry receive non-vanishing masses, and $\mathcal{O}(v^2/M^2)$ corrections to the KK masses appear. Furthermore, as the Higgs VEV generates off-diagonal entries in the mass matrices in question, mixing between the various modes appears (see section 3.3.2). We will see in section 4.2 that this mixing leads to flavour non-universalities and consequently tree level FCNCs mediated not only by the heavy gauge KK modes, but also by the Z boson.

The effects of EWSB can in principle also be treated exactly. To this end the Higgs VEV is included already for the derivation and solution of the bulk EOMs, by appropriately modifying the BCs on the IR brane. This implies distortions of the wave functions and shifts in the masses of the zero and KK modes, with respect

to the unbroken case. On the other hand due to the orthogonality of the bulk wave functions, in this approach no mixing between the various modes appears.

While the perturbative approach is more intuitive and therefore most widely used in the literature (see e. g. [40, 88, 89, 91]), in various analyses the exact approach has been exploited [58, 73, 74, 76, 92]. In two recent independent analyses [40, 93] it has been shown explicitly that in fact the perturbative approximation is valid here and the two approaches lead to equivalent results.

3.4 Fermion masses and the flavour structure

3.4.1 Effective 4D Yukawa couplings

In section 3.2.4 we have constructed the most general Yukawa coupling (3.31) consistent with the symmetries and the field content of the custodially protected RS model. For the moment we restrict ourselves to only the fermionic zero modes (u_L^i, d_L^i), u_R^i and d_R^i $(i = 1, 2, 3)$. The impact of taking into account also the fermionic KK modes will briefly be discussed in section 3.4.4. In contrast to the phenomenologically important mixing between gauge boson zero and KK modes discussed in section 3.3.2, it turns out that the effect of KK fermions, albeit of a similar origin, turns out to be a subleading effect and therefore phenomenologically negligible in most cases [35, 37].

At the zero mode level the Yukawa interactions (3.31) result, after EWSB, in non-vanishing masses for the fermionic zero modes $u_{L,R}^i$ and $d_{L,R}^i$ $(i = 1, 2, 3)$. In addition the flavour misalignment between the Yukawa coupling matrices λ^u and λ^d leads to the CKM mixing apparent in charged current interactions.

Inserting the Higgs representation (3.30) and the fermionic KK decomposition into (3.31), performing the (trivial) integral over the extra dimension $0 \leq y \leq L$ and restricting ourselves to the fermion zero modes, we find for the effective 4D Yukawa interactions

$$\begin{aligned}\mathcal{L}_{\text{Yuk}}^{\text{4D}} &= -\frac{h^0}{\sqrt{2}L}\sum_{i,j=1}^{3}\Big[\lambda_{ij}^u f_L^{(0)}(y=L,c_Q^i) f_R^{(0)}(y=L,c_u^j)\,\bar{u}_L^i u_R^j \\ &\qquad\qquad +\lambda_{ij}^d f_L^{(0)}(y=L,c_Q^i) f_R^{(0)}(y=L,c_d^j)\,\bar{d}_L^i d_R^j\Big] + h.c. \\ &\equiv -\frac{h^0}{\sqrt{2}L}\sum_{i,j=1}^{3}\Big[\lambda_{ij}^u f_i^Q f_j^u\,\bar{u}_L^i u_R^j + \lambda_{ij}^d f_i^Q f_j^d\,\bar{d}_L^i d_R^j\Big] + h.c.\,, \end{aligned} \tag{3.71}$$

where we introduced the short hand notation $f_i^{Q,u,d}$ for the relevant fermion shape

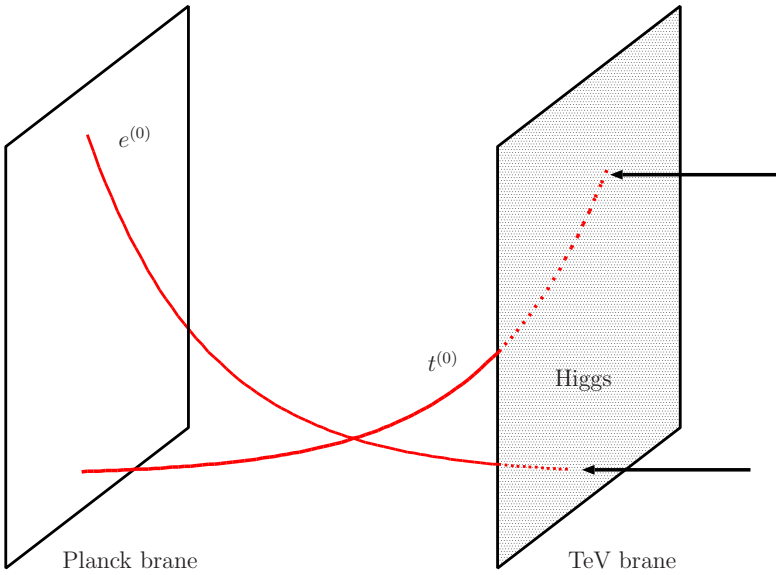

Figure 3.2: *Localisation of fermionic zero modes, leading to exponentially suppressed overlaps with the Higgs field living on the IR brane (figure taken from [87]).*

functions on the IR brane.

The mass matrices for the fermionic zero modes are then given by

$$m^u_{ij} = \frac{v}{\sqrt{2}} Y^u_{ij}\,, \qquad m^d_{ij} = \frac{v}{\sqrt{2}} Y^d_{ij}\,, \tag{3.72}$$

where we introduced the *effective* 4D Yukawa coupling matrices

$$Y^{u,d}_{ij} = \frac{e^{kL}}{L} \lambda^{u,d}_{ij} f^Q_i f^{u,d}_j\,. \tag{3.73}$$

The factor e^{kL} enters when replacing the Higgs field h^0 by its VEV $v_0 = e^{kL} v$.

We observe that the effective 4D Yukawa coupling matrices $Y^{u,d}$ depend on *both* the fundamental 5D Yukawa couplings $\lambda^{u,d}$ *and* on the overlap of the zero mode bulk profiles with the Higgs living on the IR brane, $f^{Q,u,d}$. Consequently even for naturally large 5D Yukawa couplings $\lambda^{u,d} k \sim \mathcal{O}(1)$ it is possible to obtain very hierarchical $Y^{u,d}$ matrices if the fermionic overlaps with the IR brane are very small. In order to illustrate this effect, we sketch in figure 3.2 the fermionic bulk profiles for the top quark and the electron. We observe that while the top quark needs to be localised close to the IR brane, the light quarks and leptons live close to the UV brane and are exponentially suppressed on the IR brane. Consequently their overlap with the Higgs boson in exponentially small.

The fermion mass matrices $m^{u,d}$ in (3.72) have to be diagonalised by means of bi-unitary transformations

$$\mathrm{diag}(m_u, m_c, m_t) = \mathcal{U}_L^\dagger \, m^u \, \mathcal{U}_R \,, \tag{3.74}$$

$$\mathrm{diag}(m_d, m_s, m_b) = \mathcal{D}_L^\dagger \, m^d \, \mathcal{D}_R \,, \tag{3.75}$$

where $\mathcal{U}_{L,R}$ and $\mathcal{D}_{LR}$ are unitary 3×3 matrices parameterising the field transformations in the left- and right-handed up and down sectors, respectively. The misalignment between left-handed up- and down-type quarks is then given by the CKM matrix

$$V_{\mathrm{CKM}} = \mathcal{U}_L^\dagger \mathcal{D}_L \,. \tag{3.76}$$

Note that in contrast to the SM, where only V_{CKM} is physical, in RS models with bulk fermions due to the flavour non-universal gauge couplings all four matrices $\mathcal{U}_{L,R}$, $\mathcal{D}_{LR}$ are physical.

3.4.2 Analogy with the Froggatt-Nielsen scenario

Having a closer look at the effective 4D Yukawa couplings $Y^{u,d}$ in (3.73), we observe [35, 76] that their structure is completely analogous to that analysed by Froggatt and Nielsen (FN) [13] in the context of a spontaneously broken flavour symmetry.

In that pioneering work a global $U(1)_F$ flavour symmetry has been introduced, under which the various quark fields carry different charges while the SM Higgs H is neutral under $U(1)_F$. In order to allow for non-vanishing flavour mixing, the flavour symmetry is spontaneously broken by the VEV of a scalar Φ, the so-called flavon field, that transforms as gauge singlet, but is (singly) charged under $U(1)_F$. In order to obtain small flavour violating effects consistent with observation, the flavon VEV $\langle\Phi\rangle$ has to be much smaller than its mass $m_\Phi \sim \Lambda$. The effective flavour violating parameter is then given by $\epsilon = \langle\Phi\rangle/\Lambda \ll 1$.

The case of bulk fermions in the RS background can in fact be quite easily related to the case of a $U(1)_F$ FN-symmetry [35]. This straight correspondence is summarised in table 3.1. We see that the flavour $U(1)_F$ symmetry corresponds to translations along the extra-dimensional coordinate $0 \leq y \leq L$, under which the metric is self-similar. The Higgs field, living on the IR brane, is external to this self-similarity of the bulk. The fermions, on the other hand, are localised along the extra dimension by means of their bulk mass parameters $c_{Q,u,d}$, i. e. the bulk mass parameters can be interpreted as charges under self-similarity transformations. Self-similarity is broken explicitly by the presence of the IR brane, giving rise to the symmetry breaking parameter $e^{-kL} \ll 1$.

Due to this nice one-to-one correspondence, having at hand the formulae of [13], it is easy to derive analytic expressions for the quark masses and flavour mixing

Froggatt-Nielsen symmetry	bulk fermions in RS
$U(1)_F$ symmetry	self-similarity along y
$U(1)_F$ charges $Q_F = a_i, b_i, d_i$	bulk mass parameters $c^i_{Q,u,d}$
VEV of scalar Φ $(Q_F = 1)$	IR brane at $y = L$
$\epsilon = \langle\Phi\rangle/\Lambda \ll 1$	warp factor e^{-kL}

Table 3.1: *Correspondence between FN symmetry and bulk fermions in RS [35].*

matrices $\mathcal{U}_{L,R}, \mathcal{D}_{L,R}$ in terms of the fundamental flavour parameters of the model. The result can be found in appendix A.2 [35, 76]. These formulae make the dependence on the Yukawa couplings $\lambda^{u,d}$ and in particular their complex phases explicit and consequently improve the formerly used naïve estimates [38, 39] significantly.

3.4.3 Flavour hierarchies and the RS-GIM mechanism

In order to understand the generic hierarchical structure of quark masses $m_i^{u,d}$ and mixing matrices $\mathcal{U}_{L,R}, \mathcal{D}_{L,R}$, we now have a closer look at the estimated results [38, 39] that can be obtained from the expressions in appendix A.2 in the limit of completely anarchic, i. e. structureless, Yukawa couplings $\lambda^{u,d}$. Then the formulae in question simplify to

$$m_i^{u,d} \sim \frac{v}{\sqrt{2}} \frac{e^{kL}}{L} \bar{\lambda}^{u,d} f_i^Q f_i^{u,d}\,, \tag{3.77}$$

where $\bar{\lambda}^{u,d}$ is the average value of the (anarchic) 5D Yukawa couplings, and

$$(\mathcal{U}_L)_{ij}, (\mathcal{D}_L)_{ij} \sim \frac{f_i^Q}{f_j^Q}\,, \qquad (\mathcal{U}_R)_{ij} \sim \frac{f_i^u}{f_j^u}\,, \qquad (\mathcal{D}_R)_{ij} \sim \frac{f_i^d}{f_j^d} \qquad (i < j)\,. \tag{3.78}$$

We observe that the required hierarchical pattern of the quark masses and CKM angles can be explained by the hierarchies [38, 39]

$$f_1^Q \ll f_2^Q \ll f_3^Q\,, \qquad f_1^u \ll f_2^u \ll f_3^u\,, \qquad f_1^d \ll f_2^d \ll f_3^d \tag{3.79}$$

in the fermionic shape functions. In fact this hierarchical pattern can naturally be obtained from $\mathcal{O}(1)$ bulk mass parameters fulfilling

$$c_Q^1 > c_Q^2 > 1/2\,, \qquad c_Q^3 < 1/2\,, \tag{3.80}$$

$$c_u^1 < c_u^2 < -1/2\,, \qquad c_u^3 > -1/2\,, \tag{3.81}$$

$$c_d^1 < c_d^2 < c_d^3 < -1/2\,. \tag{3.82}$$

Here $|c^3_{Q,u}| < 1/2$ is required in order to account for the large top quark mass.

Now it is crucial for the flavour structure of the RS model in question (as well as for all FN-like scenarios) that the hierarchy in the fermionic bulk profiles (3.79) needed to explain the hierarchical quark masses immediately leads to hierarchical flavour mixing matrices $\mathcal{U}_{L,R}, \mathcal{D}_{LR}$, as can be seen from (3.78). As all flavour violating effects are proportional to off-diagonal elements of the flavour mixing matrices in question, we can thus conclude that the strong suppression of fermion masses with respect to the EW scale directly leads to an exponential suppression of all FCNC processes in the model in question. This mechanism is known as the *RS-GIM mechanism* [39] and helps to suppress most flavour observables below their current experimental bounds, see e. g. [35, 36, 39, 74, 85, 94–99]. A problem arises however in the $K^0 - \bar{K}^0$ mixing sector, where for $M \simeq (2-3)$ TeV the generic CP-violating effects are by roughly two orders of magnitude too large [35, 85, 98]. We will study this and other K and B physics constraints on the RS model with custodial protection in detail in chapter 5.

To summarise we have seen that with slight hierarchies in the bulk mass parameters the observed hierarchical pattern in quark masses and mixings can be reproduced without the need for exponentially small parameters. In other words, the origin of the flavour hierarchies in the SM is traced back to the 5D bulk mass parameters. Clearly, while the hierarchies in the flavour sector are thus naturally explained, for a complete interpretation of flavour a theory predicting the actual values of the bulk mass parameters $c_{Q,u,d}$ and also the Yukawa couplings $\lambda^{u,d}$ is still missing.

3.4.4 Impact of fermionic KK modes

Taking into account also the fermionic KK modes originating from all degrees of freedom of the multiplets $\xi^i_{1,2,3}$ and restricting onesself to the first KK excitation, it is straightforward to derive explicit expressions for the mass matrices of $Q_{\rm em} = +5/3$, $Q_{\rm em} = +2/3$ and $Q_{\rm em} = -1/3$ quarks. Those are found to be 9×9, 18×18 and 12×12 matrices, respectively, that have been presented in [40].

Even at tree level these higher KK fermion modes thus affect flavour observables through their mixing with the SM fermions. Depending on the particular structure of the Yukawa interactions, like-charged fermions of any KK level mix with each other. Consequently non-unitarity effects in the 3×3 mixing matrices $\mathcal{U}_{L,R}, \mathcal{D}_{LR}$ are induced. Besides that, the small admixture of higher KK fermion modes to SM fermions modifies their gauge couplings since SM fermions and KK fermion modes couple in general differently to the various gauge boson modes. This is true not only for the heavy KK gauge bosons, but in particular also for the Z boson, as fermions with different weak isospin mix with each other.

Recently it has been claimed [76,99] that the effects of fermionic KK modes are non-negligible and and have an important impact on the results obtained. Therefore we have studied this effect numerically by diagonalising the fermion mass matrices given in [40]. In opposition to [76, 99] but in agreement with most of the existing literature (see e. g. [38] for a naïve analytic estimate) we find that the impact of the fermionic KK modes on FCNC observables constitutes in general a small effect below the 10% level. In view of other uncertainties, such as the neglect of higher KK gauge boson modes, we therefore do not consider these effects any further, but restrict our attention to the fermionic zero mode sector. For further details we refer the reader to [35, 36].

Inspired by these observations, in [37] the effects of the fermionic KK modes have been studied analytically by integrating out the heavy fields and thus reducing the flavour sector to an effective 3×3 structure. In accordance with our results in [35, 36] also this analytic approach showed that the effects of KK fermions on FCNC observables are generally small.

3.5 Parameters of the model

3.5.1 Parameter counting

After presenting in section 3.2 the fundamental 5D action of the custodially protected RS model in question, and analysing in sections 3.3 and 3.4 the gauge and flavour sectors of the model, we now quantify the new parameters present in the theory.

Geometry. In principle the RS1 set-up introduced two geometric parameters, namely the curvature scale k and the length L of the extra dimension. However as we aim to explain the hierarchy between the Planck and the EWSB scale, $e^{kL} \sim \mathcal{O}(10^{16})$ is required. Consequently in order to simplify our phenomenological analysis in chapter 5, we fix $e^{kL} = 10^{16}$ and treat

$$f = ke^{-kL} \tag{3.83}$$

as the only free parameter coming from space-time geometry. This approximation is justified as physical observables depend only weakly on the exact value of kL. We note that recently it has been observed [100] that abandoning the aim to solve the gauge hierarchy problem and allowing $e^{kL} \sim \mathcal{O}(10^3)$ can solve some of the generic problems of RS models and allow for a smaller gauge KK scale in accordance with electroweak precision constraints. On the other hand, the authors of [101] claim that the "ε_K problem" [35, 85, 98] can not be solved in this Little RS scenario.

Gauge sector. As the P_{LR} symmetry relates the gauge couplings of $SU(2)_L$ and $SU(2)_R$ to each other, in spite of the larger gauge group G_{bulk} in (3.1), we have as in the SM three independent gauge couplings

$$g_s\,, \qquad g\,, \qquad g_X\,, \tag{3.84}$$

for $SU(3)_c$, $SU(2)_L \times SU(2)_R$ and $U(1)_X$, respectively.

As already mentioned in section 3.2.1, throughout this work g_s, g and g_X denote the 5D gauge couplings that are not dimensionless. Neglecting the impact of brane kinetic terms, the simple tree level matching condition

$$g^{4D} = \frac{g}{\sqrt{L}} \tag{3.85}$$

relates the fundamental 5D to the effective 4D gauge coupling constants, with analogous relations yielding $g_{s,X}^{\text{4D}}$.

Higgs sector. As in the model in question we have introduced an elementary Higgs boson confined to the IR brane (see section 3.2.3), the Higgs sector is completely analogous to the one of the SM. In particular it is completely described by the two parameters μ and λ entering the Higgs potential.

Thus in summary, outside the flavour sector the custodially protected RS model introduces only one new parameter, namely the new physics scale f in (3.83).

Flavour parameters. In the SM the quark flavour sector is completely determined by the up- and down-quark Yukawa couplings, which can efficiently parameterised by the six quark masses and the three mixing angles and a single complex phase of the CKM matrix.

In the RS model in question the flavour sector is more complicated. In addition to the 3×3 complex 5D Yukawa coupling matrices

$$\lambda^u\,, \qquad \lambda^d \tag{3.86}$$

also the three hermitian 3×3 bulk mass matrices

$$c_Q\,, \qquad c_u\,, \qquad c_d \tag{3.87}$$

are present and constitute new sources of flavour violation.

In order to determine the number of physical parameters in the flavour sector, we make use of the flavour symmetries of the theory [39]. As $\lambda^{u,d}$ are arbitrary

complex matrices, they come along with 9 real parameters and 9 complex phases each. Furthermore the bulk mass matrices $c_{Q,u,d}$ are hermitian, containing each 6 real parameters and three phases. Altogether this counting leads to 36 real parameters and 27 complex phases. Not all of these however are physical and some of them can be eliminated by the flavour symmetry $U(3)^3$ of the 5D theory which exists in the limit of vanishing $\lambda^{u,d}$ and $c_{Q,u,d}$. Note that this flavour symmetry is identical to the one present in the SM, and as in the SM 9 real parameters and 17 phases can be eliminated by making use of this symmetry. One phase cannot be removed as it corresponds to the unbroken $U(1)_B$ baryon number symmetry.

We are then left with 27 real parameters and 10 complex phases to be compared with 9 real parameters and one complex phase in the SM. Evidently the new 18 real parameters and 9 phases come from the three bulk mass matrices c_Q, c_u and c_d.

As the lepton sector has been implemented in a completely analogous manner, see section 3.2.2, the same counting of parameters applies also to the latter sector.

3.5.2 Explicit parameterisation of the RS flavour sector

Finally, in order to allow for an efficient parameter scan of the 5D theory, as described in section 5.2, we derive an explicit parameterisation of the RS flavour sector in terms of physical parameters only which was first presented in [35]. To this end we choose to work in a basis where the bulk mass matrices are real and diagonal,

$$c_{Q,u,d} = \mathrm{diag}(c^1_{Q,u,d}, c^2_{Q,u,d}, c^3_{Q,u,d})\,. \tag{3.88}$$

Note that this can always be achieved by appropriate field redefinitions of $\xi^i_{1,2,3}$. The challenge is now to find a parameterisation of the 5D Yukawa couplings $\lambda^{u,d}$ in this particular basis.

We start by a singular value decomposition of the 5D Yukawa matrices,

$$\lambda^u = \frac{1}{k} e^{i\phi_u} U_u^\dagger D_u V_u\,, \qquad \lambda^d = \frac{1}{k} e^{i\phi_d} U_d D_d V_d\,, \tag{3.89}$$

where the $D_{u,d}$ are real and diagonal, and $U_{u,d}, V_{u,d} \in SU(3)$. The factor $1/k$ has been included in order to make $D_{u,d}$ dimensionless. The singular value decomposed representation contains redundancies which we get rid of in the following.

In order to parameterise the matrices $U_{u,d}, V_{u,d}$ we use the Euler decomposition for $SU(3)$ matrices [102]

$$U(\alpha, a, \gamma, c, \beta, b, \theta, \phi) = e^{i\lambda_3\alpha} e^{i\lambda_2 a} e^{i\lambda_3\gamma} e^{i\lambda_5 c} e^{i\lambda_3\beta} e^{i\lambda_2 b} e^{i\lambda_3\theta} e^{i\lambda_8\phi}\,, \tag{3.90}$$

where λ_i $(i = 1, \ldots, 8)$ are the Gell-Mann matrices. We notice that a, b, c are real mixing angles and $\alpha, \gamma, \beta, \theta, \phi$ are complex phases, with their physical ranges given by $[0, 2\pi)$ and $[0, \pi/2)$, respectively. In the following we work out which of the phases in $U_{u,d}, V_{u,d}$ are indeed physical.

In the basis in which $c_{Q,d,u}$ are diagonal and real we still have the freedom to make the following diagonal rephasing

$$Q_L \to e^{i\lambda_3 \alpha_{U_d}} e^{-i\lambda_8 \phi_{U_u}} Q_L \,, \tag{3.91}$$

$$u_R \to e^{-i\phi_u} e^{-i\lambda_3 \theta_{V_u}} e^{-i\lambda_8 \phi_{V_u}} u_R \,, \tag{3.92}$$

$$d_R \to e^{-i\phi_d} e^{-i\lambda_3 \theta_{V_d}} e^{-i\lambda_8 \phi_{V_d}} d_R \,. \tag{3.93}$$

Furthermore the unitary matrices U, V in a singular value decomposition are defined only up to an internal diagonal rephasing

$$UDV = (Ue^{i\lambda_3 A + i\lambda_8 B}) D (e^{-i\lambda_3 A - i\lambda_8 B} V) = U' D V' \,. \tag{3.94}$$

Using this freedom and an additional rephasing of the quark fields, we find the equivalence

$$\begin{aligned} \lambda^u k &= U_u^\dagger(0, a_{U_u}, \gamma_{U_u}, c_{U_u}, \beta_{U_u}, b_{U_u}, \theta_{U_u}, 0)\, D_u\, V_u(\alpha_{V_u}, a_{V_u}, \gamma_{V_u}, c_{V_u}, \beta_{V_u}, b_{V_u}, 0, 0) \\ &= U_u^\dagger(0, a_{U_u}, \gamma_{U_u} + r, c_{U_u}, \beta_{U_u} - r, b_{U_u}, \theta_{U_u}, r/\sqrt{3})\, D_u \\ &\qquad V_u(\alpha_{V_u}, a_{V_u}, \gamma_{V_u} + r, c_{V_u}, \beta_{V_u} - r, b_{V_u}, 0, r/\sqrt{3}) \,. \end{aligned} \tag{3.95}$$

The entries $r/\sqrt{3}$ can again be rotated to zero due to the freedom to rephase the quark zero modes. Using this invariance parameterised by r allows us to choose $\gamma_{U_u} = 0$. We can now define λ^u and λ^d in terms of physical parameters only

$$\lambda^u k = U_u^\dagger(0, a_{U_u}, 0, c_{U_u}, \beta_{U_u}, b_{U_u}, \theta_{U_u}, 0)\, D_u\, V_u(\alpha_{V_u}, a_{V_u}, \gamma_{V_u}, c_{V_u}, \beta_{V_u}, b_{V_u}, 0, 0) \,, \tag{3.96}$$

$$\lambda^d k = U_d(0, a_{U_d}, \gamma_{U_d}, c_{U_d}, \beta_{U_d}, b_{U_d}, 0, 0)\, D_d\, V_d(\alpha_{V_d}, a_{V_d}, \gamma_{V_d}, c_{V_d}, \beta_{V_d}, b_{V_d}, 0, 0) \,, \tag{3.97}$$

with $D_u = \mathrm{diag}(y_u^1, y_u^2, y_u^3)$ and $D_d = \mathrm{diag}(y_d^1, y_d^2, y_d^3)$. Altogether we thus find 18 real parameters and 10 physical phases contained in the 5D Yukawa couplings. Together with the 9 real parameters contained in the bulk mass matrices $c_{Q,u,d}$, this confirms the counting of section 3.5.1.

4 Implications for flavour physics

4.1 Preliminaries

Having presented in chapter 3 the details of the RS model with custodial protection, we are now prepared to study its impact on flavour physics observables. To this end we first discuss the origin of FCNC processes mediated at the tree level in the model in question. Subsequently we evaluate in sections 4.3 and 4.4 the various new contributions to observables related to $K^0 - \bar{K}^0$ and $B_{d,s} - \bar{B}_{d,s}$ mixings and to rare K and B decays, respectively. A detailed numerical analysis of all these observables follows in chapter 5. Our extensive study of $\Delta F = 2$ and $\Delta F = 1$ observables in the custodially protected RS model has also been published in [35, 36], to which we refer the reader for further details.

4.2 Flavour changing neutral currents at tree level

4.2.1 General structure

In section 2.2.3 we have seen that the bulk profiles of the zero mode fermions are not flat along the fifth dimension, but depend exponentially on the respective bulk mass parameters. This exponential dependence has been used in section 3.4 to naturally generate the observed hierarchies in the SM flavour sector, i. e. to explain the strong hierarchies in the quark masses and CKM mixings without the need for exponentially small parameters.

The different localisations of fermion zero modes leads not only to flavour dependent overlaps with the Higgs field, but also to flavour non-universal couplings to the KK modes of the gauge bosons present in the theory. With the bulk profiles $g(y)$ and $\tilde{g}(y)$ derived in section 2.2.2 (see (3.50), (3.51)), we find that these

couplings depend on the overlap integrals

$$\mathcal{I}^{+}_{L,R}(c_\psi) = \frac{1}{L}\int_0^L dy\, f^{(0)}_{L,R}(y,c_\psi)^2 g(y)\,, \qquad \mathcal{I}^{-}_{L,R}(c_\psi) = \frac{1}{L}\int_0^L dy\, f^{(0)}_{L,R}(y,c_\psi)^2 \tilde{g}(y)\,, \tag{4.1}$$

for a given fermion ψ and for gauge bosons with $(++)$ or $(-+)$ BCs, respectively. Here $\mathcal{I}^{+}_{L,R}(c_\psi)$ enters the couplings of $G^{(1)A}$, $A^{(1)}$ and $Z^{(1)}$, while the $Z^{(1)}_X$ couplings are proportional to $\mathcal{I}^{-}_{L,R}(c_\psi)$. As $g(y)$ and $\tilde{g}(y)$ are only slightly different from each other, due to the different BCs for the respective gauge bosons on the UV brane, it turns out that $\mathcal{I}^{+}_{L,R}(c_\psi)$ and $\mathcal{I}^{-}_{L,R}(c_\psi)$ differ from each other only at the $\mathcal{O}(1\%)$ level. Note that in the flavour eigenbasis the couplings to KK gauge bosons are flavour diagonal but non-universal. As the KK gauge bosons are localised exponentially towards the IR brane, the overlap integrals can be approximated by

$$\mathcal{I}^{\pm}_{L,R}(c_\psi) \sim \sqrt{kL}\, f^{(0)}_{L,R}(y=L,c_\psi)^2\,, \tag{4.2}$$

where the geometric enhancement factor $\sqrt{kL}$ appears due to the numerical value of the gauge KK profile on the IR brane. While this estimate turns out to be very useful to understand the rough size of NP effects, in our numerical analysis in chapter 5 we will of course evaluate the necessary overlap integrals exactly.

When transforming the fermion sector to the mass eigenbasis by means of the unitary transformation matrices $\mathcal{U}_{L,R}, \mathcal{D}_{L,R}$ defined in (3.74), (3.75), we find the couplings of the neutral gauge KK modes to down-type quarks, relevant for K and B physics, to be proportional to

$$\bar{\Delta}^{ij\pm}_L = (\mathcal{D}^\dagger_L)_{ik}\, \mathcal{I}^{\pm}_L(c^k_Q)\, (\mathcal{D}_L)_{kj}\,, \tag{4.3}$$

$$\bar{\Delta}^{ij\pm}_R = (\mathcal{D}^\dagger_R)_{ik}\, \mathcal{I}^{\pm}_R(c^k_d)\, (\mathcal{D}_R)_{kj}\,, \tag{4.4}$$

where summation over $k = 1,2,3$ is understood. Similar expressions hold in the case of up-type quarks. We observe that flavour non-diagonal couplings $i \neq j$ are generated already at the tree level, despite the unitarity of the flavour mixing matrices $\mathcal{D}_{L,R}$. This is a direct consequence of the flavour non-universality of the overlap integrals $\mathcal{I}^{\pm}_{L,R}(c_\psi)$.

It is interesting to consider the size of the flavour violating couplings in question. In section 3.4 we have estimated the off-diagonal elements of $\mathcal{D}_{L,R}$ to be

$$(\mathcal{D}_L)_{ij} \sim \frac{f^Q_i}{f^Q_j}\,, \qquad (\mathcal{D}_R)_{ij} \sim \frac{f^d_i}{f^d_j} \qquad (i<j)\,. \tag{4.5}$$

Together with the approximation in (4.2) we thus find for the size of $\bar{\Delta}^{ij\pm}$:

$$\bar{\Delta}^{ij\pm}_L \sim \sqrt{kL}\, f^Q_i f^Q_j\,, \qquad \bar{\Delta}^{ij\pm}_R \sim \sqrt{kL}\, f^d_i f^d_j\,. \tag{4.6}$$

This structure clearly reminds us of the structure of the effective Yukawa couplings $Y^{u,d}$ in (3.73). In fact the main difference is that the flavour violating gauge couplings are proportional to two fermion shape functions of the same chirality, while in the Yukawa couplings both chiralities are present. As in order to explain the observed quark mass and CKM pattern, hierarchical bulk profiles of both left- and right-handed quarks are required, both $\bar{\Delta}_L^{ij\pm}$ and $\bar{\Delta}_R^{ij\pm}$ turn out to be strongly suppressed, in particular when light quarks are involved in the interaction,

$$\bar{\Delta}_{L,R}^{sd\pm} \ll \bar{\Delta}_{L,R}^{bd\pm} \ll \bar{\Delta}_{L,R}^{bs\pm} \ll 1\,. \tag{4.7}$$

This hierarchical pattern constitutes another explicit manifestation of the RS-GIM mechanism [39] discussed already in section 3.4.3.

While the flavour non-universal interactions of the gauge boson KK modes lead to tree level FCNCs, the zero mode gauge profiles of $G^{(0)A}$, $A^{(0)}$ and $Z^{(0)}$ are flat along the 5D bulk, so that the relevant overlap integrals reduce to the normalisation condition of the fermion zero modes. Consequently the corresponding couplings are flavour universal. As QCD and QED are unaffected by the Higgs VEV, the zero mode gluons and photon are already in their mass eigenbasis. Therefore the unitarity of the mixing matrices $\mathcal{D}_{L,R}$ is effective in this case, and no tree level FCNCs mediated by the SM gluons or photon arise. The case of the Z boson however is different, as here EWSB induces mixing with the heavy KK modes $Z^{(1)}$ and $Z_X^{(1)}$, see section 3.3.

Having collected the basic ingredients, we are now ready to discuss the tree level flavour violating couplings of KK gluons and photons and the electroweak gauge bosons Z, Z_H and Z'. As in our phenomenological analysis we are interested in K and B physics observables, we focus on the tree level flavour violating couplings of down-type quarks, given in (4.3) and (4.4).

4.2.2 KK gluons

Let us start by considering the case of KK gluons, as these turn out to yield important NP contributions to meson-antimeson mixing discussed in section 4.3. As $SU(3)_c$ is unaffected by EWSB, the gluonic KK tower does not receive corrections to their masses. Consequently no mixing between the various modes appears. The flavour violating couplings of the first KK gluon modes can therefore directly be deduced to be

$$G_\mu^{(1)A}\, \bar{d}_{L,R}^i d_{L,R}^j \quad : \qquad -i\gamma_\mu t^A \Delta_{L,R}^{ij}(G^{(1)})\,, \tag{4.8}$$

where t^A are the $SU(3)_c$ generators and we have defined

$$\Delta_{L,R}^{ij}(G^{(1)}) = \frac{g_s}{\sqrt{L}} \bar{\Delta}_{L,R}^{ij+}\,. \tag{4.9}$$

4.2.3 KK photon

The case of the first KK mode of the photon is equally straightforward. Again $A^{(1)}$ is already a mass eigenstate, so that its flavour violating coupling is given by

$$A_\mu^{(1)}\, \bar{d}^i_{L,R} d^j_{L,R} \quad : \qquad -i\gamma_\mu \Delta^{ij}_{L,R}(A^{(1)})\,, \tag{4.10}$$

with

$$\Delta^{ij}_{L,R}(A^{(1)}) = \frac{Q_{\rm em} e}{\sqrt{L}} \bar{\Delta}^{ij+}_{L,R}\,. \tag{4.11}$$

We observe that this coupling is suppressed by the electric charge $Q_{\rm em} = -1/3$ of down-type quarks and by the smallness of the (5D) electromagnetic coupling e with respect to the KK gluon coupling.

4.2.4 Electroweak gauge bosons Z, Z_H and Z'

The derivation of flavour violating couplings of the electroweak gauge bosons Z, Z_H and Z',

$$V_\mu\, \bar{d}^i_{L,R} d^j_{L,R} \quad : \quad -i\gamma_\mu \Delta^{ij}_{L,R}(V) \qquad (V = Z, Z_H, Z')\,, \tag{4.12}$$

is complicated by the fact that these gauge bosons are linear combinations of the gauge eigenstates $Z^{(0)}$, $Z^{(1)}$ and $Z_X^{(1)}$. While the $Z^{(0)}$, being a gauge zero mode, does not contribute to the flavour violating couplings in question, the couplings of $Z^{(1)}$ and $Z_X^{(1)}$, given by

$$\Delta^{ij}_{L,R}(Z^{(1)}) = \frac{g}{\sqrt{L}\cos\psi}\left(T^3_L - Q_{\rm em}\sin^2\psi\right)\bar{\Delta}^{ij+}_{L,R}\,, \tag{4.13}$$

$$\Delta^{ij}_{L,R}(Z^{(1)}_X) = \frac{g}{\sqrt{L}\cos\phi}\left(T^3_R - (T^3_R + Q_X)\sin^2\phi\right)\bar{\Delta}^{ij-}_{L,R}\,, \tag{4.14}$$

are flavour changing and therefore relevant. Here the angles ψ and ϕ have been defined in (3.43) and (3.14), respectively. Further, the required electroweak quantum numbers of $d_{L,R}$ quarks are collected in table 4.1.

In order to determine the flavour violating couplings of the mass eigenstates Z, Z_H and Z', we have to make use of the gauge boson mixing worked out in section 3.3.2. We then obtain

$$\Delta^{ij}_{L,R}(Z) = \frac{M_Z^2}{M^2}\left[-\mathcal{I}_1^+ \Delta^{ij}_{L,R}(Z^{(1)}) + \mathcal{I}_1^- \cos\phi\, \cos\psi \Delta^{ij}_{L,R}(Z_X^{(1)})\right]\,, \tag{4.15}$$

$$\Delta^{ij}_{L,R}(Z_H) = \cos\xi\, \Delta^{ij}_{L,R}(Z^{(1)}) + \sin\xi\, \Delta^{ij}_{L,R}(Z_X^{(1)})\,, \tag{4.16}$$

$$\Delta^{ij}_{L,R}(Z') = -\sin\xi\, \Delta^{ij}_{L,R}(Z^{(1)}) + \cos\xi\, \Delta^{ij}_{L,R}(Z_X^{(1)})\,, \tag{4.17}$$

	T_L^3	T_R^3	Q_X	Q_{em}
d_L	$-1/2$	$-1/2$	$2/3$	$-1/3$
d_R	0	-1	$2/3$	$-1/3$

Table 4.1: *Electroweak quantum numbers of down-type zero modes. $T^3_{L,R}$ are the third component weak isospins of $SU(2)_{L,R}$ and Q_X is the $U(1)_X$ charge. The electric charge is then defined as $Q_{em} = T^3_L + T^3_R + Q_X$.*

where we neglected the KK fermion contributions that turn out to be subleading and therefore irrelevant in all cases [35, 37].

Let us have a look at these couplings in the limit of exact P_{LR} symmetry. In this limit $\mathcal{I}_1^+ = \mathcal{I}_1^- \equiv \mathcal{I}_1$, $\bar{\Delta}^{ij+}_{L,R} = \bar{\Delta}^{ij-}_{L,R} \equiv \bar{\Delta}^{ij}_{L,R}$, and ξ is given by (3.67). Inserting this into (4.15)–(4.17), we find

$$\Delta^{ij}_{L,R}(Z) = \frac{M_Z^2}{M^2}\frac{g}{\sqrt{L}}\,\mathcal{I}_1 \cos\psi \left(T^3_R - T^3_L\right) \bar{\Delta}^{ij}_{L,R}\,, \tag{4.18}$$

$$\Delta^{ij}_{L,R}(Z_H) = \frac{g}{\sqrt{2L}}\left(T^3_L \cos\phi\cos\psi + T^3_R\frac{\cos\phi}{\cos\psi} - Q_X\frac{\sin^2\psi(1+\cos^2\phi)}{\cos\phi\cos\psi}\right)\bar{\Delta}^{ij}_{L,R}\,, \tag{4.19}$$

$$\Delta^{ij}_{L,R}(Z') = \frac{g}{\sqrt{2L}}\left(T^3_R - T^3_L\right)\bar{\Delta}^{ij}_{L,R}\,. \tag{4.20}$$

From (4.18) and (4.20) we can see that in the limit of exact P_{LR} symmetry the flavour violating couplings of Z and Z' both depend on the difference $T^3_R - T^3_L$. Consequently, as already discussed for the Z boson in section 2.3.4, if the fermion in question is an eigenstate of the $P_{L,R}$ symmetry, requiring in particular $T^3_L = T^3_R$, its flavour changing couplings to the Z and Z' bosons are protected and vanish in the limit of unbroken P_{LR} symmetry. As we can see from the fermion representations in (3.16)–(3.18) and more explicitly in table 4.1, this is the case for left-handed down-type quarks d^i_L, but *not* for right-handed down-type quarks d^i_R. Consequently, while the $Z d^i_L \bar{d}^j_L$ and $Z' d^i_L \bar{d}^j_L$ couplings are protected by P_{LR}, the couplings $Z d^i_R \bar{d}^j_R$ and $Z' d^i_R \bar{d}^j_R$ are not. In the case of Z_H we find that the emerging structure is more complicated, see (4.19), and $T^3_{L,R}$ and Q_X would have to satisfy a complicated triple correlation in order to make this coupling vanish. Therefore we deduce that both $Z_H d^i_L \bar{d}^j_L$ and $Z_H d^i_R \bar{d}^j_R$ are not protected by the P_{LR} symmetry.

In order to estimate the efficiency of the P_{LR} symmetry, let us finally have a look by how much the couplings of Z and Z' are suppressed in the case of P_{LR} symmetry broken by BCs on the UV brane. On the one hand we find that $\bar{\Delta}^{ij\pm}_{L,R}$ deviate from each other by roughly 1%, while $\mathcal{I}_1^+ = \mathcal{I}_1^-$ holds at the level $\mathcal{O}(10^{-4})$. Consequently $\Delta^{ij}_L(Z)$ is suppressed by roughly two orders of magnitude with respect to the

unprotected case. On the other hand in the case of Z' the dominant P_{LR} breaking effect appears in the mixing angle ξ that receives corrections at the $\mathcal{O}(10\%)$ level. Therefore the custodial protection mechanism is less effective in that case and $\Delta_L^{ij}(Z')$ turns out to be suppressed by only one order of magnitude. Our numerical analysis in section 5.4.1 confirms these findings.

We note that the above conclusions are not affected by the inclusion of the effects of KK fermions, which has been checked both analytically [37] and numerically [35].

4.2.5 Higgs boson

Finally we consider tree level FCNCs mediated by the Higgs boson. In the SM the Higgs Yukawa coupling matrices are diagonalised simultaneously with the fermion mass matrices, so that in the mass eigenbasis for fermions all Higgs couplings are necessarily flavour conserving. In the so-called zero mode approximation, i. e. when neglecting the fermionic KK modes as done in the present analysis, the situation is completely analogous, so that tree level Higgs FCNCs are absent in this limit.

However the situation changes when the effects of KK fermions are taken into account, as due to the presence of their KK masses, the mass matrices are no longer proportional to the respective Yukawa coupling matrices. Therefore both matrices are no longer diagonalised simultaneously and tree level flavour changing Higgs couplings arise.

While in most other cases the impact of KK fermions has been found to be a sub-leading effect, the case of Higgs FCNC is potentially different as here new $\Delta F = 2$ and $\Delta F = 1$ operator contributions are generated, that can have an important impact on predictions for FCNC observables. The most prominent example are the rare decays $B_{s,d} \to \mu^+\mu^-$ whose branching ratios can receive large enhancements only in the presence of scalar operators. Therefore we now estimate the size of the relevant Higgs vertices by making use of the mass insertion approximation describing the mixing of fermion zero modes with their heavy KK partners [35]. We note that this simple estimate qualitatively agrees both with the explicit analytic derivation [37, 76] and with the exact numerical result [35].

To this end we consider diagrams with one heavy-light transition on a fermion line (denoted by +), see figure 4.1. As the Higgs vertex in that case contains a $P_R = (1+\gamma^5)/2$ projector, while the heavy-light mass insertion comes along with a $P_L = (1-\gamma^5)/2$, the leading contribution from the $1/M$ part of the fermion propagator vanishes, and only the non-leading $\not{p}/M^2$ contribution survives. When acting on the external fermion, the additional $\not{p}/M$ results in the strong chiral suppression m_i^d/M.

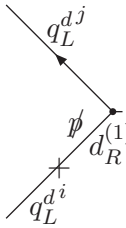

$$\sim \lambda^d_{jk}(\lambda^d)^\dagger_{ki}\,\tfrac{e^{kL}}{kL}\,f_i^Q\,f_j^Q\,\tfrac{v\,m_i^d}{M^2}\ .$$

Figure 4.1: *Leading KK fermion contribution to flavour violating Higgs couplings.*

When considering also diagrams with two mass insertions on the fermion lines, it turns out that for such contributions the chiral suppression is even stronger, so that the above contribution of a single mass insertion is indeed the dominant one [35]. We thus conclude that in the model in question where the Higgs field is confined to the IR brane, Higgs contributions to FCNC processes are strongly chirally suppressed, in addition to the usual RS-GIM suppression, and therefore negligible.

4.3 Meson-antimeson mixing

4.3.1 $\Delta F = 2$ processes in the SM

In the SM particle-antiparticle mixing in the neutral K and $B_{d,s}$ meson systems is governed by box diagrams with virtual $W^\pm$ bosons and up-type quarks running in the loop. The resulting effective Hamiltonian describing $K^0 - \bar{K}^0$ mixing reads

$$\left[\mathcal{H}_{\text{eff}}^{\Delta S=2}\right]_{\text{SM}} = \frac{G_F^2}{16\pi^2}M_W^2\left[\lambda_c^{(K)^2}\eta_1 S_c + \lambda_t^{(K)^2}\eta_2 S_t + 2\lambda_c^{(K)}\lambda_t^{(K)}\eta_3 S_{ct}\right](\bar{s}d)_{V-A}(\bar{s}d)_{V-A}\,, \tag{4.21}$$

where $\lambda_i^{(K)} = V_{is}^* V_{id}$ is the relevant CKM factor, and S_t, S_c and S_{ct} are the one-loop box functions that can be found for instance in [103]. The factors η_i are QCD corrections evaluated at the NLO level in [104–108]. Note that in writing $\left[\mathcal{H}_{\text{eff}}^{\Delta S=2}\right]_{\text{SM}}$ we neglected the poorly known long-distance (LD) contributions arising from virtual intermediate pion states. As the latter are CP-conserving, they influence only the mass difference ΔM_K but not the CP-violating parameter ε_K. Here and in the following we adopt the notations and conventions of [109] in order to allow for an easy comparison with the results obtained in the Littlest Higgs model with T-parity (LHT) [109–111]. An explicit numerical comparison is presented in section 5.5.3.

We stress that in the SM, and also in the LHT model, only a single operator

$$(\bar{s}d)_{V-A}(\bar{s}d)_{V-A} = [\bar{s}\gamma_\mu(1-\gamma_5)d]\otimes[\bar{s}\gamma^\mu(1-\gamma_5)d] \tag{4.22}$$

contributes to $K^0 - \bar{K}^0$ mixing. In the next section we will see that this situation changes drastically in the presence of the new RS tree level contributions.

The SM contribution to the off-diagonal mixing amplitude M_{12}^K is then obtained as

$$\left(M_{12}^K\right)_{\rm SM} = \frac{G_F^2}{12\pi^2} F_K^2 \hat{B}_K m_K M_W^2 \left[\lambda_c^{(K)*2} \eta_1 S_c + \lambda_t^{(K)*2} \eta_2 S_t + 2\lambda_c^{(K)*} \lambda_t^{(K)*} \eta_3 S_{ct}\right] . \tag{4.23}$$

All relevant numerical input parameters are collected in table 5.2.

The SM contribution to $B_{d,s} - \bar{B}_{d,s}$ mixings can be found in a completely analogous manner. It reads

$$(M_{12}^q)_{\rm SM} = \frac{G_F^2}{12\pi^2} F_{B_q}^2 \hat{B}_{B_q} m_{B_q} M_W^2 \left[\left(\lambda_t^{(q)*}\right)^2 \eta_B S_t\right] \qquad (q = d, s) , \tag{4.24}$$

where both charm quark and LD contributions are negligible in this case.

4.3.2 RS tree level contributions

The new tree level contributions to meson-antimeson mixing arising in the presence of RS KK modes have been considered at numerous places in the literature [39, 74, 85, 94–97]. The first complete analysis of these effects, including also the effects of electroweak gauge bosons and performing the full renormalisation group analysis at next-to-leading order has been presented by us in [35], on which the subsequent presentation is based. In order to allow for a transparent notation, we concentrate here on the case of $K^0 - \bar{K}^0$ mixing. The respective formulae relevant for $B_{d,s} - \bar{B}_{d,s}$ mixings can then straightforwardly be obtained by properly adjusting all flavour indices.

The new RS tree level contributions from the exchange of KK gluons, Z_H and Z' gauge bosons and the KK photon lead to the effective new Hamiltonian

$$\begin{aligned}\left[\mathcal{H}_{\rm eff}^{\Delta S=2}\right]_{\rm KK} = \frac{1}{4M^2} \big[&C_1^{VLL}(M)\mathcal{Q}_1^{VLL} + C_1^{VRR}(M)\mathcal{Q}_1^{VRR} \\ &+ C_1^{LR}(M)\mathcal{Q}_1^{LR} + C_2^{LR}(M)\mathcal{Q}_2^{LR}\big] ,\end{aligned} \tag{4.25}$$

with the Wilson coefficients evaluated at a scale $\mu = \mathcal{O}(M)$. Here we work in the operator basis used in [112] which is defined as

$$\mathcal{Q}_1^{VLL} = (\bar{s}\gamma_\mu P_L d)\,(\bar{s}\gamma^\mu P_L d) , \tag{4.26}$$

$$\mathcal{Q}_1^{VRR} = (\bar{s}\gamma_\mu P_R d)\,(\bar{s}\gamma^\mu P_R d) , \tag{4.27}$$

$$\mathcal{Q}_1^{LR} = (\bar{s}\gamma_\mu P_L d)\,(\bar{s}\gamma^\mu P_R d) , \tag{4.28}$$

$$\mathcal{Q}_2^{LR} = (\bar{s} P_L d)\,(\bar{s} P_R d) , \tag{4.29}$$

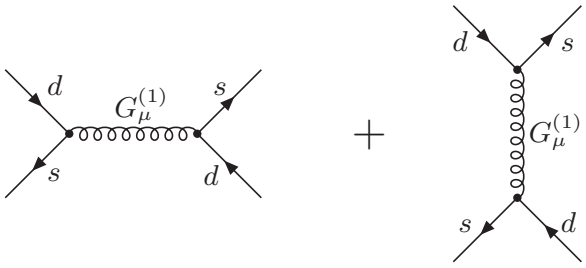

Figure 4.2: *Tree level contribution of KK gluons to $K^0 - \bar{K}^0$ mixing. Similar diagrams contribute to $B_{d,s} - \bar{B}_{d,s}$ mixings.*

with $P_{R,L} = (1 \pm \gamma^5)/2$ being the chirality projectors. The Wilson coefficients are then given by the sums of the various contributions

$$C_i(M) = C_i(M)^G + C_i(M)^{Z_H,Z'} + C_i(M)^A \,, \tag{4.30}$$

with the various contributions discussed in what follows. The case of $B_{d,s} - \bar{B}_{d,s}$ is completely analogous.

We have seen that due to the mixing between the various gauge boson modes, also the tree level Z couplings become flavour violating. Naïvely one might now think that these couplings yield the dominant contribution to $\Delta F = 2$ processes, as the Z propagator is not suppressed by the KK mass $1/M^2$. However we have found in section 4.2 that the flavour violating Z vertex is suppressed by an additional factor M_Z^2/M^2 with respect to the KK gauge boson vertices. Consequently, as a $\Delta F = 2$ Feynman diagram contains two such vertices, the Z contributions are suppressed with respect to the KK gauge contributions by an additional factor M_Z^2/M^2. In addition the left-handed Z couplings are further suppressed thanks to the custodial protection mechanism. Consequently the Z boson contributions to meson-antimeson mixing in the custodially protected RS model are negligible with respect to the dominant KK contributions. Explicit expressions for the Z contributions to the Wilson coefficients in question have been derived in [35]. Z contributions to $\Delta F = 2$ processes in the model without protection have also been considered in [74].

KK gluon contributions. We start by evaluating the tree level contributions of the KK gluons, that have been assumed to yield the dominant effect in most of the existing literature, see e. g. [39, 85, 101]. To this end we consider the Feynman diagrams shown in figure 4.2. Using the flavour violating KK gluon couplings derived in section 4.2, see (4.9), we find for the contribution of the first gluonic

KK mode to the $\Delta S = 2$ effective Hamiltonian

$$\begin{aligned}\left[\mathcal{H}_{\text{eff}}^{\Delta S=2}\right]^G = \frac{1}{2M^2}\Big[&\left(\Delta_L^{sd}(G^{(1)})\right)^2 (\bar{s}_L\gamma_\mu t^a d_L)\,(\bar{s}_L\gamma^\mu t^a d_L)\\ &+ \left(\Delta_R^{sd}(G^{(1)})\right)^2 (\bar{s}_R\gamma_\mu t^a d_R)\,(\bar{s}_R\gamma^\mu t^a d_R)\\ &+ 2\Delta_L^{sd}(G^{(1)})\Delta_R^{sd}(G^{(1)})\,(\bar{s}_L\gamma_\mu t^a d_L)\,(\bar{s}_R\gamma^\mu t^a d_R)\Big]\,. \quad (4.31)\end{aligned}$$

This Hamiltonian has to be translated to the operator basis (4.26)–(4.29) with the help of appropriate Fierz transformations. A straightforward calculation yields

$$C_1^{VLL}(M)^G = \frac{2}{3}\left(\Delta_L^{sd}(G^{(1)})\right)^2\,, \quad (4.32)$$

$$C_1^{VRR}(M)^G = \frac{2}{3}\left(\Delta_R^{sd}(G^{(1)})\right)^2\,, \quad (4.33)$$

$$C_1^{LR}(M)^G = -\frac{2}{3}\Delta_L^{sd}(G^{(1)})\Delta_R^{sd}(G^{(1)})\,, \quad (4.34)$$

$$C_2^{LR}(M)^G = -4\Delta_L^{sd}(G^{(1)})\Delta_R^{sd}(G^{(1)})\,. \quad (4.35)$$

***Z_H* and *Z'* contributions.** We now turn to the contributions of the heavy electroweak gauge bosons Z_H and Z' to $K^0 - \bar{K}^0$ mixing. As to leading order their masses are equal, $M_{Z_H} = M_{Z'} = M$, it is most straightforward to consider their contributions simultaneously. To this end we have to evaluate diagrams similar to those shown in figure 4.2, but with Z_H and Z' being exchanged. Making then use of the relation

$$\cos^2\xi + \sin^2\xi = 1\,, \quad (4.36)$$

the explicit dependence of ξ drops out of the formulae in question, and we can write the result in terms of $\Delta_{L,R}^{sd}(Z^{(1)})$ and $\Delta_{L,R}^{sd}(Z_X^{(1)})$ defined in (4.13), (4.14). We have

$$\begin{aligned}C_1^{VLL}(M)^{Z_H,Z'} &= 2\left[\left(\Delta_L^{sd}(Z^{(1)})\right)^2 + \left(\Delta_L^{sd}(Z_X^{(1)})\right)^2\right]\,,\\ C_1^{VRR}(M)^{Z_H,Z'} &= 2\left[\left(\Delta_R^{sd}(Z^{(1)})\right)^2 + \left(\Delta_R^{sd}(Z_X^{(1)})\right)^2\right]\,,\\ C_1^{LR}(M)^{Z_H,Z'} &= 4\left[\Delta_L^{sd}(Z^{(1)})\Delta_R^{sd}(Z^{(1)}) + \Delta_L^{sd}(Z_X^{(1)})\Delta_R^{sd}(Z_X^{(1)})\right]\,,\\ C_2^{LR}(M)^{Z_H,Z'} &= 0\,. \quad (4.37)\end{aligned}$$

We note that the calculation of the relevant Feynman diagrams in this case leads directly to an effective Hamiltonian in the basis (4.26)–(4.29), without the necessity of Fierz transformations. Consequently, in contrast to the case of KK gluon exchanges, no contribution to the Wilson coefficient $C_2^{LR}(M)$ is generated. This result has important implications for the interplay of various contributions in $K^0 - \bar{K}^0$ and $B_{d,s} - \bar{B}_{d,s}$ mixings, analysed in detail in section 5.3.1.

KK photon contributions. Evaluating finally the contributions of the KK photon to the $\Delta S = 2$ effective Hamiltonian, we find

$$C_1^{VLL}(M)^A = 2\left[\Delta_L^{sd}(A^{(1)})\right]^2 , \tag{4.38}$$

$$C_1^{VRR}(M)^A = 2\left[\Delta_R^{sd}(A^{(1)})\right]^2 , \tag{4.39}$$

$$C_1^{LR}(M)^A = 4\Delta_L^{sd}(A^{(1)})\Delta_R^{sd}(A^{(1)}) , \tag{4.40}$$

$$C_2^{LR}(M)^A = 0 , \tag{4.41}$$

where $\Delta_{L,R}^{ij}(A^{(1)})$ has been defined in (4.11). Also in this case we observe that no contribution to $C_2^{LR}(M)$ is generated.

Combination of contributions. Having determined the various KK contributions to $K^0 - \bar{K}^0$ mixing, we can now combine them by means of (4.30). Analogous results hold in the case of $B_d - \bar{B}_d$ and $B_s - \bar{B}_s$ mixings, where in all formulae "sd" has to be replaced by "bd" and "bs", respectively.

In order to estimate the size of EW contributions when compared to the KK gluon exchanges we add the various KK contributions and evaluate the respective couplings. This leads to

$$C_1^{VLL}(M) = (0.67 + 0.02 + 0.56)\frac{g_s^2}{L}(\bar{\Delta}_L^{ij})^2 = 1.25\frac{g_s^2}{L}(\bar{\Delta}_L^{ij})^2 , \tag{4.42}$$

$$C_1^{VRR}(M) = (0.67 + 0.02 + 0.98)\frac{g_s^2}{L}(\bar{\Delta}_R^{ij})^2 = 1.67\frac{g_s^2}{L}(\bar{\Delta}_R^{ij})^2 , \tag{4.43}$$

$$C_1^{LR}(M) = (-0.67 + 0.04 + 1.13)\frac{g_s^2}{L}\bar{\Delta}_L^{ij}\bar{\Delta}_R^{ij} = 0.50\frac{g_s^2}{L}\bar{\Delta}_L^{ij}\bar{\Delta}_R^{ij} , \tag{4.44}$$

$$C_2^{LR}(M) = (-4 + 0 + 0)\frac{g_s^2}{L}\bar{\Delta}_L^{ij}\bar{\Delta}_R^{ij} = -4\frac{g_s^2}{L}\bar{\Delta}_L^{ij}\bar{\Delta}_R^{ij} , \tag{4.45}$$

where the three contributions correspond to KK gluon, KK photon and combined Z_H and Z' exchanges respectively. In order to obtain these expressions, we have neglected the small difference between $\bar{\Delta}_{L,R}^{ij+}$ and $\bar{\Delta}_{L,R}^{ij-}$, and the running of the electroweak gauge couplings between the electroweak scale M_Z and the KK scale M. As already mentioned, the Wilson coefficient $C_2^{LR}(M)$ receives only KK gluon contributions at the scale $\mu = \mathcal{O}(M)$.

We observe that the electroweak contributions are dominated by Z_H and Z' exchanges[1] and in the case of C_1^{VLL}, C_1^{VRR} and C_1^{LR} amount to $+87\%$, $+150\%$ and -175% corrections to the KK gluon contribution. In particular the sign of $C_1^{LR}(M)$ is reversed. On the other hand the $A^{(1)}$ contributions turn out to be negligible in all cases, being suppressed by the small electromagnetic coupling and the electric

[1] In fact, due to the custodial protection of $Z' d_L^i \bar{d}_L^j$ couplings it is the Z_H that dominates.

charge of down-type quarks. We conclude that the electroweak gauge boson contributions to the Wilson coefficients C_1^{VLL}, C_1^{VRR} and C_1^{LR} at $\mu = M$ are of the same order as the KK gluon contributions and have to be taken into account. At first sight this finding may seem surprising. One should remember however that KK gluon contributions similarly to electroweak contributions are suppressed by their large masses M and the main difference between these contributions results from gauge couplings, colour factors and weak charges. Our analysis shows that with the exception of $C_2^{LR}(M)$ all these effects conspire to make the electorweak heavy gauge boson contributions to be as important as the KK gluon contributions in the effective $\Delta F = 2$ Hamiltonian.

4.3.3 Renormalisation group evolution

Having calculated the effective $\Delta F = 2$ Hamiltonian at the KK scale $\mu = M$, we now have to perform its renormalisation group evolution down to a low energy scale μ_0, where the relevant hadronic matrix elements can be evaluated with the help of lattice QCD.

As the SM operator $(\bar{s}d)_{V-A}\,(\bar{s}d)_{V-A}$ does not mix with the other $\Delta F = 2$ operators present in $\mathcal{H}_{\text{eff}}^{\Delta S=2}$, we can perform the renormalisation group running separately for the SM effective Hamiltonian $[\mathcal{H}_{\text{eff}}^{\Delta S=2}]_{\text{SM}}$ and the KK contribution $[\mathcal{H}_{\text{eff}}^{\Delta S=2}]_{\text{KK}}$. The same statement applies of course to the case of $B_{d,s} - \bar{B}_{d,s}$ mixing.

Performing then the renormalisation group evolution for $[\mathcal{H}_{\text{eff}}^{\Delta S=2}]_{\text{KK}}$, one finds that $\mathcal{Q}_1^{VLL}$ and $\mathcal{Q}_1^{VRR}$ renormalise without mixing with other operators and that their evolution is the same as QCD is a non-chiral theory. On the other hand $\mathcal{Q}_1^{LR}$ and $\mathcal{Q}_2^{LR}$ mix under renormalisation so that the RG evolution operator is a 2×2 matrix. The outcome of this analysis is an effective Hamiltonian relevant at the low energy scale μ_0

$$\begin{aligned}\left[\mathcal{H}_{\text{eff}}^{\Delta S=2}\right]_{\text{KK}} = \frac{1}{4M^2}\,\big[&C_1^{VLL}(\mu_0)\mathcal{Q}_1^{VLL} + C_1^{VRR}(\mu_0)\mathcal{Q}_1^{VRR} \\ &+ C_1^{LR}(\mu_0)\mathcal{Q}_1^{LR} + C_2^{LR}(\mu_0)\mathcal{Q}_2^{LR}\big]\,,\end{aligned} \tag{4.46}$$

with analogous expressions for the $\Delta B = 2$ Hamiltonians.

In order to determine then the new KK contribution to the off-diagonal mixing amplitude M_{12}^K,

$$2m_K\left(M_{12}^K\right)_{\text{KK}}^{*} = \langle \bar{K}^0|\left[\mathcal{H}_{\text{eff}}^{\Delta S=2}\right]_{\text{KK}}|K^0\rangle\,, \tag{4.47}$$

one has to evaluate the hadronic matrix elements

$$\langle \bar{K}^0|\mathcal{Q}_i(\mu)|K^0\rangle \equiv \langle \mathcal{Q}_i(\mu)\rangle\,, \tag{4.48}$$

	μ_0	B_1	B_4	B_5
$K^0 - \bar{K}^0$	2.0 GeV	0.57	0.81	0.56
$B_{d,s} - \bar{B}_{d,s}$	4.6 GeV	0.87	1.15	1.73

Table 4.2: *Values of the parameters B_i in the $\overline{MS}$-NDR scheme obtained in [113] ($K^0 - \bar{K}^0$) and [114] ($B_{d,s} - \bar{B}_{d,s}$). The scale μ_0 at which the Wilson coefficients C_i are evaluated is given in the second column.*

which are conveniently parameterised as follows:

$$\langle \mathcal{Q}_1^{VLL}(\mu)\rangle = \langle \mathcal{Q}_1^{VRR}(\mu)\rangle = \frac{2}{3} m_K^2 F_K^2 B_1^{VLL}(\mu)\,, \tag{4.49}$$

$$\langle \mathcal{Q}_1^{LR}(\mu)\rangle = -\frac{1}{3} R^K(\mu) m_K^2 F_K^2 B_1^{LR}(\mu)\,, \tag{4.50}$$

$$\langle \mathcal{Q}_2^{LR}(\mu)\rangle = \frac{1}{2} R^K(\mu) m_K^2 F_K^2 B_2^{LR}(\mu)\,. \tag{4.51}$$

Here the non-perturbative parameters B_i can be determined on the lattice. They are related to the parameters B_1, B_5 and B_4 calculated in [113, 114] as follows

$$B_1^{VLL}(\mu) \equiv B_1\,, \quad B_1^{LR}(\mu) \equiv B_5\,, \quad B_2^{LR}(\mu) \equiv B_4\,, \tag{4.52}$$

and their numerical values are given in Table 4.2. It should be stressed that $B_i(\mu)$ are not renormalisation group invariant parameters in contrast to $\hat{B}_K$ in (4.23). However having at hand the results of [112–114] it is easier to use them in this way.

Finally the matrix elements of the left-right operators $\mathcal{Q}_{1,2}^{LR}$ receive the chiral enhancement factor

$$R^K(\mu) = \left(\frac{m_K}{m_s(\mu) + m_d(\mu)}\right)^2\,, \tag{4.53}$$

which yields an $\mathcal{O}(20)$ enhancement of the $\mathcal{Q}_{1,2}^{LR}$ contributions with respect to $\mathcal{Q}_1^{VLL}, \mathcal{Q}_1^{VRR}$. Additionally $\mathcal{Q}_2^{LR}$ is also strongly enhanced by the effects of renormalisation group running.

Collecting all these results we can determine the new tree level contributions to the off-diagonal element M_{12}^K. We find ($\mu_L = 2\,\text{GeV}$)

$$\begin{aligned}\left(M_{12}^K\right)_{\text{KK}} = \frac{m_K F_K^2}{12 M^2}\Big[&\left(C_1^{VLL}(\mu_L) + C_1^{VRR}(\mu_L)\right) B_1^K \\ &- \frac{1}{2} R^K(\mu_L) C_1^{LR}(\mu_L) B_5^K + \frac{3}{4} R^K(\mu_L) C_2^{LR}(\mu_L) B_4^K\Big]^*\,. \end{aligned} \tag{4.54}$$

In the case of $B_{d,s} - \bar{B}_{d,s}$ mixings, a completely analogous calculation yields ($q = d, s$)

$$(M_{12}^q)_{\rm KK} = \frac{m_{B_q} F_{B_q}^2}{12 M^2} \Big[\left(C_1^{VLL}(\mu_b) + C_1^{VRR}(\mu_b)\right) B_1^q - \frac{1}{2} R^q(\mu_b) C_1^{LR}(\mu_b) B_5^q + \frac{3}{4} R^q(\mu_b) C_2^{LR}(\mu_b) B_4^q \Big]^* , \quad (4.55)$$

where the hadronic matrix elements are evaluated at the scale $\mu_b = 4.6\,\text{GeV}$.

We note that in the latter case the chiral enhancement of the left-right-operators is much less effective,

$$R^q(\mu) = \left(\frac{m_{B_q}}{m_b(\mu) + m_q(\mu)} \right)^2 \sim \mathcal{O}(1) \,. \quad (4.56)$$

We would like to caution the reader that in (4.54) and (4.55) we omitted explicit flavour indices K, q for the Wilson coefficients C_i, although they differ from each other as different Δ^{ij} are involved. In addition the scales μ_L and μ_b are different from each other.

The values for B_i in the $\overline{\rm MS}$-NDR scheme that we will use in our analysis have been extracted from [113] and [114] for the $K^0 - \bar{K}^0$ system and $B_{s,d}^0 - \bar{B}_{s,d}^0$ system, respectively. They are collected in Table 4.2, together with the relevant values of μ_0.

The final results for M_{12}^i in the custodially protected RS model are then given by

$$M_{12}^i = (M_{12}^i)_{\rm SM} + (M_{12}^i)_{\rm KK} \qquad (i = K, d, s) \,, \quad (4.57)$$

with $(M_{12}^i)_{\rm SM}$ given in (4.23), (4.24), and $(M_{12}^i)_{\rm KK}$ in (4.54), (4.55).

4.3.4 Observables in the $\Delta F = 2$ sector

The physics of particle-antiparticle mixing in the neutral K and $B_{d,s}$ meson systems is completely described by the off-diagonal mixing elements

$$M_{12}^i - \frac{i}{2}\Gamma_{12}^i \qquad (i = K, d, s) \,, \quad (4.58)$$

where the dispersive part M_{12}^i has been evaluated above, and the absorptive part Γ_{12}^i in unaffected by the new RS contributions. Note that in the case of $B_{d,s} - \bar{B}_{d,s}$ mixings $\Gamma_{12} \ll M_{12}$. Phenomenological observables related to meson-antimeson mixing thus depend on $|M_{12}^i|$ and $\arg(M_{12}^i)$, and in certain cases also Γ_{12}^i.

Below we collect all formulae for $\Delta F = 2$ observables that we use in our numerical analysis. We would like to emphasise that, although physical observables are phase convention independent, some of the formulae collected in this section depend on the phase convention chosen for the CKM matrix and yield correct results only if the standard phase convention is consistently used.

Let us start with the $K^0 - \bar{K}^0$ system. The mass splitting between the two eigenstates K_L and K_S is given by

$$\Delta M_K = 2\left[\mathrm{Re}\left(M_{12}^K\right)_{\mathrm{SM}} + \mathrm{Re}\left(M_{12}^K\right)_{\mathrm{KK}}\right] \tag{4.59}$$

and is a CP-conserving observable. Unfortunately the SM contribution is subject to considerable theoretical uncertainties, stemming from poorly known long-distance dynamics. The CP-violating parameter

$$\varepsilon_K = \frac{\kappa_\varepsilon e^{i\varphi_\varepsilon}}{\sqrt{2}(\Delta M_K)_{\mathrm{exp}}}\left[\mathrm{Im}\left(M_{12}^K\right)_{\mathrm{SM}} + \mathrm{Im}\left(M_{12}^K\right)_{\mathrm{KK}}\right], \tag{4.60}$$

extracted from $K \to \pi\pi$ decays, is theoretically much cleaner and consequently provides stringent constraints on the NP flavour structure [56]. Here $\varphi_\varepsilon = (43.51 \pm 0.05)^\circ$ and $\kappa_\varepsilon = 0.92 \pm 0.02$ [53] takes into account that $\varphi_\varepsilon \neq \pi/4$ and includes an additional effect from the imaginary part of the 0-isospin amplitude in $K \to \pi\pi$.

In the $B_{d,s}^0 - \bar{B}_{d,s}^0$ systems it is useful to define the parameterisation [115]

$$M_{12}^q = (M_{12}^q)_{\mathrm{SM}} + (M_{12}^q)_{\mathrm{KK}} = (M_{12}^q)_{\mathrm{SM}}\, C_{B_q} e^{2i\varphi_{B_q}}, \tag{4.61}$$

where

$$\left(M_{12}^d\right)_{\mathrm{SM}} = \left|\left(M_{12}^d\right)_{\mathrm{SM}}\right| e^{2i\beta}, \qquad \beta = -\arg(V_{td}) \simeq 22^\circ, \tag{4.62}$$

$$(M_{12}^s)_{\mathrm{SM}} = |(M_{12}^s)_{\mathrm{SM}}|\, e^{2i\beta_s}, \qquad \beta_s = -\arg(-V_{ts}) \simeq -1^\circ. \tag{4.63}$$

For the mass differences in the $B_{d,s}^0 - \bar{B}_{d,s}^0$ systems we then have

$$\Delta M_q = 2\,|(M_{12}^q)_{\mathrm{SM}} + (M_{12}^q)_{\mathrm{KK}}| = (\Delta M_q)_{\mathrm{SM}} C_{B_q} \qquad (q = d, s). \tag{4.64}$$

The CP-violating phases of M_{12}^q can be determined by measuring the time dependent CP-asymmetries in $B_d \to \psi K_S$ and $B_s \to \psi\phi$ decays, respectively. As these decays are tree-dominated in the SM and therefore free from direct CP-violation also in the presence of new KK contributions, they serve as a theoretically clean probe of CP-violation in $B_d - \bar{B}_d$ and $B_s - \bar{B}_s$ mixings, respectively. From the data one can then extract the coefficients

$$S_{\psi K_S} = \sin(2\beta + 2\varphi_{B_d}), \tag{4.65}$$

$$S_{\psi\phi} = \sin(2|\beta_s| - 2\varphi_{B_s}) \tag{4.66}$$

of $\sin(\Delta M_d t)$ and $\sin(\Delta M_s t)$ in the time dependent CP-asymmetries in question. In the presence of non-vanishing φ_{B_d} and φ_{B_s} these two asymmetries do not measure β and β_s but $(\beta + \varphi_{B_d})$ and $(|\beta_s| - \varphi_{B_s})$, respectively.

The last quantities we will consider in this section are the width differences $\Delta\Gamma_s$ and the semileptonic CP-asymmetry $A^s_{\rm SL}$, related to $B_s - \bar{B}_s$ mixing, and defined respectively as

$$\Delta\Gamma_s = \Gamma^s_L - \Gamma^s_H \,, \tag{4.67}$$

$$A^s_{\rm SL} = \frac{\Gamma(\bar{B}_s \to \ell^+ X) - \Gamma(B_s \to \ell^- X)}{\Gamma(\bar{B}_s \to \ell^+ X) + \Gamma(B_s \to \ell^- X)} \,. \tag{4.68}$$

Width difference and semileptonic CP-asymmetry are obtained by diagonalising the 2×2 Hamiltonian which describes the $B_s - \bar{B}_s$ system. Neglecting terms of $\mathcal{O}(m_b^4/m_t^4)$, they can simply be written as

$$\Delta\Gamma_s = -\Delta M_s \, {\rm Re}\left(\frac{\Gamma^s_{12}}{M^s_{12}}\right) , \qquad A^s_{\rm SL} = {\rm Im}\left(\frac{\Gamma^s_{12}}{M^s_{12}}\right) . \tag{4.69}$$

Theoretical predictions of both $\Delta\Gamma_s$ and $A^s_{\rm SL}$ thus require the calculation of the off-diagonal matrix element Γ^s_{12}, subject to non-perturbative QCD effects. Important theoretical improvements have been achieved thanks to advances in lattice studies of $\Delta B = 2$ four-fermion operators [114] and to the NLO perturbative calculations of the corresponding Wilson coefficients [116, 117]. In our numerical analysis we will use [116]

$${\rm Re}\left(\frac{\Gamma^s_{12}}{M^s_{12}}\right)^{\rm SM} = -(2.6 \pm 1.0) \cdot 10^{-3} \,, \qquad {\rm Im}\left(\frac{\Gamma^s_{12}}{M^s_{12}}\right)^{\rm SM} = (2.6 \pm 0.5) \cdot 10^{-5} \,. \tag{4.70}$$

In the presence of new CP-violating phases beyond the CKM one we can then write

$$\frac{\Delta\Gamma_s}{\Gamma_s} = -\left(\frac{\Delta M_s}{\Gamma_s}\right)^{\rm exp} \left[{\rm Re}\left(\frac{\Gamma^s_{12}}{M^s_{12}}\right)^{\rm SM} \frac{\cos 2\varphi_{B_s}}{C_{B_s}} - {\rm Im}\left(\frac{\Gamma^s_{12}}{M^s_{12}}\right)^{\rm SM} \frac{\sin 2\varphi_{B_s}}{C_{B_s}} \right] , \tag{4.71}$$

$$A^s_{\rm SL} = {\rm Im}\left(\frac{\Gamma^s_{12}}{M^s_{12}}\right)^{\rm SM} \frac{\cos 2\varphi_{B_s}}{C_{B_s}} - {\rm Re}\left(\frac{\Gamma^s_{12}}{M^s_{12}}\right)^{\rm SM} \frac{\sin 2\varphi_{B_s}}{C_{B_s}} \,. \tag{4.72}$$

It is important to note that with ${\rm Re}(\Gamma^s_{12}/M^s_{12}) \gg {\rm Im}(\Gamma^s_{12}/M^s_{12})$, even a small φ_{B_s} can induce an order of magnitude enhancement of $A^s_{\rm SL}$ relative to the SM. Simultaneously a non-vanishing φ_{B_s} would result in a suppression of $\Delta\Gamma_s/\Gamma_s$

Finally, we recall the correlation between $A^s_{\rm SL}$ and $S_{\psi\phi}$ [118, 119]

$$A^s_{\rm SL} = -\frac{|\Delta\Gamma_s|}{\Delta M_s} \frac{S_{\psi\phi}}{\sqrt{1 - S^2_{\psi\phi}}} \,, \tag{4.73}$$

where we assumed $(\Delta\Gamma_s)_{\rm SM} > 0$. A similar expression has been pointed out earlier in [120, 121]. As this correlation is valid in any NP model in which Γ_{12}^s is not affected by NP contributions and the $B_s \to \psi\phi$ decays are free from direct CP-violation, we will see below that the correlation in question also exists in the RS model considered here. It has been observed also in the LHT model analysed in [109, 111, 122].

4.4 Rare K and B decays

4.4.1 General remarks

Having derived analytic expressions for the most important $\Delta F = 2$ observables in the custodially protected RS model, we now analyse the new tree level contributions to rare K and B decays in this model. While partial studies of the new RS effects on rare decay branching ratios have been presented in [39, 94, 96], a first complete analysis of these effects in the custodially protected RS model has been given by us in [36]. The following discussion of the new RS effects in $K \to \pi\nu\bar{\nu}$, $B \to X_{d,s}\nu\bar{\nu}$, $K_L \to \pi^0\ell^+\ell^-$ ($\ell = e, \mu$), $K_L \to \mu^+\mu^-$ and $B_{d,s} \to \mu^+\mu^-$ is based on the latter publication. Throughout this section, we use the notations and conventions of the corresponding analysis performed in the LHT model [122, 123].

4.4.2 The $K \to \pi\nu\bar{\nu}$ system

The $K \to \pi\nu\bar{\nu}$ decays, being theoretically very clean and extremely suppressed in the SM, are known to be one of the best probes of NP in the flavour sector. Recent reviews of these decays both in and beyond the SM can be found in [124, 125], here we just quote for completeness the presently available SM predictions, obtained at the NNLO level,

$$Br(K_L \to \pi^0\nu\bar{\nu})_{\rm SM} = (2.76 \pm 0.40) \cdot 10^{-11} \qquad [126, 127] \tag{4.74}$$

and

$$Br(K^+ \to \pi^+\nu\bar{\nu})_{\rm SM} = (8.5 \pm 0.7) \cdot 10^{-11} \qquad [128]\,. \tag{4.75}$$

Unfortunately the $K \to \pi\nu\bar{\nu}$ decays are experimentally very challenging, so that for $Br(K_L \to \pi^0\nu\bar{\nu})$ only an upper bound [129]

$$Br(K_L \to \pi^0\nu\bar{\nu})_{\rm exp} < 6.7 \cdot 10^{-8} \qquad (90\%\,\text{C.L.}) \tag{4.76}$$

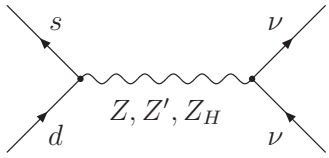

Figure 4.3: *Tree level contributions of Z, Z' and Z_H to the $s \to d\nu\bar{\nu}$ effective Hamiltonian.*

is available, while the present measurement of $Br(K^+ \to \pi^+\nu\bar{\nu})$ [130]

$$Br(K^+ \to \pi^+\nu\bar{\nu})_{\text{exp}} = (17.3^{+11.5}_{-10.5}) \cdot 10^{-11} \tag{4.77}$$

is still plagued by large uncertainties.

While a significant deviation of any of these branching ratios on its own from the respective SM prediction would already be a spectacular sign of NP, it is even more interesting to study both decays simultaneously. In [131] we have pointed out that the stringent two-branch correlation observed e. g. in the LHT model [122, 123] and in the minimal 3-3-1 model [132] provides a clean test of the universality of CP-violating phases in $K^0 - \bar{K}^0$ mixing and the $K \to \pi\nu\bar{\nu}$ system. In fact one of the most common reasons for the absence of such correlation is the presence of the new $\mathcal{Q}_i^{LR}$ operators contributing to the $\Delta S = 2$ effective Hamiltonian.

In order to calculate the $K \to \pi\nu\bar{\nu}$ branching ratios we have to consider the effective Hamiltonian $[\mathcal{H}_{\text{eff}}^{\nu\bar{\nu}}]^K$ governing the $s \to d\nu\bar{\nu}$ transition. In the SM it is given as follows

$$[\mathcal{H}_{\text{eff}}^{\nu\bar{\nu}}]^K_{\text{SM}} = g^2_{\text{SM}} \sum_{\ell=e,\mu,\tau} \left[\lambda_c^{(K)} X^{\ell}_{\text{NNL}}(x_c) + \lambda_t^{(K)} X(x_t)\right] (\bar{s}d)_{V-A} (\bar{\nu}_\ell \nu_\ell)_{V-A} + h.c.\,, \tag{4.78}$$

where $x_i = m_i^2/M_W^2$, $\lambda_i^{(K)} = V_{is}^* V_{id}$ and V_{ij} are the elements of the CKM matrix. $X^{\ell}_{\text{NNL}}(x_c)$ and $X(x_t)$ comprise internal charm and top quark contributions, respectively. They are known to high accuracy including NNLO QCD corrections [126, 127, 133]. For convenience we have introduced the effective coupling

$$g^2_{\text{SM}} = \frac{G_F}{\sqrt{2}} \frac{\alpha}{2\pi \sin^2\theta_W}\,. \tag{4.79}$$

In the custodially protected RS model the couplings of the Z boson and the new heavy modes Z_H and Z' are flavour violating already at the tree level, see section 4.2. Consequently new contributions to $[\mathcal{H}_{\text{eff}}^{\nu\bar{\nu}}]^K$ mediated by these gauge bosons exist, shown by the diagram in figure 4.3. On the other hand the KK gluons and photon cannot contribute to the effective Hamiltonian in question, as

they do not couple to neutrinos. Evaluating then the diagram in figure 4.3 we find the new contributions to $[\mathcal{H}_{\rm eff}^{\nu\bar{\nu}}]^K$ with $i = Z, Z_H, Z'$

$$[\mathcal{H}_{\rm eff}^{\nu\bar{\nu}}]_i^K = \frac{\Delta_L^{\nu\nu}(i)}{M_i^2}\left[\Delta_L^{sd}(i)(\bar{s}_L\gamma^\mu d_L) + \Delta_R^{sd}(i)(\bar{s}_R\gamma^\mu d_R)\right](\bar{\nu}_L\gamma_\mu\nu_L) + h.c.\,. \tag{4.80}$$

The flavour violating couplings $\Delta_{L,R}^{sd}(Z)$, $\Delta_{L,R}^{sd}(Z_H)$ and $\Delta_{L,R}^{sd}(Z')$ have been calculated in section 4.2. The flavour conserving neutrino couplings $\Delta_L^{\nu\nu}(Z)$, $\Delta_L^{\nu\nu}(Z_H)$ and $\Delta_L^{\nu\nu}(Z')$ are collected in appendix A.3. Note that $\Delta_R^{\nu\nu}(i) \equiv 0$, as the right-handed neutrinos are introduced as pure gauge singlets.

Combining then the new contributions of Z, Z_H and Z' in (4.80) with the SM contribution in (4.78),

$$[\mathcal{H}_{\rm eff}^{\nu\bar{\nu}}]^K = [\mathcal{H}_{\rm eff}^{\nu\bar{\nu}}]_{\rm SM}^K + [\mathcal{H}_{\rm eff}^{\nu\bar{\nu}}]_Z^K + [\mathcal{H}_{\rm eff}^{\nu\bar{\nu}}]_{Z_H}^K + [\mathcal{H}_{\rm eff}^{\nu\bar{\nu}}]_{Z'}^K\,, \tag{4.81}$$

we find for the total effective Hamiltonian mediating the $s \to d\nu\bar{\nu}$ transition

$$\begin{aligned}[\mathcal{H}_{\rm eff}^{\nu\bar{\nu}}]^K = g_{\rm SM}^2 \sum_{\ell=e,\mu,\tau}\Big[\lambda_c^{(K)}X_{\rm NNL}^\ell(x_c) + \lambda_t^{(K)}X_K^{V-A}\Big](\bar{s}d)_{V-A}(\bar{\nu}_\ell\nu_\ell)_{V-A} \\ + g_{\rm SM}^2 \sum_{\ell=e,\mu,\tau}\Big[\lambda_t^{(K)}X_K^V\Big](\bar{s}d)_V(\bar{\nu}_\ell\nu_\ell)_{V-A} + h.c.\,.\end{aligned} \tag{4.82}$$

In order to allow for a transparent presentation of our analytic results we have introduced the functions

$$X_K^{V-A} = X(x_t) + \sum_{i=Z,Z_H,Z'}(X_i^K)^{V-A}\,, \tag{4.83}$$

$$X_K^V = \sum_{i=Z,Z_H,Z'}(X_i^K)^V\,. \tag{4.84}$$

This structure generalises the one encountered in the LHT model, where due to the specific operator structure of that model only the function X_K^{V-A} was present [123]. The various contributions $i = Z, Z_H, Z'$ are given by

$$(X_i^K)^{V-A} = \frac{1}{\lambda_t^{(K)}}\frac{\Delta_L^{\nu\nu}(i)}{4M_i^2 g_{\rm SM}^2}\left[\Delta_L^{sd}(i) - \Delta_R^{sd}(i)\right]\,, \tag{4.85}$$

$$(X_i^K)^V = \frac{1}{\lambda_t^{(K)}}\frac{\Delta_L^{\nu\nu}(i)}{2M_i^2 g_{\rm SM}^2}\Delta_R^{sd}(Z)\,. \tag{4.86}$$

Note that, as we have seen in section 3.3, to leading order in v^2/M^2 the masses of Z_H and Z' are equal,

$$M_{Z_H} = M_{Z'} = M\,. \tag{4.87}$$

Having at hand the effective Hamiltonian for $s \to d\nu\bar{\nu}$ transitions (4.82) it is now straightforward to obtain explicit expressions for the branching ratios $Br(K^+ \to \pi^+\nu\bar{\nu})$ and $Br(K_L \to \pi^0\nu\bar{\nu})$.

We observe that while in the SM only a single operator $(\bar{s}d)_{V-A}(\bar{\nu}\nu)_{V-A}$ is present, in the RS model in question also the operator $(\bar{s}d)_V(\bar{\nu}\nu)_{V-A}$ contributes. This is a direct consequence of both the $\Delta_L^{sd}(i)$ and $\Delta_R^{sd}(i)$ couplings being non-zero. Indeed in section 5.4.1 we will see that in most cases $\Delta_R^{sd}(Z)$ yields the dominant contribution.

Therefore both matrix elements $\langle\pi|(\bar{s}d)_{V-A}|K\rangle$ and $\langle\pi|(\bar{s}d)_V|K\rangle$ have to be evaluated. Fortunately, as both K and π are pseudoscalar mesons, only the vector current part contributes and we simply have

$$\langle\pi|(\bar{s}d)_{V-A}|K\rangle = \langle\pi|(\bar{s}d)_V|K\rangle \,. \tag{4.88}$$

This means that effectively, as in the LHT model, the NP contributions can be collected in a single function that generalises the SM one $X(x_t)$. Denoting this function by

$$X_K \equiv X_K^{V-A} + X_K^V \equiv |X_K| e^{i\,\theta_X^K} \,, \tag{4.89}$$

we can make use of the formulae of Section 3.3 in [123] to analyse the impact of new contributions on the branching ratios for $K^+ \to \pi^+\nu\bar{\nu}$ and $K_L \to \pi^0\nu\bar{\nu}$. The expressions for the branching ratios in question then read

$$Br(K^+ \to \pi^+\nu\bar{\nu}) = \kappa_+ \Big[\tilde{r}^2 A^4 R_t^2 |X_K|^2 + 2\tilde{r}\bar{P}_c(x) A^2 R_t |X_K| \cos\beta_X^K + \bar{P}_c(x)^2\Big], \tag{4.90}$$

$$Br(K_L \to \pi^0\nu\bar{\nu}) = \kappa_L \tilde{r}^2 A^4 R_t^2 |X_K|^2 \sin^2\beta_X^K \,, \tag{4.91}$$

where [126–128, 134],

$$\kappa_+ = (5.36 \pm 0.03)\cdot 10^{-11} \,, \qquad \kappa_L = (2.31 \pm 0.01)\cdot 10^{-10} \,, \tag{4.92}$$

$$\bar{P}_c(x) = \left(1 - \frac{\lambda^2}{2}\right)(0.42 \pm 0.05) \,, \tag{4.93}$$

$$\tilde{r} = \left|\frac{V_{ts}}{V_{cb}}\right| \,, \qquad A = \frac{|V_{cd}V_{cb}^*|}{\lambda^3} \,, \qquad R_t = \left|\frac{V_{td}V_{tb}^*}{V_{cd}V_{cb}^*}\right| \,, \tag{4.94}$$

with $P_c(x)$ including both the NNLO corrections [126–128] and long-distance contributions [135]. Finally we have defined

$$\beta_X^K = \beta - \beta_s - \theta_X^K \,. \tag{4.95}$$

Note that, in contrast to the real function $X(x_t)$, the new function X_K is complex implying new CP-violating effects that can be best tested in the correlation between the two $K \to \pi\nu\bar{\nu}$ modes.

4.4.3 $B \to X_s \nu\bar{\nu}$ and $B \to X_d \nu\bar{\nu}$

Having at hand the effective Hamiltonian (4.82) governing $s \to d\nu\bar{\nu}$ transitions, it is straightforward to generalise it to the case of $b \to q\nu\bar{\nu}$ ($q = d, s$). To this end we only have to properly adjust all flavour indices. In addition the charm quark contributions can safely be neglected in this case, being suppressed by $m_c \ll m_t$ and the relevant CKM factors. The effective Hamiltonian for $b \to q\nu\bar{\nu}$ is then given as follows:

$$[\mathcal{H}_{\rm eff}^{\nu\bar{\nu}}]^{B_q} = g_{\rm SM}^2 \sum_{\ell=e,\mu,\tau} \left[\lambda_t^{(q)} X_q^{V-A}\right] (\bar{b}q)_{V-A} (\bar{\nu}_\ell \nu_\ell)_{V-A} + g_{\rm SM}^2 \sum_{\ell=e,\mu,\tau} \left[\lambda_t^{(q)} X_q^{V}\right] (\bar{b}q)_{V} (\bar{\nu}_\ell \nu_\ell)_{V-A} + h.c.\,, \tag{4.96}$$

with

$$X_q^{V-A} = X(x_t) + \sum_{i=Z,Z_H,Z'} (X_i^q)^{V-A}\,, \tag{4.97}$$

$$X_q^{V} = \sum_{i=Z,Z_H,Z'} (X_i^q)^{V} \tag{4.98}$$

and ($i = Z, Z_H, Z'$)

$$(X_i^q)^{V-A} = \frac{1}{\lambda_t^{(q)}} \frac{\Delta_L^{\nu\nu}(i)}{4M_i^2 g_{\rm SM}^2} \left[\Delta_L^{bq}(i) - \Delta_R^{bq}(i)\right]\,, \tag{4.99}$$

$$(X_i^q)^{V} = \frac{1}{\lambda_t^{(q)}} \frac{\Delta_L^{\nu\nu}(i)}{2M_i^2 g_{\rm SM}^2} \Delta_R^{bq}(i)\,. \tag{4.100}$$

Again all relevant $\Delta_{L,R}^{bq}(i)$ can be found in section 4.2.

The effective Hamiltonian for $b \to q\nu\bar{\nu}$ governs exclusive decays like $B \to K\nu\bar{\nu}$ and $B \to K^*\nu\bar{\nu}$ and the inclusive modes $B \to X_{s,d}\nu\bar{\nu}$. A recent model-independent study [136] showed that a combined analysis of all these channels can provide important information on the NP operator structure. Unfortunately however the decays in question are experimentally challenging. In addition our analysis in [36] revealed that the NP effects in the exclusive modes $B \to K\nu\bar{\nu}$ and $B \to K^*\nu\bar{\nu}$ are small within the custodially protected RS model. Therefore in the present work we focus only on the inclusive modes $B \to X_{s,d}\nu\bar{\nu}$.

From the effective Hamiltonian we can easily derive the expressions for $Br(B \to X_{s,d}\nu\bar{\nu})$. As in the inclusive modes $B \to X_{s,d}\nu\bar{\nu}$ there is no interference between left- and right-handed contributions, the formulae of [123] generalise to

$$\frac{Br(B \to X_q \nu\bar{\nu})}{Br(B \to X_q \nu\bar{\nu})_{\rm SM}} = \frac{\left|X_q^{V-A} + \frac{X_q^V}{2}\right|^2 + \left|\frac{X_q^V}{2}\right|^2}{X(x_t)^2} \qquad (q = d, s)\,. \tag{4.101}$$

In the SM and models with Constrained Minimal Flavour Violation (CMFV) [11, 12,121], in which all flavour violation is governed by the CKM matrix and only SM operators are relevant, the decays $K \to \pi\nu\bar{\nu}$ and $B \to X_{s,d}\nu\bar{\nu}$ are governed by a single real and flavour universal function X. In the custodially protected RS model on the other hand the functions $X^{V-A,V}_{K,d,s}$ depend on the quark flavours involved, through the flavour indices in the $\Delta^{ij}_{L,R}$ $(i,j = s,d,b)$ couplings and through the $1/\lambda_t^{(q)}$ $(q = K,d,s)$ factor in front of the new RS contributions. These factors introduce also new sources of CP-violation, so that $X^{V-A,V}_{K,d,s}$ are generally complex in the model in question. Consequently the universality of NP effects in $K \to \pi\nu\bar{\nu}$ and $B \to X_{s,d}\nu\bar{\nu}$ can be badly violated in the model in question, being a clear sign of physics beyond the CMFV hypothesis. We will elaborate more on this issue in section 5.5.2.

4.4.4 The $K_L \to \pi^0\ell^+\ell^-$ decays

We now turn our attention to rare decays with charged leptons in the final state, starting with the $K_L \to \pi^0\ell^+\ell^-$ decays which are dominated by CP-violating contributions. In the SM the main contribution comes from the indirect (mixing-induced) CP-violation and its interference with the directly CP-violating contribution [137–139]. Both direct CP-violation alone and the CP-conserving contribution are suppressed by roughly one order of magnitude. As the dominant indirectly CP-violating contributions are practically determined by the measured decays $K_S \to \pi^0\ell^+\ell^-$ and the parameter ε_K, the decays in question belong to the theoretically cleanest rare K decays, although they cannot compete with the $K \to \pi\nu\bar{\nu}$ ones in this aspect. In addition they are not as sensitive to new directly CP-violating contributions, that are very clearly exposed in the $K_L \to \pi^0\nu\bar{\nu}$ decay. Still as pointed out in [140], in the presence of large new CP-violating phases the direct CP-violating contribution can become the dominant contribution and the branching ratios for $K_L \to \pi^0\ell^+\ell^-$ can be enhanced by a factor of $2-3$ with the effect being stronger in the case of $K_L \to \pi^0\mu^+\mu^-$ [139]. In addition the correlation between the two branching ratios in question can provide important information on the operator structure of the NP flavour sector [139, 141, 142].

First of all we recall that in the SM neglecting QCD corrections the top quark contribution to the effective Hamiltonian governing $s \to d\ell^+\ell^-$ transitions reads

$$\begin{aligned}\left[\mathcal{H}^{\ell\bar{\ell}}_{\rm eff}\right]^K_{\rm SM} = &-g^2_{\rm SM}\left[\lambda_t^{(K)}Y(x_t)\right](\bar{s}d)_{V-A}(\bar{\ell}\ell)_{V-A}\\ &+4g^2_{\rm SM}\sin^2\theta_W\left[\lambda_t^{(K)}Z(x_t)\right](\bar{s}d)_{V-A}(\bar{\ell}\ell)_V + h.c.\,. \qquad (4.102)\end{aligned}$$

Here $Y(x_t)$ and $Z(x_t)$ are one-loop functions, analogous to $X(x_t)$, that result from various penguin and box diagrams. The charm contributions and QCD corrections

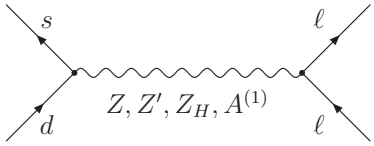

Figure 4.4: *Tree level contributions of Z, Z_H, Z' and $A^{(1)}$ to the $s \to d\ell^+\ell^-$ effective Hamiltonian.*

are irrelevant for the discussion presented below and will be included only in the numerical analysis later on. We also remark that in principle also dipole operators could be included here, but that in K decays, as discussed in [143], they can be fully neglected due to their suppression by m_s. Finally, the operator basis chosen in (4.102) differs from the one used to study QCD corrections [143] but is very suitable for the discussion of modifications of the functions $Y(x_t)$ and $Z(x_t)$ due to NP contributions which we will consider next.

Similarly to $[\mathcal{H}_{\rm eff}^{\nu\bar{\nu}}]^K$ in (4.82) also $\left[\mathcal{H}_{\rm eff}^{\ell\bar{\ell}}\right]^K$ receives tree level contributions of the gauge bosons Z, Z_H and Z', and as now charged leptons appear in the final state, also the KK photon $A^{(1)}$ contributes. The relevant Feynman diagrams are shown in figure 4.4. We note that the flavour violating $\bar{s}d$ vertices are the same as already encountered in the case of $s \to d\nu\bar{\nu}$ transitions. The leptonic couplings of Z, Z_H, Z' and $A^{(1)}$ can be found in appendix A.3.

The evaluation of the diagrams in figure 4.4 gives then ($i = Z, Z_H, Z', A^{(1)}$)

$$\begin{aligned}\left[\mathcal{H}_{\rm eff}^{\ell\bar{\ell}}\right]_i^K = \frac{1}{M_i^2}&\left[\Delta_L^{bs}(i)(\bar{s}_L\gamma^\mu d_L) + \Delta_R^{bs}(i)(\bar{s}_R\gamma^\mu d_R)\right]\\ &\cdot\left[\Delta_L^{\ell\ell}(i)(\bar{\ell}_L\gamma_\mu\ell_L) + \Delta_R^{\ell\ell}(i)(\bar{\ell}_R\gamma_\mu\ell_R)\right] + h.c.\,,\end{aligned} \tag{4.103}$$

which contains additional operators relative to (4.102). Also in this case to the desired $\mathcal{O}(v^2/M^2)$ level of accuracy

$$M_{Z_H} = M_{Z'} = M_{A^{(1)}} = M\,. \tag{4.104}$$

Again, as in the case of $s \to d\nu\bar{\nu}$, the complete effective Hamiltonian governing $s \to d\ell^+\ell^-$ transitions is given by the sum of the various contributions,

$$\left[\mathcal{H}_{\rm eff}^{\ell\bar{\ell}}\right]^K = \left[\mathcal{H}_{\rm eff}^{\ell\bar{\ell}}\right]_{\rm SM}^K + \left[\mathcal{H}_{\rm eff}^{\ell\bar{\ell}}\right]_Z^K + \left[\mathcal{H}_{\rm eff}^{\ell\bar{\ell}}\right]_{Z_H}^K + \left[\mathcal{H}_{\rm eff}^{\ell\bar{\ell}}\right]_{Z'}^K + \left[\mathcal{H}_{\rm eff}^{\ell\bar{\ell}}\right]_{A^{(1)}}^K\,. \tag{4.105}$$

Defining then the functions $Y_K^{V-A,V}$ and $Z_K^{V-A,V}$ through

$$Y_K^{V-A} = Y(x_t) + \sum_{i=Z,Z_H,Z',A^{(1)}} (Y_i^K)^{V-A}\,, \tag{4.106}$$

$$Z_K^{V-A} = Z(x_t) + \sum_{i=Z,Z_H,Z',A^{(1)}} (Z_i^K)^{V-A}\,, \tag{4.107}$$

$$Y_K^{V} = \sum_{i=Z,Z_H,Z',A^{(1)}} (Y_i^K)^{V}\,, \tag{4.108}$$

$$Z_K^{V} = \sum_{i=Z,Z_H,Z',A^{(1)}} (Z_i^K)^{V}\,, \tag{4.109}$$

with the contributions of the various gauge bosons ($i = Z, Z_H, Z', A^{(1)}$) given by

$$(Y_i^K)^{V-A} = -\frac{1}{\lambda_t^{(K)}}\frac{\left[\Delta_L^{\ell\ell}(i) - \Delta_R^{\ell\ell}(i)\right]}{4M_i^2 g_{\rm SM}^2}\left[\Delta_L^{sd}(Z) - \Delta_R^{sd}(i)\right]\,, \tag{4.110}$$

$$(Z_i^K)^{V-A} = \frac{1}{\lambda_t^{(K)}}\frac{\Delta_R^{\ell\ell}(i)}{8M_i^2 g_{\rm SM}^2\sin^2\theta_W}\left[\Delta_L^{sd}(i) - \Delta_R^{sd}(i)\right]\,, \tag{4.111}$$

$$(Y_i^K)^{V} = -\frac{1}{\lambda_t^{(K)}}\frac{\left[\Delta_L^{\ell\ell}(i) - \Delta_R^{\ell\ell}(i)\right]}{2M_i^2 g_{\rm SM}^2}\Delta_R^{sd}(i)\,, \tag{4.112}$$

$$(Z_i^K)^{V} = \frac{1}{\lambda_t^{(K)}}\frac{\Delta_R^{\ell\ell}(i)}{4M_i^2 g_{\rm SM}^2\sin^2\theta_W}\Delta_R^{sd}(i)\,, \tag{4.113}$$

we finally find for the effective Hamiltonian governing $s \to d\ell^+\ell^-$ transitions

$$\begin{aligned}\left[\mathcal{H}_{\rm eff}^{\ell\bar\ell}\right]^K = &-g_{\rm SM}^2\left[\lambda_t^{(K)}Y_K^{V-A}\right](\bar s d)_{V-A}(\bar\ell\ell)_{V-A}\\ &+4g_{\rm SM}^2\sin^2\theta_W\left[\lambda_t^{(K)}Z_K^{V-A}\right](\bar s d)_{V-A}(\bar\ell\ell)_{V}\\ &-g_{\rm SM}^2\left[\lambda_t^{(K)}Y_K^{V}\right](\bar s d)_{V}(\bar\ell\ell)_{V-A}\\ &+4g_{\rm SM}^2\sin^2\theta_W\left[\lambda_t^{(K)}Z_K^{V}\right](\bar s d)_{V}(\bar\ell\ell)_{V} + h.c.\,.\end{aligned} \tag{4.114}$$

From (4.114) one can now easily obtain the branching ratios for the $K_L \to \pi^0\ell^+\ell^-$ decays. As in the case of $K \to \pi\nu\bar\nu$ also here the relation (4.88) for the matrix elements in question holds. Consequently the formulae valid in the LHT model [123] are valid also here, when we define

$$Y_K = Y_K^{V-A} + Y_K^V \equiv |Y_K|e^{i\theta_Y^K}\,, \tag{4.115}$$

$$Z_K = Z_K^{V-A} + Z_K^V \equiv |Z_K|e^{i\theta_Z^K}\,. \tag{4.116}$$

One then finds (see [138, 139, 141–143] for a derivation of these formulae)

$$Br(K_L \to \pi^0 \ell^+ \ell^-) = \left(C^\ell_{\rm dir} \pm C^\ell_{\rm int} \, |a_s| + C^\ell_{\rm mix} \, |a_s|^2 + C^\ell_{\rm CPC}\right) \cdot 10^{-12} \,, \qquad (4.117)$$

where

$$C^e_{\rm dir} = (4.62 \pm 0.24)(\omega_{7V}^2 + \omega_{7A}^2) \,, \qquad C^\mu_{\rm dir} = (1.09 \pm 0.06)(\omega_{7V}^2 + 2.32\omega_{7A}^2) \,, \qquad (4.118)$$

$$C^e_{\rm int} = (11.3 \pm 0.3)\omega_{7V} \,, \qquad C^\mu_{\rm int} = (2.63 \pm 0.06)\omega_{7V} \,, \qquad (4.119)$$

$$C^e_{\rm mix} = 14.5 \pm 0.05 \,, \qquad C^\mu_{\rm mix} = 3.38 \pm 0.20 \,, \qquad (4.120)$$

$$C^e_{\rm CPC} \simeq 0 \,, \qquad C^\mu_{\rm CPC} = 5.2 \pm 1.6 \,, \qquad (4.121)$$

$$|a_s| = 1.2 \pm 0.2 \qquad (4.122)$$

with

$$\omega_{7V} = \frac{1}{2\pi} \left[P_0 + \frac{|Y_K|}{\sin^2\theta_W} \frac{\sin\beta^K_Y}{\sin(\beta - \beta_s)} - 4|Z_K| \frac{\sin\beta^K_Z}{\sin(\beta - \beta_s)} \right] \left[\frac{{\rm Im}\,\lambda_t^{(K)}}{1.4 \cdot 10^{-4}} \right] , \qquad (4.123)$$

$$\omega_{7A} = -\frac{1}{2\pi} \frac{|Y_K|}{\sin^2\theta_W} \frac{\sin\beta^K_Y}{\sin(\beta - \beta_s)} \left[\frac{{\rm Im}\,\lambda_t^{(K)}}{1.4 \cdot 10^{-4}} \right] . \qquad (4.124)$$

Here $P_0 = 2.88 \pm 0.06$ [143] includes NLO QCD corrections and

$$\beta^K_Y = \beta - \beta_s - \theta^K_Y \,, \qquad \beta^K_Z = \beta - \beta_s - \theta^K_Z \qquad (4.125)$$

with θ^K_Y, θ^K_Z defined in (4.115), (4.116), respectively.

The effect of the NP contributions is mainly felt in ω_{7A}, as the corresponding contributions in ω_{7V} cancel each other to a large extent.

The present experimental bounds

$$Br(K_L \to \pi^0 e^+ e^-)_{\rm exp} < 28 \cdot 10^{-11} \qquad [144] \,, \qquad (4.126)$$

$$Br(K_L \to \pi^0 \mu^+ \mu^-)_{\rm exp} < 38 \cdot 10^{-11} \qquad [145] \qquad (4.127)$$

are still by one order of magnitude larger than the SM predictions [142]

$$Br(K_L \to \pi^0 e^+ e^-)_{\rm SM} = 3.54^{+0.98}_{-0.85} \left(1.56^{+0.62}_{-0.49}\right) \cdot 10^{-11} \,, \qquad (4.128)$$

$$Br(K_L \to \pi^0 \mu^+ \mu^-)_{\rm SM} = 1.41^{+0.28}_{-0.26} \left(0.95^{+0.22}_{-0.21}\right) \cdot 10^{-11} \,. \qquad (4.129)$$

The values in parentheses correspond to the destructive interference between directly and indirectly CP-violating contributions. A recent discussion of the theoretical status of this interference sign can be found in [146] where the results of [139, 141, 147] are critically analysed. From this discussion, constructive interference seems to be favoured though more work is necessary.

4.4.5 Short-distance contribution to $K_L \to \mu^+\mu^-$

Another interesting rare K mode is the decay $K_L \to \mu^+\mu^-$, whose short-distance (SD) contributions are governed by the effective Hamiltonian (4.114). In contrast to the decays discussed until now, the SD contribution calculated here is only a part of a dispersive contribution to $K_L \to \mu^+\mu^-$ that is by far dominated by the absorptive contribution with two internal photon exchanges. Consequently the SD contribution constitutes only a small fraction of the branching ratio. Moreover, because of long-distance (LD) contributions to the dispersive part of $K_L \to \mu^+\mu^-$, the extraction of the SD part from the data is subject to considerable uncertainties. The most recent estimate gives [148]

$$Br(K_L \to \mu^+\mu^-)_{\rm SD} \leq 2.5 \cdot 10^{-9}\,, \tag{4.130}$$

to be compared with $(0.8 \pm 0.1) \cdot 10^{-9}$ in the SM [149].

When evaluating the SD contribution to $K_L \to \mu^+\mu^-$ two simplifications occur. First when evaluating the relevant hadronic matrix elements $\langle 0|(\bar{s}d)_{V-A}|K_L\rangle$ and $\langle 0|(\bar{s}d)_V|K_L\rangle$ only the axial part contributes, as K_L is pseudoscalar, so that

$$\langle 0|(\bar{s}d)_V|K_L\rangle = 0\,. \tag{4.131}$$

Then, due to the conserved vector current the vector component of the $\mu\bar{\mu}$-vertex drops out as well and as in the SM only the axial current component of the $\mu\bar{\mu}$-vertex is relevant. Therefore the only SD operator contributing to $K_L \to \mu^+\mu^-$ is the SM $(V-A)\otimes(V-A)$ one. Consequently following [140] in the custodially protected RS model we find

$$Br(K_L \to \mu^+\mu^-)_{\rm SD} = 2.08 \cdot 10^{-9} \left[\bar{P}_c\,(Y_K) + A^2 R_t \left|Y_K^{V-A}\right| \cos\bar{\beta}_Y^K\right]^2\,, \tag{4.132}$$

where we have defined

$$\bar{\beta}_Y^K \equiv \beta - \beta_s - \bar{\theta}_Y^K\,, \qquad |V_{td}| = A\lambda^3 R_t\,, \tag{4.133}$$

$$\bar{P}_c\,(Y_K) \equiv \left(1 - \frac{\lambda^2}{2}\right) P_c\,(Y_K)\,, \tag{4.134}$$

with $P_c\,(Y_K) = 0.113 \pm 0.017$ [149].

4.4.6 $B_s \to \mu^+\mu^-$ and $B_d \to \mu^+\mu^-$

The last rare decays on our list are the leptonic modes $B_s \to \mu^+\mu^-$ and $B_d \to \mu^+\mu^-$. In contrast to the decay $K_L \to \mu^+\mu^-$ considered previously, these decays are short-distance dominated. As in the SM their branching ratios receive a strong

chiral suppression, they can be largely enhanced in models where scalar operator contributions are generated for which the chirality suppression in absent. This happens for instance in the MSSM and other two Higgs doublet models at large $\tan\beta$. In the RS model in question however it turns out that flavour violating Higgs couplings are strongly chirally suppressed in addition to the usual RS-GIM suppression, see section 4.2. In addition the flavour conserving $H\bar{\mu}\mu$ vertex is suppressed by the small muon mass. Consequently Higgs contributions in this case are completely irrelevant and the branching ratios in question are governed by the new tree level Z, Z_H, Z' and $A^{(1)}$ contributions, in addition to the SM Z penguin and box diagrams.

The effective Hamiltonians for $b \to q\ell^+\ell^-$ transitions can then straightforwardly be obtained from $\left[\mathcal{H}_{\rm eff}^{\ell\bar{\ell}}\right]^K$ in (4.114) by properly adjusting all flavour indices. We note that, in contrast to the $s \to d\ell^+\ell^-$ transition, now also the dipole operator contributions mediating the decay $b \to q\gamma$ become relevant. The new RS contributions to the corresponding operators $\mathcal{Q}_{7\gamma}$ and $\mathcal{Q}_{8G}$ appear first at the one-loop level and consequently are beyond the scope of this work. In the following we will denote the total contribution of the dipole operators to the effective Hamiltonian in question simply by $\mathcal{H}_{\rm eff}(b \to q\gamma)$. We then find ($q = d, s$)

$$\begin{aligned}\left[\mathcal{H}_{\rm eff}^{\ell\bar{\ell}}\right]^{B_q} &= \mathcal{H}_{\rm eff}(b \to q\gamma) - g_{\rm SM}^2 \left[\lambda_t^{(q)} Y_q^{V-A}\right] (\bar{b}q)_{V-A}(\bar{\ell}\ell)_{V-A} \\ &\quad - g_{\rm SM}^2 \left[\lambda_t^{(q)} Y_q^{V}\right] (\bar{b}q)_{V}(\bar{\ell}\ell)_{V-A} \\ &\quad + 4g_{\rm SM}^2 \sin^2\theta_W \left[\lambda_t^{(q)} Z_q^{V-A}\right] (\bar{b}q)_{V-A}(\bar{\ell}\ell)_{V} \\ &\quad + 4g_{\rm SM}^2 \sin^2\theta_W \left[\lambda_t^{(q)} Z_q^{V}\right] (\bar{b}q)_{V}(\bar{\ell}\ell)_{V} + h.c.\,. \end{aligned} \tag{4.135}$$

In analogy to $Y_K^{V-A,V}, Z_K^{V-A,V}$ defined in (4.106)–(4.113), the relevant functions can be obtained from the latter formulae by making the index replacements

$$K \longrightarrow q\,, \qquad sd \longrightarrow bq\,. \tag{4.136}$$

Since the dipole operators $\mathcal{H}_{\rm eff}(b \to q\gamma)$ do not contribute to the $B_{d,s} \to \mu^+\mu^-$ decays, we can now evaluate the new RS contributions to the branching ratios in question. To this end we notice that as in the case of $K_L \to \mu^+\mu^-$ effectively only the SM $(V-A)\otimes(V-A)$ operators contribute. Consequently the only relevant functions are Y_q^{V-A} and we find ($q = d, s$)

$$Br(B_q \to \mu^+\mu^-) = \tau(B_q)\frac{G_F^2}{\pi}\left(\frac{\alpha}{4\pi\sin^2\theta_W}\right)^2 F_{B_q}^2 m_\mu^2 m_{B_q}\sqrt{1-4\frac{m_\mu^2}{m_{B_q}^2}}\left|\lambda_t^{(q)} Y_q^{V-A}\right|^2 . \tag{4.137}$$

Consequently the deviations from the SM predictions are simply given by

$$\frac{Br(B_q \to \mu^+\mu^-)}{Br(B_q \to \mu^+\mu^-)_{\rm SM}} = \frac{|Y_q^{V-A}|^2}{Y(x_t)^2}\,. \tag{4.138}$$

5 Global numerical analysis

5.1 Goals

We are now ready to present a global numerical analysis of the $\Delta F = 2$ and $\Delta F = 1$ observables calculated in the previous chapter within the custodially protected RS model. Therefore, after presenting some technical details of the parameter scan and collecting the experimental and theoretical input used throughout our analysis, we will turn our attention to observables related to meson-antimeson mixing in the model in question. In that context we will address the following questions:

1. What is the generic structure of the NP contributions?
2. Is it possible to obtain a simultaneous agreement with all $\Delta F = 2$ data, in particular with the ε_K parameter?
3. How much fine-tuning in the fundamental 5D Yukawa couplings is necessary in order to achieve this?
4. Can possible slight tensions in the SM, in particular between various CP-violating observables, be resolved?
5. What amount of CP-violation in $B_s - \bar{B}_s$ mixing is predicted?

Subsequently, we will study the impact of the new RS contributions on rare K and B decay branching ratios. In this context the following questions will be of interest:

6. Which of the various NP contributions is the most important one? What pattern of deviations from the SM can therefore be expected?
7. How would this pattern change if the custodial protection mechanism was absent?
8. By how much do the various K and B meson decay rates deviate from their SM predictions?
9. What are the correlations among various observables predicted in this framework?
10. Are simultaneous large NP effects in the various meson systems possible?

After having successfully addressed all of these topics, we will compare our results with those found within minimal flavour violating (MFV) models and within the Littlest Higgs model with T-parity (LHT), with the latter being an example of models with new sources of flavour and CP-violation but only SM operators. We will see that the specific patterns of flavour and CP-violating effects observed can help to distinguish between these models and more generally between the various frameworks of flavour violation beyond the SM.

5.2 Numerical strategy

Before presenting the answers to all the questions listed above, in this section we briefly summarise how the numerical analysis has been performed. The strategy for this analysis has been developed in [35] for the study of NP effects in $\Delta F = 2$ observables. For further details on the parameter scan, we refer the reader to that paper. The straightforward extension to include also $\Delta F = 1$ observables has been presented in [36].

In order to be able to determine the size of NP effects in the model under consideration, we have to restrict ourselves to those regions of the parameter space of the model that reproduce the experimentally observed quark masses and CKM mixing parameters and are consistent with the data on electroweak precision observables.

Due to the explicit custodial symmetry of the model, the electroweak precision data can be fulfilled for

$$M \gtrsim (2-3)\,\text{TeV} \tag{5.1}$$

with only moderate constraints on the fermion bulk mass parameters c. Therefore throughout our numerical analysis, we set

$$f = 1\,\text{TeV} \qquad \Longrightarrow \qquad M \simeq 2.5\,\text{TeV}\,, \tag{5.2}$$

so that the first KK modes should be detectable via direct searches at the LHC. Furthermore the bulk mass parameter of the third generation left-handed quark doublet c_Q^3 is chosen randomly in the range

$$0.1 \leq c_Q^3 \leq 0.5\,. \tag{5.3}$$

Similarly the parameters of the 5D Yukawa couplings λ^u, λ^d in the parameterisation of section 3.5.2 are varied over their physical ranges, with the restriction

$$\left|\lambda_{ij}^{u,d}\right| k \leq 3 \tag{5.4}$$

in order to maintain the perturbative calculability of the model at least up to the first two KK excitations [39, 85]. See [35] for further technical details.

	$\mu = 2\,\text{GeV}$	$\mu = 4.6\,\text{GeV}$	$\mu = 172\,\text{GeV}$	$\mu = 3\,\text{TeV}$
$m_u(\mu)$	3.0(10) MeV	2.5(8) MeV	1.6(5) MeV	1.4(5) MeV
$m_d(\mu)$	6.0(15) MeV	4.9(12) MeV	3.2(8) MeV	2.7(7) MeV
$m_s(\mu)$	110(15) MeV	90(12) MeV	60(8) MeV	50(7) MeV
$m_c(\mu)$	1.04(8) GeV	0.85(7) GeV	0.55(4) GeV	0.45(4) GeV
$m_b(\mu)$	—	4.2(1) GeV	2.7(1) GeV	2.2(1) GeV
$m_t(\mu)$	—	—	162(2) GeV	135(2) GeV

Table 5.1: *Renormalised quark masses at various scales, evaluated using NLO running. The 1σ uncertainties are given in brackets.*

In order to perform the parameter scan efficiently, instead of randomly choosing the remaining bulk mass parameters $c_Q^{1,2}$, $c_u^{1,2,3}$ and $c_d^{1,2,3}$, we make use of the Froggatt-Nielsen-like formulae of appendix A.2 in order to determine their values necessary to fit the quark masses collected in table 5.1 and the CKM parameters given in table 5.2. Having thus fixed a specific parameter point, we check numerically whether the SM quark masses and CKM parameters are indeed reproduced within their experimental 2σ ranges.

For those parameter points passing this test[1], we subsequently evaluate all relevant $\Delta F = 2$ observables, using the analytic results of section 4.3. All necessary input parameters can be found in table 5.2. In particular we analyse the pattern of NP effects in $K^0 - \bar{K}^0$ and $B_{d,s} - \bar{B}_{d,s}$ mixings and determine the amount of fine-tuning required to fit the data on ε_K and other $\Delta F = 2$ observables. After that we restrict the parameter space to those regions that fulfil, in addition to the SM quark masses and CKM mixings, also all available $\Delta F = 2$ constraints simultaneously. For those regions we determine the possible size of deviations in those $\Delta F = 2$ observables that have not been measured so far: the CP-asymmetries $S_{\psi\phi}$ and A_{SL}^s and the width difference $\Delta\Gamma_s$.

Throughout the analysis of $\Delta F = 2$ processes we show the results obtained in terms of density plots rather than scatter plots, as the former carry the additional information of how likely a certain effect is, i. e. we get a notion of the *typical* size of effects within the RS model with custodial protection.

[1] Scanning for RS parameter points that are able to reproduce the SM quark masses and mixing angles in fact turns out to be the most time-consuming part of the numerical analysis. Therefore in order to avoid this sophisticated step, in [40] an alternative parameterisation of the RS flavour sector has been presented. In contrast to the parameterisation used throughout the present analysis, in the latter case the SM quark masses and CKM parameters appear as explicit parameters and do not need to be fitted. The remaining flavour parameters, apart from the 5D bulk masses, can then be expressed in terms of the mixing angles and complex phases of the flavour mixing matrices $\mathcal{D}_L$, $\mathcal{U}_R$ and $\mathcal{D}_R$.

$\lambda = \lvert V_{us}\rvert = 0.226(2)$	$G_F = 1.16637 \cdot 10^{-5}\,\text{GeV}^{-2}$
$\lvert V_{ub}\rvert = 3.8(4) \cdot 10^{-3}$	$M_W = 80.403(29)\,\text{GeV}$
$\lvert V_{cb}\rvert = 4.1(1) \cdot 10^{-2}$ [2]	$\alpha(M_Z) = 1/127.9$
$\gamma = 75(25)^\circ$	$\sin^2\theta_W = 0.23122$
$\Delta M_K = 0.5292(9) \cdot 10^{-2}\,\text{ps}^{-1}$	$m_K^0 = 497.648\,\text{MeV}$
$\lvert\varepsilon_K\rvert = 2.232(7) \cdot 10^{-3}$ [1]	$m_{B_d} = 5279.5\,\text{MeV}$
$\Delta M_d = 0.507(5)\,\text{ps}^{-1}$	$m_{B_s} = 5366.4\,\text{MeV}$ [1]
$\Delta M_s = 17.77(12)\,\text{ps}^{-1}$	$\eta_1 = 1.32(32)$ [104]
$S_{\psi K_S} = 0.671(24)$ [150]	$\eta_3 = 0.47(5)$ [105, 106]
$\bar{m}_c = 1.30(5)\,\text{GeV}$	$\eta_2 = 0.57(1)$
$\bar{m}_t = 162.7(13)\,\text{GeV}$	$\eta_B = 0.55(1)$ [107, 108]
$F_K = 156(1)\,\text{MeV}$ [151]	$F_{B_s} = 245(25)\,\text{MeV}$
$\hat{B}_K = 0.75(7)$	$F_{B_d} = 200(20)\,\text{MeV}$
$\hat{B}_{B_s} = 1.22(12)$	$F_{B_s}\sqrt{\hat{B}_{B_s}} = 270(30)\,\text{MeV}$
$\hat{B}_{B_d} = 1.22(12)$	$F_{B_d}\sqrt{\hat{B}_{B_d}} = 225(25)\,\text{MeV}$
$\hat{B}_{B_s}/\hat{B}_{B_d} = 1.00(3)$ [152]	$\xi = 1.21(4)$ [152]
$\tau(B_s) = 1.470(26)\,\text{ps}$	$\alpha_s(M_Z) = 0.118(2)$ [1]
$\tau(B_d) = 1.530(9)\,\text{ps}$ [1]	

Table 5.2: *Values of the experimental and theoretical quantities used as input parameters.*

In order to extend the analysis to include also $\Delta F = 1$ rare decays, we again restrict ourselves to those regions of the parameter space that are consistent with the experimental $\Delta F = 2$ constraints. For those points we determine the size of NP effects in the $\Delta F = 1$ observables discussed in section 4.4. The results of this analysis are shown as *blue* points in the figures of section 5.4. As we are primarily interested in that potion of the parameter space which is only moderately fine-tuned, we will show in *orange* those points for which the constraint on the fine-tuning measure $\Delta_{\text{BG}}(\varepsilon_K) < 20$ is satisfied. Accordingly the statements in the text concerning the possible size of NP effects correspond to the points with moderate fine-tuning.

Apart from determining the typical size of NP effects, we are mainly interested in studying possible correlations among the various observables and looking for specific patterns of effects that can help to distinguish this model from other NP frameworks. As examples we discuss in some detail how the custodially protected RS model can be distinguished from the class of models with (constrained) MFV and from the LHT model.

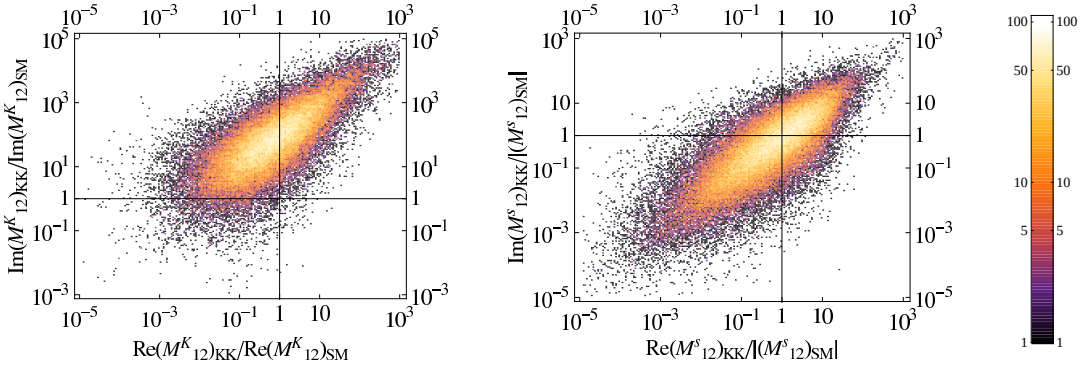

Figure 5.1: *Left:* $\mathrm{Re}(M_{12}^K)_{KK}/\,\mathrm{Re}(M_{12}^K)_{SM}$ *and* $\mathrm{Im}(M_{12}^K)_{KK}/\,\mathrm{Im}(M_{12}^K)_{SM}$*, plotted on logarithmic axes. Right:* $\mathrm{Re}(M_{12}^s)_{KK}$ *and* $\mathrm{Im}(M_{12}^s)_{KK}$*, normalised to* $|(M_{12}^s)_{SM}|$ *and plotted on logarithmic axes.*

5.3 $\Delta F = 2$ observables and fine-tuning

5.3.1 Pattern of NP contributions

In order to understand the impact of RS physics on $\Delta F = 2$ observables, we first consider the effect on the off-diagonal mixing amplitudes M_{12}^i $(i = K, d, s)$. We recall that these amplitudes are affected in a significant manner by tree level KK gluon and Z_H exchanges, while the effects of Z', Z and the KK photon turned out to be additionally suppressed and therefore irrelevant. Consequently, in addition to the SM operator $\mathcal{Q}_1^{VLL}$ also the new operator $\mathcal{Q}_1^{VRR}$ and the chirally enhanced $\mathcal{Q}_{1,2}^{LR}$ ones receive relevant NP contributions, with the contribution to $\mathcal{Q}_2^{LR}$ being generated exclusively by KK gluon exchanges.

As a starting point we show in figure 5.1 the pure KK contributions to M_{12}^K and M_{12}^s, normalised to the SM short-distance contributions. Specifically, in the left panel, $\mathrm{Im}(M_{12}^K)_{\mathrm{KK}}/\,\mathrm{Im}(M_{12}^K)_{\mathrm{SM}}$ is plotted as a function of $\mathrm{Re}(M_{12}^K)_{\mathrm{KK}}/\,\mathrm{Re}(M_{12}^K)_{\mathrm{SM}}$. We observe that while specific regions of the parameter space predict NP contributions to $\mathrm{Re}(M_{12}^K)$ by several orders of magnitude above the SM contribution and therefore in clear conflict with the data on ΔM_K, typically the RS contribution to $\mathrm{Re}(M_{12}^K)$ is of comparable size to the SM short-distance contribution. Consequently, thanks to the poorly known long-distance SM contributions, an agreement with the data on ΔM_K can naturally be obtained. The situation appears to be very different in the case of $\mathrm{Im}(M_{12}^K)$, where the KK contribution typically exceeds the SM contribution by almost two orders of magnitude. While the KK contribution to M_{12}^K generically has an arbitrary $\mathcal{O}(1)$ complex phase, so that $\mathrm{Re}(M_{12}^K)_{\mathrm{KK}}$ and $\mathrm{Im}(M_{12}^K)_{\mathrm{KK}}$ are expected of comparable size, the situation in the SM is funda-

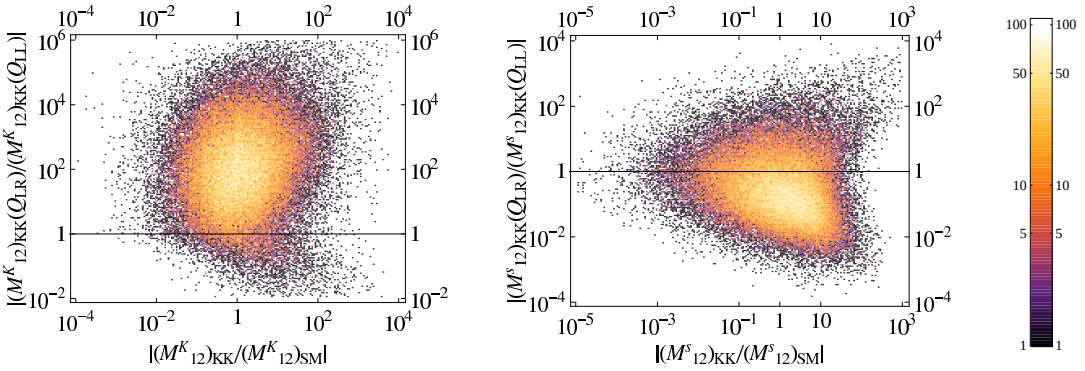

Figure 5.2: *The ratio of the contribution of only $\mathcal{Q}^{LR}_{1,2}$ and only $\mathcal{Q}^{VLL}_1$ to $(M^K_{12})_{KK}$ (left) and $(M^s_{12})_{KK}$ (right), as a function of $(M^i_{12})_{KK}/(M^i_{12})_{SM}$ ($i = K, s$).*

mentally different. Here, while $\mathrm{Re}(M^K_{12})_{\mathrm{SM}}$ is dominated by the purely real charm quark contributions, $\mathrm{Im}(M^K_{12})_{\mathrm{SM}}$ can only be generated by top contributions that are highly suppressed due to the smallness of $\mathrm{Im}(\lambda_t^{(K)})$. Consequently the CP-violating effects in $K^0 - \bar{K}^0$ mixing generated by KK gauge boson exchanges are generically way too large, giving rise to the so-called *ε_K problem* [85] that is indeed common to many NP models in which the chirally enhanced left-right operators are present [56].

In the right panel of figure 5.1 we show $\mathrm{Re}(M^s_{12})_{\mathrm{KK}}$ and $\mathrm{Im}(M^s_{12})_{\mathrm{KK}}$, normalised to $|(M^s_{12})_{\mathrm{SM}}|$. We observe that the absolute value of the KK gauge boson contribution is generically of roughly the same size as the SM contribution. In addition $\mathrm{Re}(M^s_{12})_{\mathrm{KK}}$ and $\mathrm{Im}(M^s_{12})_{\mathrm{KK}}$ turn out to be generally comparable in size, as the phase of $(M^s_{12})_{\mathrm{KK}}$ is arbitrary in contrast to the small phase $2\beta_s \sim -2^\circ$ of $(M^s_{12})_{\mathrm{SM}}$. Consequently we can deduce already from this figure that while the experimental constraint on ΔM_s can quite easily be satisfied, large new CP-violating effects in $B_s - \bar{B}_s$ mixing should be possible. Indeed in section 5.3.4 we will see that such effects remain possible even after imposing all existing constraints from $\Delta F = 2$ observables simultaneously.

Next in figure 5.2 we aim to analyse in more detail the operator structure of $K^0 - \bar{K}^0$ and $B_s - \bar{B}_s$ mixing. To this end we show the ratio of the contribution of only the $\mathcal{Q}^{LR}_{1,2}$ operators and only the $\mathcal{Q}^{VLL}_1$ one to $(M^i_{12})_{\mathrm{KK}}$, as a function of $(M^i_{12})_{\mathrm{KK}}/(M^i_{12})_{\mathrm{SM}}$, with $i = K$ in the left panel and $i = s$ in the right panel. We observe that the KK contributions to $K^0 - \bar{K}^0$ mixing are generally fully dominated by the $\mathcal{Q}^{LR}_{1,2}$ operator, while the $\mathcal{Q}^{VLL}_1$ contribution appears only at the percent level. As the dominant left-right contribution is due to the operator $\mathcal{Q}^{LR}_2$, which is generated only by KK gluon contributions, we conclude that the

NP effects in $K^0 - \bar{K}^0$ mixing are dominated by tree level exchanges of KK gluons, while the contributions of Z_H and Z' turn out to be subleading and in most cases irrelevant.

The situation turns out to be different in the $B_s - \bar{B}_s$ system. Here the $\mathcal{Q}_1^{VLL}$ and $\mathcal{Q}_{1,2}^{LR}$ contributions appear to be competitive in size, with $\mathcal{Q}_1^{VLL}$ even slightly dominant over $\mathcal{Q}_{1,2}^{LR}$. Consequently, as the KK gluon and Z_H contributions to $\mathcal{Q}_1^{VLL}$ are comparable, it turns out that the latter effects, although usually neglected in the literature, have to be taken into account.

The origin of this different pattern of contributions is in fact easy to understand. First of all, the matrix elements of the left-right operators are proportional to the chiral enhancement factors $R^K(\mu_L) \sim 20$ in (4.53) and $R^q(\mu_b) \sim 1$ in (4.56), respectively. Second, the $\mathcal{Q}_2^{LR}$ contributions are significantly enhanced when running from the KK scale $M \simeq 2.5\,\text{TeV}$ down to the scale μ_0, where the matrix elements of the relevant operators can be evaluated by lattice QCD. As $\mu_0 = 2.0\,\text{GeV}$ in the case of $K^0 - \bar{K}^0$ mixing, while $\mu_0 = 4.6\,\text{GeV}$ in the case of $B_s - \bar{B}_s$ mixing, the renormalisation group enhancement is weaker in the latter case. Finally, the flavour violating effects are much weaker for right-handed b quarks than for left-handed ones, as the third generation left-handed quark doublet needs to be localised much further in the IR than the right-handed one, in order to account for the large top quark mass. This additionally suppresses the $\mathcal{Q}_{1,2}^{LR}$ operator contribution with respect to the $\mathcal{Q}_1^{VLL}$ one in the $B_s - \bar{B}_s$ system, while the analogous effect in the $K^0 - \bar{K}^0$ system is much less pronounced. All these effects thus help to generate the observed pattern of contributions: While $K^0 - \bar{K}^0$ mixing is fully dominated by the $\mathcal{Q}_2^{LR}$ contribution and therefore by KK gluon exchanges, in the $B_s - \bar{B}_s$ system $\mathcal{Q}_1^{VLL}$ and therefore also the Z_H contributions are relevant. Note that the Z' contributions to $\mathcal{Q}_1^{VLL}$ are strongly suppressed by the custodial protection mechanism and therefore negligible. Similarly the KK photon contributions are small, being suppressed by the electromagnetic coupling constant and the electric charge of down-type quarks.

Finally, in both $K^0 - \bar{K}^0$ and $B_s - \bar{B}_s$ mixings, the contributions of the operator $\mathcal{Q}_1^{VRR}$ turn out to be negligible and we do not show them explicitly. This is due to the fact that the right-handed down-type quarks are generally localised further away from the IR brane than the left-handed ones.

The situation in the $B_d - \bar{B}_d$ system is very similar to the one encountered in the $B_s - \bar{B}_s$ system, as shown in the right panels of figures 5.1 and 5.2 and discussed in detail above. Therefore we omit to show the corresponding plots.

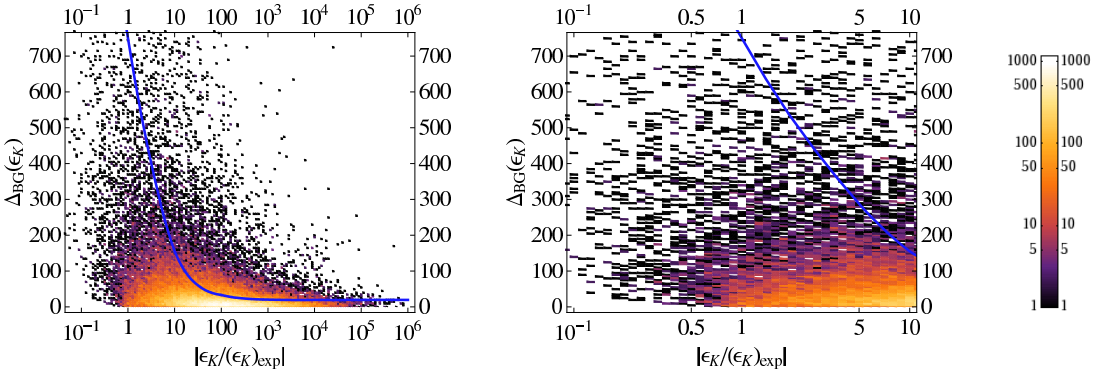

Figure 5.3: *Left: The fine-tuning $\Delta_{BG}(\varepsilon_K)$ plotted against ε_K, normalised to its experimental value. The blue line displays the average fine-tuning as a function of ε_K. Right: The same, but displaying only the phenomenologically interesting region $0.1 < |\varepsilon_K/(\varepsilon_K)_{exp}| < 10$.*

5.3.2 The ε_K constraint and fine-tuning

We have deduced already from figure 5.1 that the experimental constraint on ε_K is problematic for the RS model in question. Indeed this constraint has been used in [85] to derive a lower bound on the KK scale $M \gtrsim 20\,\text{TeV}$, assuming completely anarchic Yukawa couplings. We confirm this bound[2], see [35], by requiring that the average fine-tuning in the 5D Yukawa couplings, required to obtain ε_K in agreement with the data, does not exceed the bound $\Delta_{\text{BG}}(\varepsilon_K) = 20$. Herewith the Barbieri-Giudice (BG) [153] measure of fine-tuning, quantifying the sensitivity of a given observable O to small variations in the model parameters p_j $(j = 1, \ldots, m)$ is defined by

$$\Delta_{\text{BG}}(O) = \max_{j=1,\ldots,m} \{\Delta_{\text{BG}}(O, p_j)\}\,, \tag{5.5}$$

with

$$\Delta_{\text{BG}}(O, p_j) = \left|\frac{p_j}{O}\frac{\partial O}{\partial p_j}\right|\,. \tag{5.6}$$

The normalisation factor p_j/O appears in order not to be sensitive to the absolute size of p_j and O.

Here we follow a different approach and ask by how much the 5D Yukawa couplings have to deviate from the anarchic ansatz in order to satisfy the experimental constraint on ε_K for low KK masses in the reach of the LHC. Therefore we use, as throughout our whole numerical analysis, $M \simeq 2.5\,\text{TeV}$ and determine random sets of 5D Yukawa parameters that predict the correct quark masses and CKM

[2] Another independent confirmation has been obtained in [98], making use of the 4D two-site approach to study the model in question.

mixings. In figure 5.3 we show the fine-tuning $\Delta_{\rm BG}(\varepsilon_K)$, plotted against ε_K with the latter normalised to its experimental value. The blue curve displays the on average required fine-tuning in order to obtain a given value of ε_K. We find that while the generic prediction for ε_K is roughly by two orders of magnitude too large, in agreement with the findings in [85,98], there exist regions of the parameter space of the model, for which ε_K is in agreement with the data. We also see that while for $\varepsilon_K \sim 100(\varepsilon_K)_{\rm exp}$ the necessary fine-tuning is generally small, $\Delta_{\rm BG}(\varepsilon_K) \sim 20$, it rapidly increases with decreasing ε_K, so that for $\varepsilon_K \sim (\varepsilon_K)_{\rm exp}$ a fine-tuning of order 700 is needed on average. However we also observe that there exist regions of parameter space for which the data on ε_K can be fulfilled without significant fine-tuning. In other words we find that natural solutions to the ε_K problem are possible. Stating this we are aware of the fact that due to the $\mathcal{O}(1)$ 5D Yukawa couplings, the model is close to the perturbative limit, so that loop corrections to the tree level processes considered in this work are potentially sizable. While taking into account also these effects would certainly lead to modified predictions for given points of the parameter space, we do not expect the overall picture to be modified at the qualitative level.

5.3.3 Effects in other $\Delta F = 2$ observables

After considering in detail the potentially dangerous NP effects on CP-violation in the $K^0 - \bar{K}^0$ system, we now turn our attention to other $\Delta F = 2$ observables that have been measured with high precision. Specifically we consider the mass differences ΔM_K, ΔM_d and ΔM_s, measuring CP-conserving effects in the $K^0 - \bar{K}^0$, $B_d - \bar{B}_d$ and $B_s - \bar{B}_s$ systems, respectively. Furthermore we have a look at the CP-asymmetry $S_{\psi K_S}$, measuring the CP-violating phase in $B_d - \bar{B}_d$ mixing.

Let us begin with ΔM_K which, being sensitive to $\mathrm{Re}(M_{12}^K)$, is the CP-conserving counterpart to $\varepsilon_K \propto \mathrm{Im}(M_{12}^K)$. We concluded already from figure 5.1 that, in contrast to the case of ε_K, in the case of ΔM_K the KK gauge boson contributions do generally not give rise to unwantedly large contributions. In order to quantify this result, we consider in figure 5.4 the fine-tuning $\Delta_{\rm BG}(\Delta M_K)$ plotted against ΔM_K, with the latter normalised to its experimental value. We observe that in this case the generic RS prediction is in good agreement with the data[3]. Furthermore we find that in this case the required fine-tuning is generally much smaller than in the case of ε_K, $\Delta_{\rm BG}(\Delta M_K) \lesssim 20$, with its minimum reached for values of ΔM_K consistent with the data. We thus conclude that ΔM_K is not subject to any naturalness problem in the model in question.

[3] As in our numerical analysis we did not include the SM long-distance effects which are subject to large theoretical uncertainties, deviations of $\mathcal{O}(30\%)$ from the experimental value can be attributed to this additional contribution.

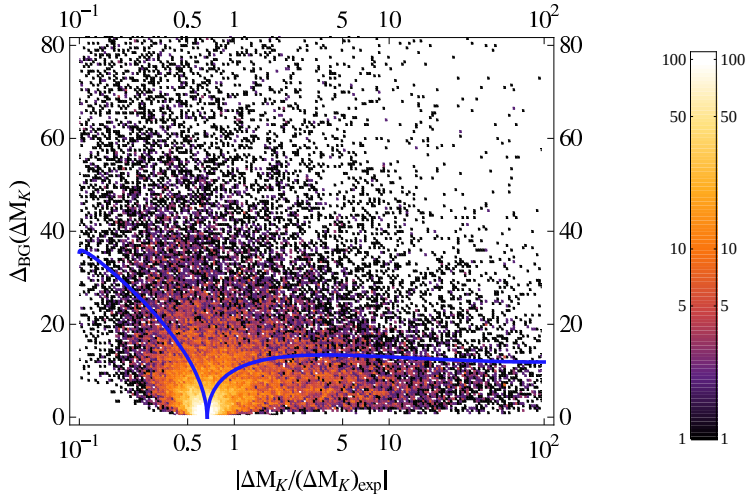

Figure 5.4: *The fine-tuning $\Delta_{BG}(\Delta M_K)$ plotted against ΔM_K, normalised to its experimental value. The blue line displays the average fine-tuning as a function of ΔM_K.*

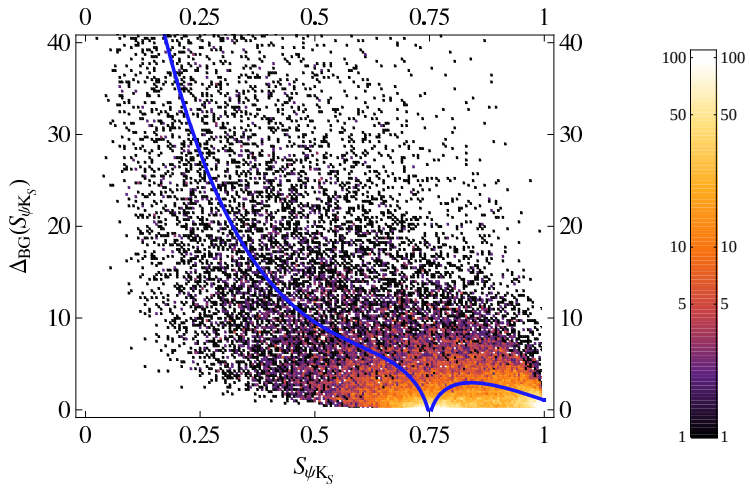

Figure 5.5: *The fine-tuning $\Delta_{BG}(S_{\psi K_S})$ plotted against $S_{\psi K_S}$. The blue line displays the average fine-tuning as a function of $S_{\psi K_S}$.*

Next we consider the CP-asymmetry $S_{\psi K_S}$, measuring CP-violating effects in $B_d - \bar{B}_d$ mixing, being measured with high precision and theoretically clean. As in the cases of ε_K and ΔM_K we consider the fine-tuning $\Delta_{\rm BG}(S_{\psi K_S})$ as a function of $S_{\psi K_S}$. The result is shown in figure 5.5. We observe that also in this case the RS prediction is generically in good agreement with the data and the associated fine-tuning is small, typically $\Delta_{\rm BG}(S_{\psi K_S}) \lesssim 5$. On the other hand, we can also see that possible slight deviations from the SM prediction, as discussed at numerous places in the literature, can easily be accounted for by the RS model with custodial protection.

As the corresponding plots for ΔM_d and ΔM_s are very similar to the ones discussed previously, we do not show them explicitly, but merely summarise briefly the result. Also for these two observables, the RS prediction is generically in good agreement with the data and the associated fine-tuning is small.

In summary thus the only problematic $\Delta F = 2$ observable is ε_K, which generically requires a large KK scale or significant fine-tuning of the 5D model parameters. However we have seen that also in that case there exist regions of the parameter space where the RS contribution is in agreement with the data without the necessity for large fine-tuning.

Until now we have considered only one $\Delta F = 2$ observable at a time, not taking into account the experimental constraints from the other observables. As it was one of our main goals to find whether all $\Delta F = 2$ constraints can be fulfilled simultaneously, we now impose also these constraints, in addition to the ones coming from the SM quark masses and CKM mixings, that have already been taken into account so far. We find that the figures shown and discussed above do not change qualitatively when the other $\Delta F = 2$ constraints are imposed on the parameter space, although the number of valid parameter points of course decreases when more constraints are imposed. We also find that indeed it is possible to fulfil *all* available $\Delta F = 2$ *simultaneously*, although large portions of the parameter space are excluded by this simultaneous analysis. As can be expected from our previous discussion, it turns out that the ε_K constraint is indeed the most restrictive one and excludes already on its own a major part of the parameter space.

5.3.4 CP-violation in $B_s - \bar{B}_s$ mixing

Having restricted our numerical analysis to only those regions of the parameter space that are consistent with all available $\Delta F = 2$ constraints, we are now prepared to consider those observables that have not yet been measured with high precision. In the $\Delta F = 2$ sector, these are the CP-asymmetry $S_{\psi\phi}$, the semi-leptonic CP-asymmetry $A^s_{\rm SL}$ and the width difference $\Delta\Gamma_s$. In all models where

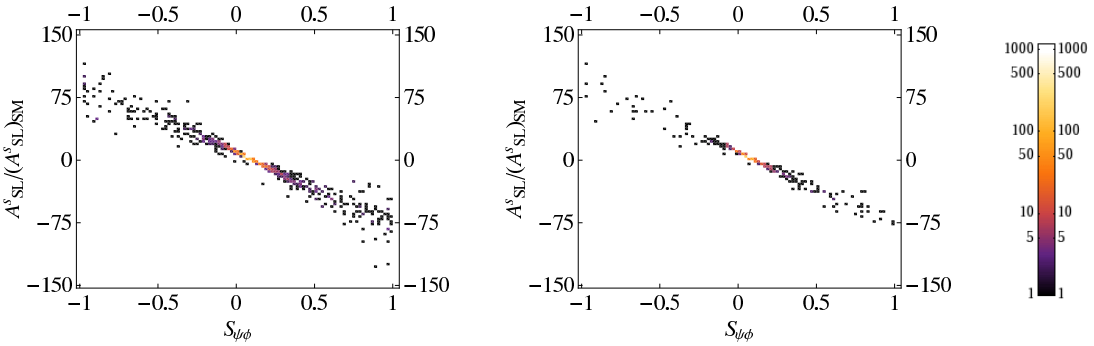

Figure 5.6: *Left: A^s_{SL}, normalised to its SM value, as a function of $S_{\psi\phi}$. In addition to the requirement of correct quark masses and CKM mixings, also the available $\Delta F = 2$ constraints are imposed. Right: The same, but in addition the condition $\Delta_{BG}(\varepsilon_K) < 20$ is imposed.*

NP does not affect the absorptive part of the off-diagonal mixing amplitude, Γ^s_{12}, and where the decay $B_s \to \psi\phi$ is dominated by the SM tree level effects [118–121], any deviation of the data from the SM prediction would be a clear signal of new CP-violating effects in $B_s - \bar{B}_s$ mixing. Consequently, if the above conditions are satisfied, the NP effects in $S_{\psi\phi}$, $A^s_{\rm SL}$ and $\Delta\Gamma_s$ are strongly correlated, so that finding one of these observables significantly different from its SM value would open the road towards large NP effects also in the other observables. On the other hand if the model-independent correlations of [118–121] are falsified by the data one day, we would have gained the interesting insight that either Γ^s_{12} is affected by NP contributions in a significant manner or the decay $B_s \to \psi\phi$ receives relevant NP contributions that lead to directly CP-violating effects in this mode. We note though that in most of the realistic NP models this is not the case so that the correlation in question is indeed predicted.

The situation recently became particularly interesting, as the data from the CDF and DØ experiments hint at the possibility that indeed the CP-violating effects in $B_s - \bar{B}_s$ mixing are enhanced by an order of magnitude with respect to their SM predictions [154–156]. Model-independent theoretical analyses have been presented in [157, 158].

In figure 5.6 we show the correlation between $S_{\psi\phi}$ and $A^s_{\rm SL}$ that emerges after imposing all available $\Delta F = 2$ constraints. We observe that $S_{\psi\phi}$ can reach any value between -1 and $+1$, so that the recent data can easily be accounted for. Due to the strong correlation with $A^s_{\rm SL}$ the latter asymmetry can be enhanced by as much as two orders of magnitude. Comparing the left and right panels of figure 5.6 to each other, we find that imposing in addition the naturalness constraint $\Delta_{\rm BG}(\varepsilon_K) < 20$ on the parameter space, the overall picture is not modified and

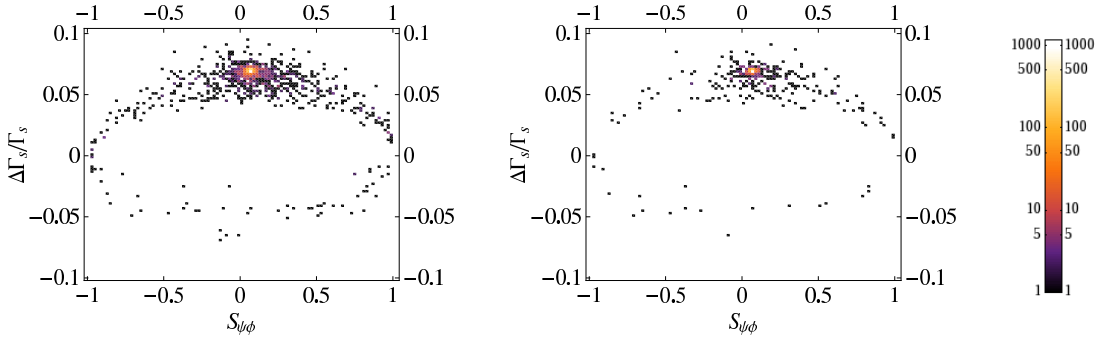

Figure 5.7: *left:* $\Delta\Gamma_s/\Gamma_s$ *as a function of* $S_{\psi\phi}$*. In addition to the requirement of correct quark masses and CKM mixings, also the available* $\Delta F = 2$ *constraints are imposed. right: The same, but in addition the condition* $\Delta_{BG}(\varepsilon_K) < 20$ *is imposed.*

large NP effects in the two CP-asymmetries are still possible. The only relevant change is the reduction of the number of points by roughly a factor of 3, while the distribution of points remains essentially the same.

We close our numerical analysis of $\Delta F = 2$ observables in the custodially protected RS model by considering the correlation between $S_{\psi\phi}$ and $\Delta\Gamma_s/\Gamma_s$ shown in figure 5.7. Due to the model-independent correlation between these two observables, a future accurate measurement of $\Delta\Gamma_s$ could help to distinguish between scenarios predicting large or small NP contributions to $S_{\psi\phi}$. We note however that this test is limited by the theoretical uncertainties in the SM prediction for $\Delta\Gamma_s$ and therefore becomes effective only if $S_{\psi\phi}$ is enhanced by more than an order of magnitude with respect to the SM. On the other hand an accurate measurement of $\Delta\Gamma_s$ will significantly reduce the present theoretical uncertainties in the correlation between $S_{\psi\phi}$ and $A^s_{\rm SL}$ [118], so that the assumptions underlying the model-independent correlation (4.73) between these two observables can eventually be tested with high precision.

5.4 Rare decay branching ratios

5.4.1 Pattern of Z, Z_H and Z' contributions

Before turning our attention to the phenomenology of rare K and B decays in the custodially protected RS model, we now analyse the relative sizes of Z, Z_H and Z' contributions to the $\Delta F = 1$ processes in question.

The NP contributions to the functions X, Y and Z calculated in section 4.4 turned out to be a product of three main components: the coupling of the respective gauge boson to the down-type quarks, the gauge boson's coupling to leptons, and finally its propagator in the low energy limit $q^2 \ll M^2$. For a given meson system characterised by (ij) there are six distinct contributions from the three gauge bosons Z, Z_H and Z' coupling to left- and right-handed down-type quarks[4], $\Delta^{ij}_{L,R}(Z)\,, \Delta^{ij}_{L,R}(Z_H)\,, \Delta^{ij}_{L,R}(Z')$. In section 4.2 we have seen that two of them, the couplings of Z and Z' to the left-handed quarks are suppressed by the custodial symmetry. Now we will analyse the numerical impact of this protection.

Flavour violating couplings to quarks: Let us start with considering the hierarchy in the flavour violating gauge couplings to SM quarks. As the flavour mixing matrices $\mathcal{D}_L$, $\mathcal{D}_R$ enter the Z, Z_H and Z' couplings in the same way, and in addition the gauge boson shape functions $g(y)$ and $\tilde{g}(y)$ are roughly equal, the source of the hierarchy in question is the mixing of gauge bosons into mass eigenstates and the suppression of $Zd^i_L\bar{d}^j_L$ and $Z'd^i_L\bar{d}^j_L$ induced by the custodial protection. Numerically, we find for the left-handed quark couplings

$$\Delta^{ij}_L(Z_H) : \Delta^{ij}_L(Z') : \Delta^{ij}_L(Z) \sim \mathcal{O}(10^4) : \mathcal{O}(10^3) : 1\,. \tag{5.7}$$

As the right-handed down-type quarks are no P_{LR}-eigenstates, the custodial protection mechanism is not effective in the case of $\Delta^{ij}_R(Z)$ and $\Delta^{ij}_R(Z')$. Consequently their hierarchy is solely determined by the mixing of gauge bosons into mass eigenstates. It is given by

$$\Delta^{ij}_R(Z_H) : \Delta^{ij}_R(Z') : \Delta^{ij}_R(Z) \sim \mathcal{O}(10^2) : \mathcal{O}(10^2) : 1\,, \tag{5.8}$$

where the above hierarchies hold for the K, B_d and B_s systems likewise, that is for $ij = sd$, $ij = bd$ and $ij = bs$, respectively.

Clearly in the presence of an exact protective P_{LR} symmetry the flavour violating couplings $\Delta^{ij}_L(Z)$ and $\Delta^{ij}_L(Z')$ would vanish identically. In this limit the same linear combination of $Z^{(1)}$ and $Z^{(1)}_X$ enters the Z and Z' mass eigenstates, so that the same cancellation of contributions is effective. Taking into account the P_{LR} symmetry breaking effects on the UV brane, the custodial protection mechanism is not exact anymore, but still powerful enough to suppress $\Delta^{ij}_L(Z)$ by two orders of magnitude. In the case of Z', the mixing angles for $Z^{(1)}$ and $Z^{(1)}_X$ are modified by roughly 10% when including the violation of the P_{LR} symmetry, see section 3.3. Accordingly, the protection is weaker in the case of Z' and $\Delta^{ij}_L(Z')$ is suppressed only by one order of magnitude compared to the case without protection.

[4]We note that in case of the Y and Z functions also the KK photon $A^{(1)}$ contributes. However its couplings to fermions are suppressed by the smallness of the electromagnetic coupling e and the electric quark charge, so that its contributions turn out to be small (if not absent) in all cases.

Flavour conserving couplings to leptons: Since leptons are significantly lighter than quarks of the same generation, we choose them to be localised towards the UV brane and set the bulk mass parameters to $c = \pm 0.7$ for left- and right-handed leptons, respectively. The assumption of degenerate bulk masses is well motivated by the observation that the flavour conserving couplings depend only very weakly on the actual value of c, provided $c > 0.5$ ($c < -0.5$ for right-handed fermions). As the couplings of gauge boson mass eigenstates are dominated by the $Z^{(0)}$ and $Z^{(1)}$ contributions[5], it turns out that their hierarchy does not depend on the particular handedness or species of leptons involved. In contrast to the Z_H and Z' couplings, the Z coupling to the lepton sector is not suppressed by an overlap integral of shape functions and hence is found to be dominant. Numerically,

$$\Delta_{L,R}^{\nu\nu,\ell\ell}(Z_H) : \Delta_{L,R}^{\nu\nu,\ell\ell}(Z') : \Delta_{L,R}^{\nu\nu,\ell\ell}(Z) \sim \mathcal{O}(10^{-1}) : \mathcal{O}(10^{-1}) : 1\,. \tag{5.9}$$

This hierarchy enters in a universal manner in the rare K, B_d and B_s decays.

Gauge boson propagators: To leading order in the v^2/M^2 expansion, the heavy neutral gauge bosons Z_H and Z' are degenerate in mass. Consequently their contribution to the functions X, Y and Z is suppressed by a factor $M_Z^2/M^2 \sim \mathcal{O}(10^{-3})$ with respect to the Z contribution.

Having at hand these considerations, we are now able to weight the contributions of Z, Z_H and Z' coupling to left- and right-handed quarks. It is obvious that the contributions from the Z_H and Z coupling to left-handed quarks are comparable in size, while the corresponding contribution from Z' is clearly negligible. The contribution from couplings to right-handed quarks is strictly dominated by the Z boson.

To finally determine the dominant overall contribution, we compare $\Delta_L^{ij}(Z)$ and $\Delta_R^{ij}(Z)$, which is shown for $ij = sd$ and $ij = bs$, respectively, by the blue points in figure 5.8. Note that the points shown in this figure fulfil all existing $\Delta F = 2$ constraints. We observe that in general the Z boson couples much more strongly to right-handed quarks than to left-handed quarks, which is a consequence of the custodial protection mechanism suppressing the latter couplings by roughly two orders of magnitude. More explicitly, we observe:

- $\Delta_R^{sd}(Z)$ is larger than $\Delta_L^{sd}(Z)$ for a dominant part of the allowed points and is on average larger than $\Delta_L^{sd}(Z)$ by two orders of magnitude.
- The dominance of $\Delta_R^{bs}(Z)$ over $\Delta_L^{bs}(Z)$ is less pronounced, but still on average $\Delta_R^{bs}(Z)$ is larger than $\Delta_L^{bs}(Z)$ by one order of magnitude.

[5]This is due to the fact that the overlap integral of a $(++)$ gauge boson with UV localised fermions is much larger than the corresponding overlap integral for a $(-+)$ gauge boson.

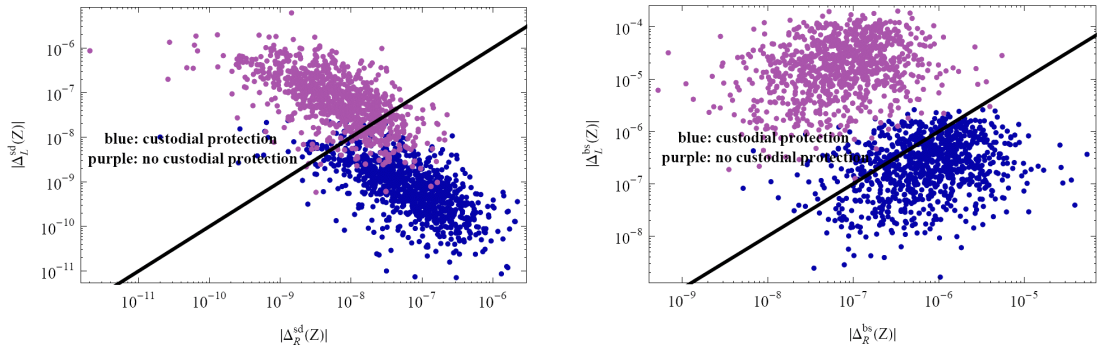

Figure 5.8: $|\Delta_L^{ij}(Z)|$ *versus* $|\Delta_R^{ij}(Z)|$ *for* $ij = sd$ *(left) and* $ij = bs$ *(right). The blue points are obtained in the custodially protected model after imposing all constraints from* $\Delta F = 2$ *observables. The purple points show the effect of removing the custodial protection. The solid lines display the equality* $|\Delta_L^{ij}(Z)| = |\Delta_R^{ij}(Z)|$.

- The values of $\Delta_R^{bs}(Z)$ are on average larger than $\Delta_R^{sd}(Z)$ by one order of magnitude, as the (b_R, s_R) system is localised closer to the IR brane than the (s_R, d_R) system.

The case of $\Delta_{L,R}^{bd}(Z)$ constitutes an intermediate scenario, and we do not show the corresponding plot explicitly. In summary we find that in the RS model with custodial protection the NP effects in $\Delta F = 1$ rare decays are dominated by the Z boson couplings to *right-handed* down-type quarks

Finally let us mention how the pattern identified above changes when the custodial protection mechanism is removed. To this end we simply remove the effects of the $Z_X^{(1)}$ gauge boson from all couplings, so that effectively an RS model with the SM gauge group in the bulk is recovered. The impact of this change is shown by the purple points in figure 5.8. We observe that now the left-handed couplings $\Delta_L^{ij}(Z)$ are enhanced by two orders of magnitude, as they are not protected by a symmetry any longer. At the same time $\Delta_R^{ij}(Z)$ decrease by roughly one order of magnitude, as they previously were dominated by the $Z_X^{(1)}$ contribution but are now suppressed by an additional factor $Q_{\rm em} \sin^2\theta_W$. Therefore in the RS model without custodial protection the rare decay branching ratios will be dominated completely by the Z boson coupling to *left-handed* quarks. Consequently the flavour phenomenology of the latter model turns out to be very different from the one of the custodially protected model, and in particular significantly larger effects in rare $B_{d,s}$ decays are possible. For further details, we refer the reader to [36, 99]. We stress that a consistent analysis of the RS model without custodial symmetry requires not only the removal of the additional gauge degrees of freedom, but that in this case a *simultaneous* analysis of electroweak precision and flavour constraints is necessary.

5.4.2 Comparison of K and $B_{d,s}$ systems

Before studying in detail the phenomenological implications for specific K and B decay branching ratios, we now aim to predict the average relative size of NP contributions in the K and B systems. On the one hand, having a closer look at the NP contributions to the functions $X_i^{V-A,V}$, $Y_i^{V-A,V}$ and $Z_i^{V-A,V}$ $(i = K, d, s)$, we observe that the possible size of NP effects depends crucially on the factors

$$\frac{1}{\lambda_t^{(K)}} \sim 2500\,, \qquad \frac{1}{\lambda_t^{(d)}} \sim 100\,, \qquad \frac{1}{\lambda_t^{(s)}} \sim 25 \tag{5.10}$$

for K, B_d and B_s systems, respectively, so that if the NP effects by themselves would not exhibit any specific hierarchy, largest effects could be expected in K physics observables, while the effects in rare $B_{d,s}$ decays should be moderate. In fact this structure has been encountered within the LHT model, where spectacular effects in rare K decays have been found [122,123,159–161]. A detailed comparison of the LHT results with the predictions of the custodially protected RS model will be given in section 5.5.3.

On the other hand in the custodially protected RS model the hierarchies given in (5.10) are partially compensated by the hierarchical structure of $\Delta_R^{sd,bd,bs}(Z)$. As however the amount of flavour violation needed to explain the SM quark masses and CKM parameters is much smaller in the right-handed sector than in the left-handed one, the hierarchies of (5.10) are only partly compensated. Having at hand numerical results for $\Delta_R^{sd,bd,bs}(Z)$ for a large number of parameter sets, we can quantify the average relative size of NP contributions in the K and B systems. We find that the size of the NP contributions on average drops by a factor of four when going from the K to the B_d system and by another factor of two when going from the B_d to the B_s system.

In fact this pattern of NP effects can be verified numerically by considering the NP effects in the functions X_i, as defined in (4.89). In the left panel of figure 5.9 we show the absolute values $|X_K|$ and $|X_s|$. We observe that while $|X_K|$ can be sizably enhanced or suppressed with respect to its SM value, the corresponding effects turn out to be small in the B_s system. In the case of $|X_d|$ that we do not show in the figure, the effects turn out to be somewhat larger, and numerically we find

$$0.60 \leq \frac{|X_K|}{X(x_t)} \leq 1.30\,, \qquad 0.90 \leq \frac{|X_d|}{X(x_t)} \leq 1.12\,, \qquad 0.95 \leq \frac{|X_s|}{X(x_t)} \leq 1.08\,. \tag{5.11}$$

This pattern implies much larger CP-conserving effects in the K than in the B_d and B_s systems, where NP effects are found to be disappointingly small. Interestingly, in contrast to the CMFV models, large effects in K and B decays do not necessarily

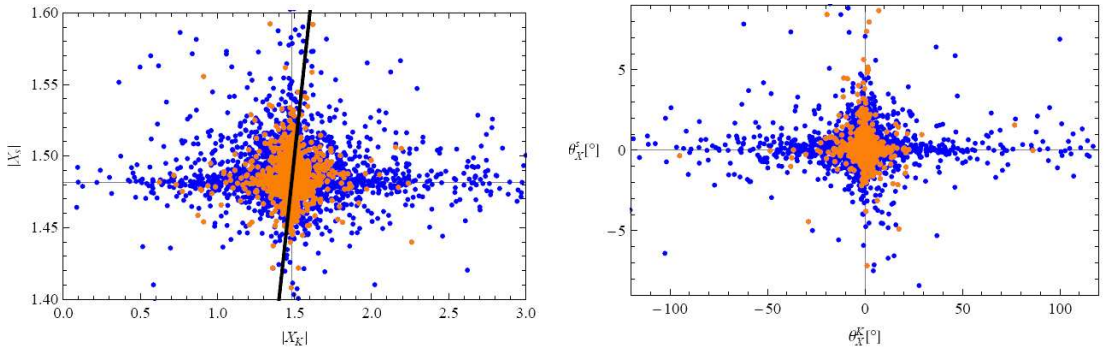

Figure 5.9: *Left: Breakdown of the universality between $|X_K|$ and $|X_s|$. The solid thick line represents the CMFV relation $|X_s| = |X_K|$ and the crossing point of the three solid lines indicates the SM prediction. Right: Breakdown of the universality between θ_X^K and θ_X^s and new sources of CP-violation. In the SM and in MFV models, $\theta_X^K = \theta_X^s = 0$.*

appear simultaneously in the RS model considered, and in fact simultaneous large effects in both systems appear to be unlikely. Consequently the flavour universality of the function X predicted in the SM and in all models with CMFV, displayed by the black line, can be strongly violated.

In the right panel of figure 5.9 we plot the new CP-violating phases θ_X^K and θ_X^s against each other. We observe that while large new CP-violating effects are possible in the K system, the effects are much less pronounced in the B_s system. The B_d system again constitutes an intermediate scenario. We find the ranges

$$-45° \leq \theta_X^K \leq 25°\,, \qquad -9° \leq \theta_X^d \leq 8°\,, \qquad -2° \leq \theta_X^s \leq 7°\,. \tag{5.12}$$

We note that non-vanishing complex phases can only occur in the presence of new sources of CP-violation beyond the standard CKM one and therefore constitute a clear sign of NP beyond the MFV hypothesis. The possible deviations from MFV in the RS model considered will be described in more detail in section 5.5.2.

The pattern of NP effects in the functions Y_i and Z_i $(i = K, d, s)$ is similar to the one encountered above, although the overall size of effects is more pronounced in these cases, due to the SM hierarchy

$$X(x_t) > Y(x_t) > Z(x_t)\,. \tag{5.13}$$

Numerical ranges for the possible NP contributions to the functions Y_i and Z_i can be found in [36].

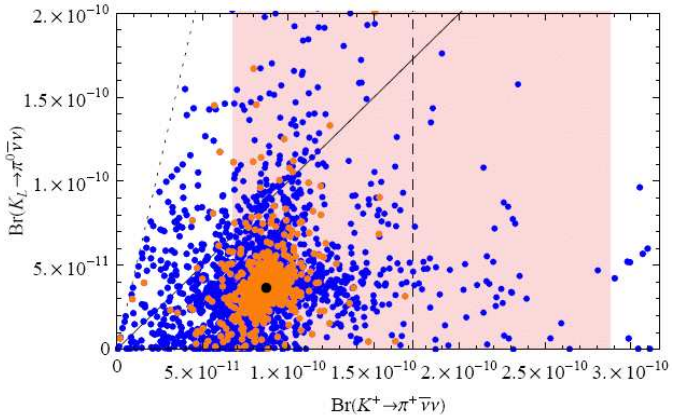

Figure 5.10: *$Br(K_L \to \pi^0\nu\bar{\nu})$ as a function of $Br(K^+ \to \pi^+\nu\bar{\nu})$. The shaded area represents the experimental 1σ-range for $Br(K^+ \to \pi^+\nu\bar{\nu})$. The GN-bound is displayed by the dotted line, while the solid line separates the two areas where $Br(K_L \to \pi^0\nu\bar{\nu})$ is larger or smaller than $Br(K^+ \to \pi^+\nu\bar{\nu})$. The black point represents the SM prediction.*

5.4.3 Rare K decays: $K \to \pi\nu\bar{\nu}$, $K_L \to \pi^0\ell^+\ell^-$, $K_L \to \mu^+\mu^-$

We have seen that large effects are to be expected in rare K decay branching ratios. Therefore we now turn our attention to the most prominent examples of this class, namely $Br(K^+ \to \pi^+\nu\bar{\nu})$, $Br(K_L \to \pi^0\nu\bar{\nu})$, $Br(K_L \to \pi^0\ell^+\ell^-)$ and $Br(K_L \to \mu^+\mu^-)$.

We have seen in section 4.4 that the $K \to \pi\nu\bar{\nu}$ decays are among the most sensitive channels for NP searches, and in addition the correlation between both decay rates can provide useful information on the correlation between $\Delta S = 2$ and $\Delta S = 1$ flavour violation [131]. Therefore we show in figure 5.10 $Br(K_L \to \pi^0\nu\bar{\nu})$ as a function of $Br(K^+ \to \pi^+\nu\bar{\nu})$. We observe that the $K^+ \to \pi^+\nu\bar{\nu}$ decay rate can be enhanced by up to a factor of 2, which could be welcome one day if the central experimental value stays around $15 \cdot 10^{-11}$ and its error decreases. $K_L \to \pi^0\nu\bar{\nu}$ turns out to be even more sensitive to RS effects, and it can be increased by as much as a factor of 3 over its SM prediction. Interestingly, no visible correlation between the two decay rates is found, so that for a given value of $Br(K^+ \to \pi^+\nu\bar{\nu})$ all values for $Br(K_L \to \pi^0\nu\bar{\nu})$ consistent with the Grossman-Nir (GN) bound [162] can be reached. As discussed in detail in [131], this non-correlation originates in the fact that in the RS model with custodial protection, the new CP-violating phases in $K^0 - \bar{K}^0$ mixing and the rare K decays turn out to be independent of each other, being a result of the $\mathcal{Q}_2^{LR}$ contribution dominating $K^0 - \bar{K}^0$ mixing.

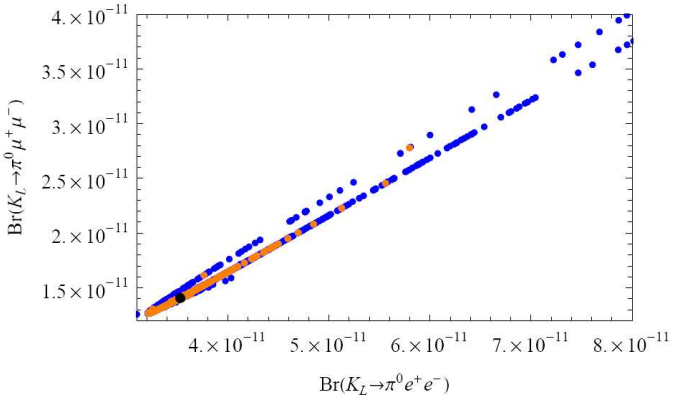

Figure 5.11: *$Br(K_L \to \pi^0\mu^+\mu^-)$ as a function of $Br(K_L \to \pi^0 e^+e^-)$, assuming constructive interference. The black point represents the SM prediction.*

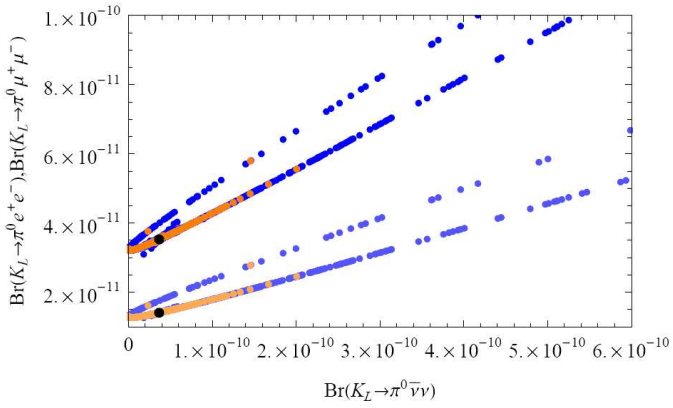

Figure 5.12: *$Br(K_L \to \pi^0 e^+e^-)$ (upper curve) and $Br(K_L \to \pi^0\mu^+\mu^-)$ (lower curve) as functions of $Br(K_L \to \pi^0\nu\bar{\nu})$. The corresponding SM predictions are represented by black points.*

Next we consider the correlation between $Br(K_L \to \pi^0\mu^+\mu^-)$ and $Br(K_L \to \pi^0 e^+e^-)$, that we show in figure 5.11. We observe that these two decays are very strongly correlated in the model in question, and both branching ratios can be enhanced by up to a factor of 1.5. As pointed out and analysed in detail in [139, 141, 142], accurately measuring the two branching ratios in question provides interesting information on the operator structure entering rare K decays. Eventually finding the correlation seen in 5.11 violated would not only rule out the RS model with custodial protection, but at the same time all NP models with no relevant scalar operator contributions to the $K_L \to \pi^0\ell^+\ell^-$ decays.

In figure 5.12 we show the correlation between $Br(K_L \to \pi^0\ell^+\ell^-)$ and $Br(K_L \to \pi^0\nu\bar{\nu})$ that has first been studied in [123] in the context of the LHT model. Also in

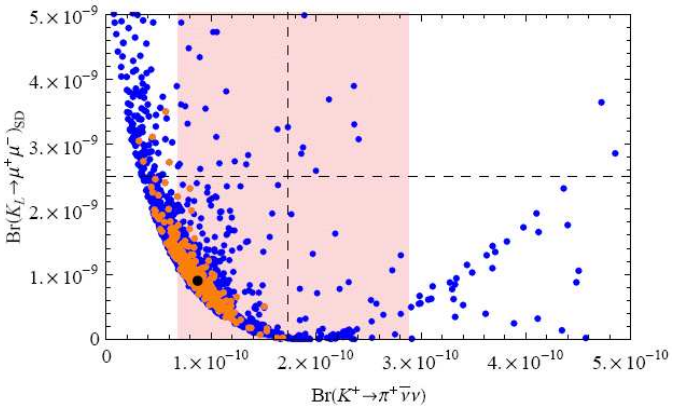

Figure 5.13: *Correlation between $K_L \to \mu^+\mu^-$ and $K^+ \to \pi^+\nu\bar{\nu}$. The black point represents the SM prediction.*

the RS model with custodial protection, we observe a strong correlation between the decay rates in question. This can easily be understood by noting that the $K_L \to \pi^0\nu\bar{\nu}$ mode is purely CP-violating and the $K_L \to \pi^0\ell^+\ell^-$ decays are by far dominated by CP-violating effects. Therefore, as in the RS model in question the CP-violating phases entering these decays are universal, a strict correlation emerges.

The fourth interesting K decay mode is $K_L \to \mu^+\mu^-$. While it receives significant long-distance contributions and is therefore theoretically much less under control, a useful upper bound on the short distance (SD) contribution, $Br(K_L \to \mu^+\mu^-)_{\rm SD} < 2.5 \cdot 10^{-9}$, can be derived [148], as mentioned already in section 4.4. In figure 5.13 we show the SD contribution to $K_L \to \mu^+\mu^-$ as a function of $Br(K^+ \to \pi^+\nu\bar{\nu})$. We observe that while in most cases the bound on $Br(K_L \to \mu^+\mu^-)_{\rm SD}$ is satisfied by the RS model in question, it can in principle be violated. However such large enhancements appear only if $Br(K^+ \to \pi^+\nu\bar{\nu})$ is suppressed with respect to its SM prediction, which is disfavoured by the data anyway. As both $K^+ \to \pi^+\nu\bar{\nu}$ and $K_L \to \mu^+\mu^-$ are CP-conserving decays, a non-trivial correlation emerges also between these two modes. Interestingly, in contrast to the roughly linear correlations seen in figures 5.11 and 5.12, the correlation between $Br(K_L \to \mu^+\mu^-)_{\rm SD}$ and $Br(K^+ \to \pi^+\nu\bar{\nu})$ appears to be an inverse one, so that for $Br(K^+ \to \pi^+\nu\bar{\nu})$ close to the experimental central value, $Br(K_L \to \mu^+\mu^-)_{\rm SD}$ is close to zero. The origin of this correlation is easy to see: In the model in question $\Delta F = 1$ processes are governed by right-handed flavour changing Z couplings, generating the current $(\bar{s}d)_{V+A}$ in addition to the SM $(\bar{s}d)_{V-A}$ one. As K_L, K^+ and π^+ are pseudoscalar mesons, the relevant matrix elements can be straightforwardly related to

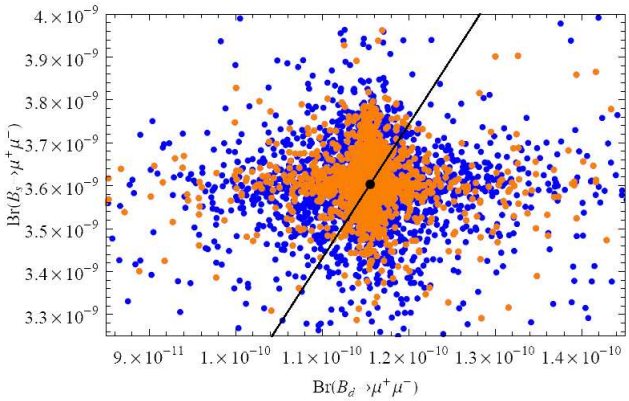

Figure 5.14: *$Br(B_s \to \mu^+\mu^-)$ versus $Br(B_d \to \mu^+\mu^-)$. The straight line represents the CMFV correlation and the black point the SM prediction.*

each other, and one finds

$$\langle \pi^+|(\bar{s}d)_{V+A}|K^+\rangle = \langle \pi^+|(\bar{s}d)_{V-A}|K^+\rangle\,, \tag{5.14}$$

$$\langle 0|(\bar{s}d)_{V+A}|K_L\rangle = -\langle 0|(\bar{s}d)_{V-A}|K_L\rangle\,. \tag{5.15}$$

Consequently, while SM and NP contributions interfere *constructively* in the case of $K^+ \to \pi^+\nu\bar{\nu}$, they interfere *destructively* in the case of $K_L \to \mu^+\mu^-$. The correlation between $K_L \to \mu^+\mu^-$ and $K^+ \to \pi^+\nu\bar{\nu}$ thus provides an interesting possibility to disentangle whether NP induces dominantly left- or right-handed FCNC contributions. Unfortunately though the power of this test is limited by the sizable theoretical uncertainties in $Br(K_L \to \mu^+\mu^-)$, and progress on this field would be very welcome.

5.4.4 Rare B decays: $B_{d,s} \to \mu^+\mu^-$, $B \to X_{s,d}\nu\bar{\nu}$

The discussion of section 5.4.2 let us anticipate that the effects in rare B decays are much less pronounced than in the case of rare K decays discussed so far. In what follows we will restrict our attention mainly to the decays $B_{s,d} \to \mu^+\mu^-$ and $B \to X_{s,d}\nu\bar{\nu}$. We remark that also the decays $B \to X_s\gamma$ and $B \to X_s\ell^+\ell^-$ have received a lot of attention during the last years and a lot of progress has been made both on the experimental and theoretical side. As these modes are affected by potentially large one-loop contributions to the dipole operators [39, 98], we leave a discussion of these modes within the RS model with custodial protection for future work.

In figure 5.14 we show the correlation between the purely leptonic decays $B_s \to \mu^+\mu^-$ and $B_d \to \mu^+\mu^-$. We observe that their branching ratios can deviate by

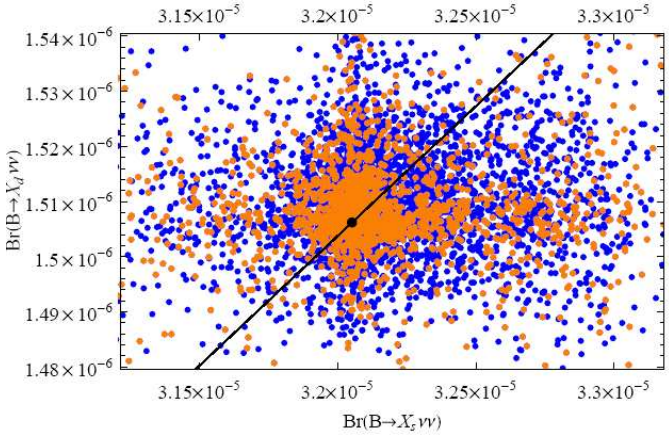

Figure 5.15: *Correlation between* $Br(B \to X_s\nu\bar{\nu})$ *and* $Br(B \to X_d\nu\bar{\nu})$. *The black line represents the universal CMFV result given by the ratio* $|V_{td}|^2/|V_{ts}|^2$, *and the black point the SM prediction.*

at most $\sim 10\%$ and $\sim 20\%$, respectively, from their SM predictions. This can be understood from the custodial protection mechanism being more powerful in B than in K physics. In addition in the custodially protected RS model no scalar operator contributions are generated that would lead to potentially large effects in the decays in question. Consequently it will be very challenging for experimentalists to disentangle a possible effect of the custodially protected RS model in these modes. Still it would be interesting to measure precisely the two branching ratios in question, as any deviation from the black line in figure 5.14 would signal flavour non-universalities and therefore the presence of a NP flavour structure beyond the CMFV hypothesis[6].

The picture emerging in the case of $Br(B \to X_s\nu\bar{\nu})$ and $Br(B \to X_d\nu\bar{\nu})$ is quite analogous, see figure 5.15. Also here the custodial protection mechanism turns out to be extremely powerful, so that the branching ratios in question can be affected by at most $\sim 5\%$ and $\sim 10\%$, respectively. At the same time, flavour universality can be strongly broken.

5.4.5 Correlations between K and B physics observables

The results presented so far lead to the conclusion that the effects of the custodially protected RS model are generally much more pronounced in K physics than in B physics. An exceptional role is herewith played by CP-violating effects in the

[6] A similarly strong correlation has been observed in the more general MFV framework, in which new operators are allowed [163].

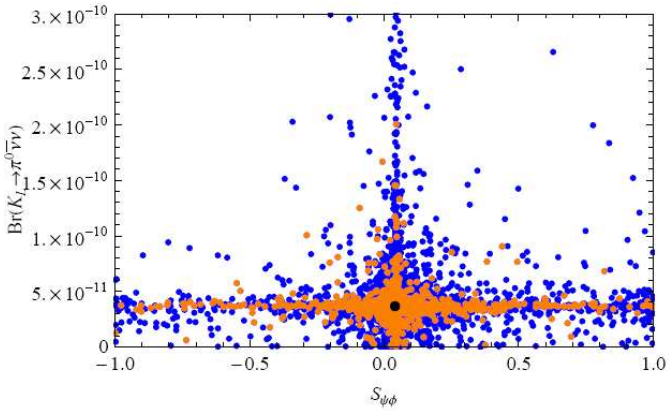

Figure 5.16: *$Br(K_L \to \pi^0\nu\bar{\nu})$ as a function of $S_{\psi\phi}$. The black point represents the SM prediction.*

$B_s - \bar{B}_s$ system, observable through the time-dependent CP-asymmetry $S_{\psi\phi}$. In the latter asymmetry, and consequently also in the semi-leptonic asymmetry $A^s_{\rm SL}$, spectacularly large effects are possible. While we have so far considered correlations only among various observables in either the K or in the B system, the aim of the present section is to study possible correlations between the two systems.

To this end, we start by considering two of the most interesting flavour observables in the model in question: In figure 5.16 we show $Br(K_L \to \pi^0\nu\bar{\nu})$ as a function of $S_{\psi\phi}$. While we can see also from this plot that large effects can emerge in either $S_{\psi\phi}$ or the $K_L \to \pi^0\nu\bar{\nu}$ decay, the apparent cross-like structure shows that *simultaneously* large effects in *both* observables turn out to be extremely unlikely. Therefore if eventually the present hints for a large value of $S_{\psi\phi}$ are confirmed, $Br(K_L \to \pi^0\nu\bar{\nu})$ is predicted by the custodially protected RS model to be close to its SM value, and finding this decay rate significantly enhanced would put the model in question in serious trouble. On the other hand, a SM-like $S_{\psi\phi}$ would open the road towards potentially large effects in the $K_L \to \pi^0\nu\bar{\nu}$ decay. The reason behind this exclusive structure is in fact easy to identify: While the rare K decays are fully dominated by the flavour non-universal effects in the right-handed quark sector, $B_s - \bar{B}_s$ mixing is roughly equally affected by the operators $\mathcal{Q}_1^{VLL}$ and $\mathcal{Q}_2^{LR}$, i. e. large flavour non-universal effects are required in the left-handed sector. Clearly large flavour breaking effects require the corresponding quark sector to be placed closer towards the IR brane. As the scale of 5D Yukawa couplings is fixed to $\mathcal{O}(1)$, in order to generate the observed pattern of quark masses, this automatically implies that the oppositely-handed quark sector has to live further in the UV, so that the flavour breaking effects in this system decrease.

Next in figure 5.17 we consider the correlation between $Br(K^+ \to \pi^+\nu\bar{\nu})$ and $Br(B_s \to \mu^+\mu^-)/Br(B_s \to \mu^+\mu^-)_{\rm SM}$. Again we observe that the RS affects can

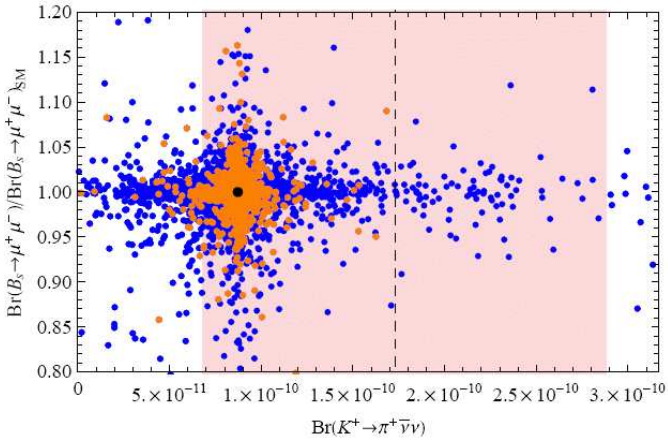

Figure 5.17: $Br(B_s \to \mu^+\mu^-)/Br(B_s \to \mu^+\mu^-)_{SM}$ *as a function of* $Br(K^+ \to \pi^+\nu\bar{\nu})$. *The shaded area represents the experimental* 1σ*-range for* $Br(K^+ \to \pi^+\nu\bar{\nu})$ *and the black point shows the SM prediction.*

be much larger in the rare K decay than in the B_s one. We also find that if a sizable NP contribution enters $Br(K^+ \to \pi^+\nu\bar{\nu})$, the non-standard effects in $Br(B_s \to \mu^+\mu^-)$ become even smaller and typically below $\sim 5\%$ for $Br(K^+ \to \pi^+\nu\bar{\nu})$ close to its experimental central value. We note however that the cross-like structure, excluding simultaneous large NP effects, is much less pronounced in this case than in case of $K_L \to \pi^0\nu\bar{\nu}$ and $S_{\psi\phi}$ considered before. This is due to the fact that now the RS effects in both $K^+ \to \pi^+\nu\bar{\nu}$ and $B_s \to \mu^+\mu^-$ are dominated by right-handed currents.

Finally in figure 5.18 we show $Br(K_L \to \mu^+\mu^-)_{\rm SD}$ as a function of $Br(B_s \to \mu^+\mu^-)$. We find that due to the much more pronounced effects in $K_L \to \mu^+\mu^-$, the flavour universal prediction of models with CMFV, displayed by the black line, can be significantly violated.

5.5 Comparison with other new physics frameworks

5.5.1 Pattern of effects in the custodially protected RS model

So far we have concentrated on the possible NP effects in various $\Delta F = 2$ and $\Delta F = 1$ flavour violating observables predicted by the RS model with custodial protection. In this context we have identified a specific pattern of effects that should help to distinguish this model from other NP frameworks. In particular we have seen that:

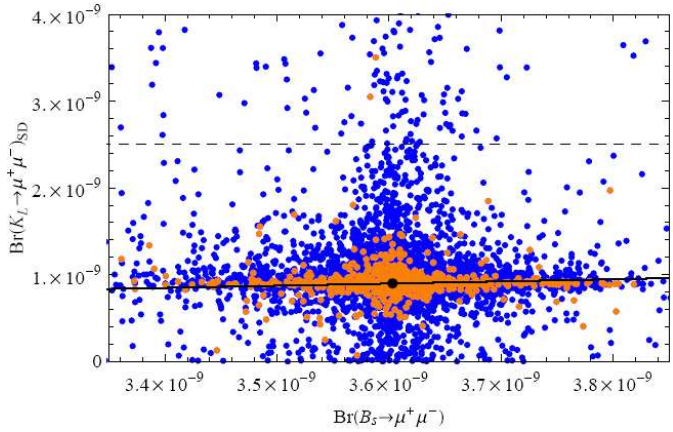

Figure 5.18: *$Br(K_L \to \mu^+\mu^-)_{SD}$ as a function of $Br(B_s \to \mu^+\mu^-)$. The dashed line indicates the upper bound on $Br(K_L \to \mu^+\mu^-)_{SD}$. The solid line shows the CMFV prediction, while the black point represents the SM.*

- Large effects are possible in CP-violation in $B_s - \bar{B}_s$ mixing, allowing for the full range $-1 \leq S_{\psi\phi} \leq 1$. Simultaneously spectacular effects are found in the semileptonic CP-asymmetry $A^s_{\rm SL}$.
- Large effects are also possible in rare K decay branching ratios, enhancing $K \to \pi\nu\bar{\nu}$ and $K_L \to \pi^0\ell^+\ell^-$ by up to factors $2-3$ and 1.5, respectively, and the SD contribution to $K_L \to \mu^+\mu^-$ up to its present upper limit.
- Interesting correlations appear between the various K decay channels, specifically:
  - A strong linear correlation appears between $K_L \to \pi^0 e^+e^-$ and $K_L \to \pi^0\mu^+\mu^-$, and between $K_L \to \pi^0\nu\bar{\nu}$ and $K_L \to \pi^0\ell^+\ell^-$.
  - The correlation between $K^+ \to \pi^+\nu\bar{\nu}$ and the SD contribution to $K_L \to \mu^+\mu^-$ is an inverse one.
  - No visible correlation appears in the $K \to \pi\nu\bar{\nu}$ system.
- Large effects in $S_{\psi\phi}$ and the rare K decays can *not* appear *simultaneously*.
- The effects in rare B decays are predicted to be small.
- The flavour universality between effects in the K, B_d and B_s systems can be strongly violated.

In order to demonstrate how this pattern of effects can serve as a tool to distinguish the RS model in question from other popular extensions of the SM, we will now show in explicit terms how such a distinction can be made in practice. To this end we concentrate on two NP frameworks. First we discuss the class of models with MFV, both constrained and general. After that we turn our attention to the

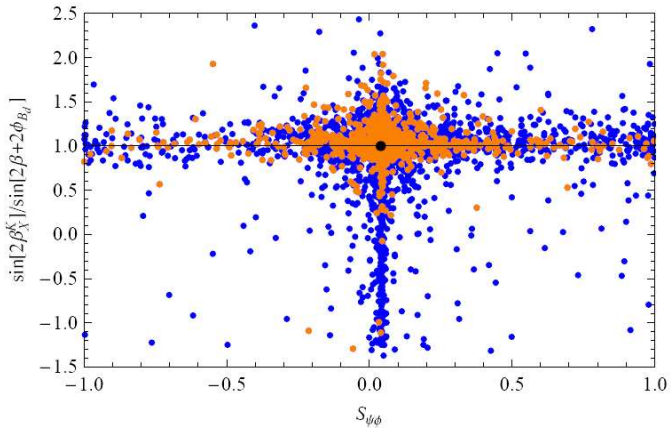

Figure 5.19: $\sin 2\beta_X^K / \sin(2\beta + 2\varphi_{B_d})$ *as a function of* $S_{\psi\phi}$*. The departure from unity (solid line) measures the size of non-MFV effects. The black point represents the SM prediction.*

LHT model, a model that contains new sources of flavour and CP-violation but generates only contributions to the SM operators.

5.5.2 Minimal flavour violation

In MFV models all flavour violation is exclusively generated by the SM Yukawa couplings, so that no new sources of flavour and CP-violation beyond the CKM ones are present [8–10]. In the constrained version of this class of models, in addition the requirement holds that no new operators mediate FCNCs beyond the ones already relevant in the SM [11, 12, 121].

It is common to both versions of MFV that no new CP-violating phases appear. Consequently one finds immediately

$$(S_{\psi\phi})_{\rm MFV} = (S_{\psi\phi})_{\rm SM} \simeq 0.04\,, \tag{5.16}$$

so that confirming one day the present hints for a large $S_{\psi\phi}$ would not only rule out the SM, but at the same time the whole class of MFV models. As we have seen before, the RS model with custodial protection is one candidate model to explain such large effects.

As in MFV models the phase of the CKM matrix is the only source of CP-violation entering universally K, B_d and B_s systems, interesting correlations among various CP-violating observables appear. One particularly clean test of this universality is given by comparing CP-violating effects in $B_d - \bar{B}_d$ mixing, measured in $S_{\psi K_S}$, to CP-violation in the $K \to \pi\nu\bar{\nu}$ system. In the latter case, the phase β_X^K defined

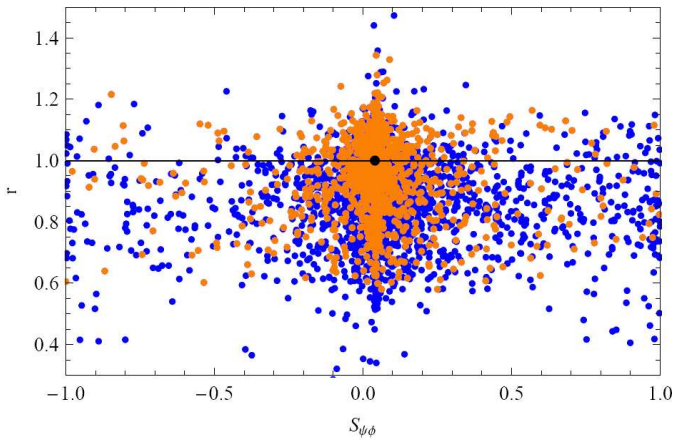

Figure 5.20: *The ratio r of (5.19) as a function of $S_{\psi\phi}$. The black point indicates the SM and CMFV value.*

in (4.95), can be determined from the measurement of both branching ratios. In the SM and all MFV models, the function X_K is real and therefore

$$S_{\psi K_S} = \sin 2\beta = (\sin 2\beta)_{K\to\pi\nu\bar{\nu}}\,, \tag{5.17}$$

holds to very good approximation [164, 165]. Consequently any deviation of the ratio

$$\frac{(\sin 2\beta)_{K\to\pi\nu\bar{\nu}}}{S_{\psi K_S}} = \frac{\sin 2\beta_X^K}{\sin(2\beta + 2\varphi_{B_d})} \tag{5.18}$$

from unity would signal the presence of new sources of CP-violation beyond the SM and MFV one. In figure 5.19 we show the ratio in (5.18) as a function of $S_{\psi\phi}$. We observe that in the custodially protected RS model, large deviations from unity for the ratio (5.18) are possible, and even its sign can be reversed. Such spectacular effects are however only possible if $S_{\psi\phi}$ is SM-like. However, even for large values of $S_{\psi\phi}$, deviations of up to 50% from the MFV prediction are possible albeit very unlikely. Clearly, as the SM prediction for $S_{\psi K_S}$ is in good agreement with the data and therefore φ_{B_d} is restricted to be small, such large effects are only possible if NP affects the $K \to \pi\nu\bar{\nu}$ decays in a significant manner.

While the general MFV hypothesis can be best tested via the comparison of various CP-violating effects, additional strong correlations appear in its constrained version also among CP-conserving observables. Several examples for tests of this flavour universality have been indicated already by the solid lines in figures 5.9, 5.14, 5.15, 5.18, where deviations from this universality line would be a clear signal of physics beyond the CMFV framework.

Another powerful probe of the CMFV hypothesis is given by the relation

$$\frac{Br(B_s \to \mu^+\mu^-)}{Br(B_d \to \mu^+\mu^-)} = \frac{\hat{B}_{B_d}}{\hat{B}_{B_s}} \frac{\tau(B_s)}{\tau(B_d)} \frac{\Delta M_s}{\Delta M_d}\, r\,, \quad r = \left|\frac{Y_s}{Y_d}\right|^2 \frac{C_{B_d}}{C_{B_s}}\,, \tag{5.19}$$

with $r = 1$ in CMFV models [166] but generally different from unity. Here $C_{B_{s,d}}$ has been defined in (4.61). In figure 5.20 we show the ratio r as a function of $S_{\psi\phi}$. We observe that in the RS model with custodial protection

$$0.6 \lessapprox r \lessapprox 1.3 \tag{5.20}$$

is possible, with this range being quite insensitive to the actual value of $S_{\psi\phi}$.

Furthermore, also the possible size of effects can be used to distinguish the CMFV class of models from scenarios beyond this hypothesis, such as the RS model considered here. As in the CMFV framework flavour violating effects enter the various meson systems in a universal manner, the constraints on the already measured decays $B \to X_s\gamma$ and $B \to X_s\ell^+\ell^-$ can be used to put upper bounds on other rare decay branching ratios, under the quite reasonable assumption that the NP effects are dominantly mediated by Z-penguins while the box contributions are subleading [167]. Including in addition also the the flavour conserving constraint from the $Zb_L\bar{b}_L$ coupling, the respective bounds become even stronger and one finds the allowed ranges

$$4.29 \cdot 10^{-11} \leq Br(K^+ \to \pi^+\nu\bar{\nu}) \leq 10.72 \cdot 10^{-11}\,, \tag{5.21}$$

$$1.55 \cdot 10^{-11} \leq Br(K_L \to \pi^0\nu\bar{\nu}) \leq 4.38 \cdot 10^{-11}\,, \tag{5.22}$$

$$1.17 \cdot 10^{-9} \leq Br(B_s \to \mu^+\mu^-) \leq 6.67 \cdot 10^{-9}\,, \tag{5.23}$$

$$0.36 \cdot 10^{-10} \leq Br(B_d \to \mu^+\mu^-) \leq 2.03 \cdot 10^{-10} \tag{5.24}$$

at the 95% confidence level [168]. We observe that while the NP effects in the rare K decays are much more restricted in the CMFV models, the situation is opposite in case of $B_{d,s}$ decays, where the CMFV framework generally allows for larger effects than the custodially protected RS model.

Finally let us mention that also the mass differences ΔM_d and ΔM_s by themselves can provide a useful test of the CMFV hypothesis, if the non-perturbative uncertainties in the relevant hadronic parameters $F_{B_d}\sqrt{\hat{B}_{B_d}}$ and $F_{B_s}\sqrt{\hat{B}_{B_s}}$ will be significantly reduced by future lattice calculations. Finding then $\Delta M_d < (\Delta M_d)_{\rm SM}$ and/or $\Delta M_s < (\Delta M_s)_{\rm SM}$ would be a clear signal of either new sources of flavour and CP-violation, or new operators in addition to the SM $\mathcal{Q}_1^{VLL}$ one, or the presence of new Majorana fermions or new heavy $U(1)$ gauge bosons contributing only at the loop level [169]. Clearly, as the RS model in question provides the first two conditions, a suppression of $\Delta M_{s,d}$ could indeed be explained in that context.

5.5.3 Littlest Higgs model with T-parity

Having discussed in detail how the RS model with custodial protection can be distinguished from the MFV class of models, we now turn our attention to models in which new sources of flavour and CP-violation are present, but no new operators are generated. A prime example of this class of models is the Littlest Higgs model with T-parity (LHT). Therefore let us briefly recall the basic structure of this particular model.

The Little Higgs class of models [41,42] aims to address the little hierarchy problem by introducing an enlarged global and local symmetry structure. The Higgs boson then arises as a pseudo-Goldstone boson, when this symmetry is spontaneously broken at the NP scale $f \sim 1\,\text{TeV}$. In order to keep the Higgs potential stable against radiative corrections, the symmetry breaking has to appear *collectively*. One of the most economical realisations of this concept is the Littlest Higgs model (LH) [45], which is based on an $SU(5) \to SO(5)$ global symmetry breaking pattern. Here, in addition to the SM gauge and matter fields new heavy gauge bosons $W_H^\pm$, Z_H and A_H, the heavy top partner T and a scalar triplet Φ with $\mathcal{O}(1\,\text{TeV})$ masses are present. Reviews can be found in [43, 44].

When studying electroweak precision observables, it turns out that an additional discrete symmetry, called T-parity [46, 47], is needed in order to allow for the new particles below the 1 TeV scale. Under this symmetry, the SM particles and the heavy top partner T_+ are even, while $W_H^\pm, Z_H, A_H$ and Φ are odd. A consistent implementation of T-parity requires also the introduction of mirror fermions – one for each quark and lepton species – that are odd under T-parity [48]. A detailed description of the LHT model has been presented in [123], where also a complete set of Feynman rules can be found[7].

While the LH model without T-parity belonged to the CMFV class of models, implying generally small effects in flavour violating observables [171,172], the mirror quarks in the LHT model introduce new sources of flavour and CP-violation, parameterised by the new mixing matrix V_{Hd} [110, 173]. Potentially large deviations from the SM and CMFV predictions in FCNC processes can thus appear [109,111,119,122,123,159,161,170,174,175]. A brief review of these analyses can be found in [160]. Interestingly however, as the couplings between SM quarks and mirror quarks, mediated by the heavy T-odd gauge bosons, are purely left-handed, no new operators beyond the SM ones arise [109, 123]. Consequently a very specific pattern of flavour violating effects emerges.

In what follows we will concentrate on those K and B physics predictions of the LHT model that can best be used to distinguish this model from the RS model

[7] Some corrections to these rules have been pointed out in [122, 161, 170].

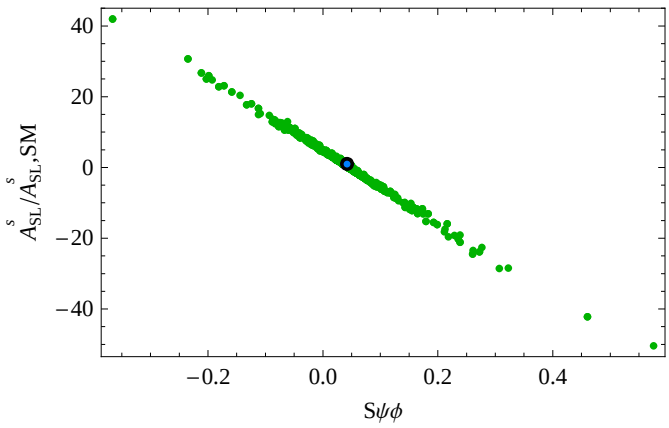

Figure 5.21: *Correlation between $S_{\psi\phi}$ and A_{SL}^s in the LHT model. The light blue point shows the contribution of the T-even sector, and the black point represents the SM prediction. The corresponding result in the custodially protected RS model has been presented in figure 5.6.*

with custodial protection. For further details and a recent numerical update we refer the reader to [122].

In figure 5.21 we show the correlation between the CP-asymmetries $S_{\psi\phi}$ and $A_{\rm SL}^s$ predicted by the LHT model. The observed strong correlation between these two observables is analogous to the one encountered in case of the custodially protected RS model in figure 5.6 and reflects the fact that both models do not induce directly CP-violating effects in the $B_s \to \psi\phi$ decay[8]. We can see that LHT dynamics can hardly generate $|S_{\psi\phi}| \gtrsim 0.2$. Consequently confirming one day the present hints for values as large as $S_{\psi\phi} \gtrsim 0.4$ [154–156] would put the LHT model under pressure and favour the custodially protected RS model.

A second clean possibility to distinguish between RS and LHT physics is offered by the correlations among the various rare K decays. While the correlations between $K_L \to \pi^0\ell^+\ell^-$ and $K_L \to \pi^0\nu\bar{\nu}$ and within the $K_L \to \pi^0\ell^+\ell^-$ system look similar in both models, the situation is completely different in case of the $K \to \pi\nu\bar{\nu}$ system. While in the custodially protected RS model (see figure 5.10) no visible correlation between the two branching ratios appeared, we observe now in figure 5.22 that the LHT model gives rise to a strong correlation. Essentially only two branches of possible points are allowed: one with approximately SM-like $K_L \to \pi^0\nu\bar{\nu}$ and one parallel to the GN bound. The origin of this striking correlation has been analysed in a model-independent manner in [131]. In the LHT model flavour and CP-violating effects in the $\Delta S = 2$ and $\Delta S = 1$ systems are strongly

[8] The somewhat more stringent correlation observed in figure 5.21 can be attributed to the more sophisticated error analysis performed in [111, 122], compared to the simplified error analysis performed here and in [35, 36] in the custodially protected RS model.

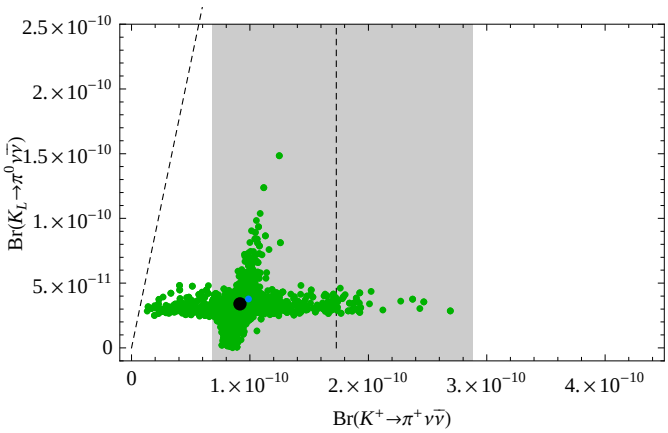

Figure 5.22: *Correlation between $Br(K^+ \to \pi^+\nu\bar{\nu})$ and $Br(K_L \to \pi^0\nu\bar{\nu})$ in the LHT model. The experimental 1σ rage and the model independent GN-bound are indicated. The light blue point shows the contribution of the T-even sector, and the black point represents the SM prediction. The corresponding result in the custodially protected RS model has been presented in figure 5.10.*

correlated, and no new operators can spoil this structure. Consequently the CP-phases governing $K^0 - \bar{K}^0$ mixing and the $K \to \pi\nu\bar{\nu}$ decays are approximately equal to each other (apart from a trivial factor 2). The correlation found in the $K \to \pi\nu\bar{\nu}$ system is thus a remnant of the strong experimental constraint on the CP-violating parameter ε_K. A similar correlation can be expected in most other NP models in which no new operators beyond the SM ones are present. The situation is fundamentally different in the custodially protected RS model. In that case $K^0 - \bar{K}^0$ mixing is dominated by the chirally enhanced operators $\mathcal{Q}^{LR}_{1,2}$, that cannot affect the rare K decays. Consequently in the latter model CP-violating effects in $K^0 - \bar{K}^0$ mixing and in the $K \to \pi\nu\bar{\nu}$ system are independent of each other and no correlation between $Br(K^+ \to \pi^+\nu\bar{\nu})$ and $Br(K_L \to \pi^0\nu\bar{\nu})$ arises. Thus finding one day the two branching ratios in question outside the range observed in figure 5.22 would not only rule out the LHT model, but would be a strong hint for new operator contributions to $K^0 - \bar{K}^0$ mixing that dilute the correlation between $\Delta S = 2$ and $\Delta S = 1$ CP-violating effects. We note that apart from the RS model with custodial protection, another famous candidate for this type of NP would be the MSSM with general flavour and CP-violating interactions.

We have seen already in section 5.4.4 that the NP operator structure can be tested also by means of the correlation between $Br(K^+ \to \pi^+\nu\bar{\nu})$ and $Br(K_L \to \mu^+\mu^-)_{\text{SD}}$, where we show the LHT prediction in figure 5.23. While in figure 5.13 we could observe that the RS model in question predicts an inverse correlation between these two modes, in the LHT model a linear correlation is found. As already

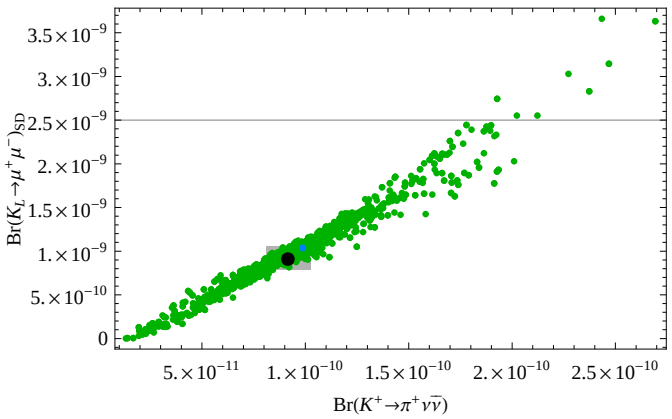

Figure 5.23: *Correlation between $Br(K^+ \to \pi^+ \nu\bar{\nu})$ and $Br(K_L \to \mu^+\mu^-)_{SD}$. The light blue point shows the contribution of the T-even sector, and the black point represents the SM prediction. The corresponding result in the custodially protected RS model has been presented in figure 5.13.*

discussed in section 5.4.4 this correlation provides a clear test of the handedness of the new flavour violating interactions. While in the custodially protected RS model the rare K decays are dominated by the flavour changing Z couplings to *right-handed* quarks, flavour violating effects in the LHT model are purely *left-handed*, thus explaining the linear correlation found in figure 5.23.

In many other cases the structure of flavour violating effects appears to be similar in the LHT model and in the custodially protected RS model. Specifically:

- Effects in K physics are generally larger than in B physics, with the exception of $B_s - \bar{B}_s$ CP-violation.
- Simultaneous large effects in K and B physics observables appear to be unlikely, although not rigorously excluded.
- Flavour universality can be strongly violated. As a consequence, correlations between various observables can differ significantly from their (C)MFV predictions.

On the other hand we have identified the following clean ways to distinguish the custodially protected RS model from the LHT model:

- The RS model in question allows for larger effects in the CP-asymmetries $S_{\psi\phi}$ and $A_{\rm SL}^s$ than the LHT model.
- The LHT model predicts a striking correlation in the $K \to \pi\nu\bar{\nu}$ system, while no visible correlation emerges in the RS model.
- The correlation between $Br(K^+ \to \pi^+ \nu\bar{\nu})$ and $Br(K_L \to \mu^+\mu^-)_{\rm SD}$ is funda-

mentally different in the two models.

Measuring one day all these observables will therefore provide a powerful tool to distinguish between these two models.

6 Summary and outlook

The Randall-Sundrum geometric background provides an appealing solution to the gauge hierarchy problem, by reducing the vast hierarchy between the electroweak and the Planck scale to a moderate hierarchy between the curvature scale k and the length L of the extra dimension. While to this end the Higgs sector needs to be placed on or near the IR brane, the gauge and fermionic matter content has to be promoted to the 5D bulk in order to avoid stringent constraints on higher-dimensional operators. For each field living in the 5D bulk then a full tower of massive (TeV scale) Kaluza-Klein states arises, in addition to the light zero mode corresponding to the respective SM field. These KK excitation are then accessible to direct searches at the LHC experiments Atlas and CMS. In addition their presence also leads to modified predictions of low-energy precision observables, both in the electroweak and in the flavour sector.

In the present thesis we have studied in detail the RS model with custodial protection of the T parameter and the flavour diagonal and non-diagonal $Zd^i_L\bar{d}^j_L$ couplings. While the stringent bounds from electroweak precision observables do not allow for RS physics with only the SM gauge group in the 5D bulk in the reach of the LHC, these constraints can be avoided by enlarging the gauge group by an additional factor $SU(2)_R$ and a discrete P_{LR} symmetry. The gauge group is then broken to the SM one by appropriate boundary conditions on the UV brane. Having introduced the full 5D action of the custodially protected RS model, we analysed in detail its various sectors.

Herewith particular emphasis has been put on the flavour sector of the model. Bulk fermions in the RS background provide an interesting interpretation of flavour. With slightly different 5D bulk mass parameters the observed hierarchies is the SM quark masses and CKM mixing parameters can be explained so that the flavour hierarchy problem is reduced to the problem of appropriately chosen $\mathcal{O}(1)$ bulk mass parameters and fundamental Yukawa couplings. Together with the exponential suppression of the effective Yukawa couplings also all flavour violating interactions turn out to be suppressed by the same flavour hierarchies. This so-called RS-GIM mechanism helps to suppress most of the otherwise dangerously large tree level FCNC contributions induced by the presence of the gauge KK modes.

After classifying the various flavour violating couplings present already at tree level

in the model in question, we have studied their impact on particle-antiparticle mixing in the neutral K and $B_{d,s}$ meson sectors. Subsequently we have evaluated the new tree level contributions to the most interesting rare K and $B_{d,s}$ decays. The study of decays like $B \to X_s\gamma$ and $B \to X_s\ell^+\ell^-$ requires the calculation of the new RS contributions to the dipole operators $\mathcal{Q}_{7\gamma}$ and $\mathcal{Q}_{8G}$ that appear first at the one-loop level, and is thus left for future work.

Having at hand analytic formulae for the $\Delta F = 2$ and $\Delta F = 1$ processes in question, we have performed an extensive numerical analysis of the new RS effects in the various observables. To this end we have performed a scan over the full parameter space of the model, with KK gauge bosons in the reach of the LHC, and fitting all quark masses and CKM parameters to their observed values.

In the $\Delta F = 2$ sector we focused mainly on the mass differences ΔM_K, ΔM_d and ΔM_s related to the $K^0 - \bar{K}^0$, $B_d - \bar{B}_d$ and $B_s - \bar{B}_s$ systems, respectively, as well as on the CP-violating parameter ε_K, the CP-asymmetries $S_{\psi K_S}$ and $S_{\psi\phi}$, the semileptonic asymmetry $A^s_{\rm SL}$ and the width difference $\Delta\Gamma_s$, probing new mixing-induced CP-violation in the various meson systems. We also analysed the required fine-tuning necessary to bring the new RS contributions to the various observables in agreement with the data. Our findings in the $\Delta F = 2$ sector can be summarised as follows:

1. The new RS effects in $K^0 - \bar{K}^0$ mixing are dominated by the contributions of the operators $\mathcal{Q}_2^{LR}$ that receive a strong chiral and QCD enhancement. Consequently tree level exchanges of KK gluons are most important.
2. The enhancement of $\mathcal{Q}_2^{LR}$ is weaker in the case of $B_{d,s} - \bar{B}_{d,s}$ mixings, so that the contributions of the operator $\mathcal{Q}_1^{VLL}$ are equally important. Consequently the electroweak gauge bosons Z_H and Z' contribute significantly to $\Delta B = 2$ observables and have to be taken into account.
3. Z contributions on the other hand are negligible in all $\Delta F = 2$ observables, being of higher order in the v^2/M^2 expansion. Furthermore their left-handed flavour violating couplings are strongly suppressed by the custodial P_{LR} symmetry.
4. A stringent constraint is placed by the CP-violating observable ε_K, which in the case of completely anarchic 5D Yukawa couplings leads to the constraint $M \gtrsim 20\,\text{TeV}$. However also for low scales $M \simeq (2-3)\,\text{TeV}$ in the reach of the LHC an agreement with the data can be obtained, if the completely anarchic ansatz is partly abandonned.
5. Generically for such low values of M a large amount of fine-tuning is required in order to obtain agreement with the ε_K data, although there exist regions in the parameter space where only a moderate tuning $\Delta_{\rm BG}(\varepsilon_K)$ is necessary.
6. All other $\Delta F = 2$ constraints can be naturally fulfilled, and a simultaneous

fit of all available data is possible.

7. Thanks to the presence of new CP-violating phases, possible slight tensions between the tree level determination of V_{ub} and the observed values for the CP-asymmetry $S_{\psi K_S}$ and the parameter ε_K arising in the SM can easily be resolved in the custodially protected RS model.

8. At the same time large deviations of the CP-asymmetry $S_{\psi\phi}$ from its tiny SM value 0.04 are possible, allowing for the full range $-1 < S_{\psi\phi} < 1$. Due to the strong correlation with the semileptonic asymmetry $A^s_{\rm SL}$ also the latter observables can be enhanced by more than two orders of magnitude.

Subsequently we quantified the size of effects in various rare decays that remain possible after imposing all existing constraints from the $\Delta F = 2$ sector analysed previously. To this end we concentrated on the branching ratios for $K_L \to \pi^0\nu\bar{\nu}$, $K^+ \to \pi^+\nu\bar{\nu}$, $K_L \to \pi^0\ell^+\ell^-$ ($\ell = \mu, e$), $K_L \to \mu^+\mu^-$, $B \to X_{s,d}\nu\bar{\nu}$ and $B_{s,d} \to \mu^+\mu^-$. Apart from determining the size of NP effects, we also studied possible correlations between the various rare K decays, between rare K and B decays, and also between $\Delta F = 1$ and $\Delta F = 2$ observables. Specifically the main results of this analysis are:

9. The new contributions to the rare decay branching ratios in question are dominated by the flavour violating Z boson couplings to *right-handed* down-type quarks. This is due to the custodial protection of $Zd^i_L\bar{d}^j_L$ couplings and to the geometric suppression $\sim 1/(kL)$ of the KK gauge boson contributions.

10. Consequently a very specific pattern of effects arises, with possible large effects in rare K decays, but much smaller in rare B decays. This pattern is very different from RS models without custodial protection, where effects of roughly equal size are expected.

11. $Br(K_L \to \pi^0\nu\bar{\nu})$, $Br(K^+ \to \pi^+\nu\bar{\nu})$, $Br(K_L \to \pi^0\ell^+\ell^-)$ and $Br(K_L \to \mu^+\mu^-)_{\rm SD}$ can be enhanced by a factor $2-3$ with repsect to their SM values. Such large effects are however excluded if $S_{\psi\phi}$ is found significantly different from its SM prediction.

12. Interesting correlations appear between the various rare K modes. In particular:

    - The $K \to \pi\nu\bar{\nu}$ decay rates appear to be totally uncorrelated, being a result of the chirally enhanced left-right contributions to ε_K that spoil the connection between $\Delta S = 2$ and $\Delta S = 1$ CP-violating phases.
    - Strict linear correlations are observed between the decays $K_L \to \pi^0\nu\bar{\nu}$, $K_L \to \pi^0\mu^+\mu^-$ and $K_L \to \pi^0 e^+e^-$. Those are a remnant of the absence of scalar operator contributions and test the universality of CP-violating phases in various rare K decays.

- An inverse correlation is found between $K^+ \to \pi^+\nu\bar{\nu}$ and the short-distance contribution to $K_L \to \mu^+\mu^-$. While this correlation in principle provides a clean test of the handedness of the relevant flavour violating interactions, it is shadowed by the poor theoretical knowledge of the long-distance contributions dominating $K_L \to \mu^+\mu^-$.

13. Effects in rare B are small, typically below $(10-20)\%$ of the SM prediction, and therefore extremely challenging for future experiments.
14. Flavour universality between the K, B_d and B_s systems is generally strongly violated.

This specific pattern of NP effects identified in the custodially protected RS model and summarised in 1.–14. allows for a clear distinction of this model from other NP frameworks. For instance observing new sources of CP-violation in $S_{\psi\phi}$, $K \to \pi\nu\bar{\nu}$ and $K_L \to \pi^0\ell^+\ell^-$ would provide a definite hint for physics beyond the MFV hypothesis. Similarly the breakdown of universality visible in the correlation between K and B physics observables of the same kind would put (C)MFV models under pressure.

The distinction from other NP models with new sources of flavour and CP-violation is more involved, although still possible as we showed explicitly for the case of the LHT model. Important information is herewith provided by the size of the CP-asymmetry $S_{\psi\phi}$ and the correlations in the rare K sector that, due to the different operator structure of the models in question, turn out to be very different.

Consequently a detailed and precise study of flavour physics observables is complementary to high-energy experiments searching directly for new particles and interactions. Important information will be provided on both sides during the coming years. On the one hand the high-energy experiments Atlas and CMS at the LHC will search directly for new particles and interactions, and on the other hand the flavour precision experiments like LHCb, SuperB and the rare K decay searches will provide further insights on the flavour structure of New Physics. Clearly in order to eventually get a definite answer what kind of New Physics lies beyond the Standard Model information from both sides are necessary.

Appendix

A.1 Warped geometry

A.1.1 Basics of differential geometry and general relativity

In this appendix we collect some basic formulae known from differential geometry that are required for calculations in curved space-times. The necessary ingredients to study fermions in a warped background are summarised in A.1.2.

A space-time is generally described by its metric

$$ds^2 = g_{MN} dx^M dx^N \,, \tag{A.1}$$

where $M, N = 1, \ldots, n$ are summed over the number of space-time dimensions. In the case of the RS metric given in (2.5) $M, N = 0, 1, 2, 3, 5$. Depending on the actual form of g_{MN} the space-time considered may be flat or curved. In case of the curved RS space-time the flat tangent space is the 5D Minkowski space-time with the metric

$$\eta_{AB} = \mathrm{diag}(1, -1, -1, -1, -1) \,. \tag{A.2}$$

In order to be able to define covariant derivatives acting on vector or tensor fields, the Christoffel symbols

$$\Gamma^N_{MK} = \frac{1}{2} g^{NR} (\partial_K g_{MR} + \partial_M g_{KR} - \partial_R g_{MK}) \tag{A.3}$$

have to be introduced. A covariant derivative of e. g. a free vector field V^M is then given by

$$D_N V^M = \partial_N V^M + \Gamma^M_{NK} V^K \,. \tag{A.4}$$

The curvature of a space-time described by the metric g_{MN} can be quantified by the Riemann tensor

$$R^K{}_{LMN} = \partial_M \Gamma^K_{LN} - \partial_N \Gamma^K_{LM} + \Gamma^K_{PM} \Gamma^P_{LN} - \Gamma^K_{PN} \Gamma^P_{LM} \,. \tag{A.5}$$

A flat space-time is characterised by $R^K{}_{LMN} \equiv 0$. The Ricci tensor is then given by the contraction

$$R_{LN} = R^K{}_{LKN}\,, \tag{A.6}$$

and the Ricci or curvature scalar is defined as

$$R = g^{LN} R_{LN}\,. \tag{A.7}$$

A space-time is called flat if $R \equiv 0$.

The Einstein equations of general relativity relate the geometry of space time to its energy content, given by the energy-momentum-tensor T_{MN}. They read

$$R_{MN} - \frac{1}{2} g_{MN} R + \Lambda g_{MN} = \kappa T_{MN}\,, \tag{A.8}$$

with Λ the cosmological constant and κ the strength of gravitational couplings.

A.1.2 Fermions in a warped background

As the Dirac matrices are related to the space-time metric via the Clifford algebra

$$\{\Gamma^M, \Gamma^N\} = 2g^{MN}\,, \tag{A.9}$$

they have to be modified with respect to those known from the flat space-time. It can straightforwardly be checked that the warped Clifford algebra (A.9) is satisfied by the warped space Dirac matrices

$$\Gamma^M = E^M_A \gamma^A\,, \qquad \gamma^A = \{\gamma^\mu, -i\gamma^5\}\,. \tag{A.10}$$

Here, γ^μ and $\gamma^5 = i\gamma^0\gamma^1\gamma^2\gamma^3$ are defined in the usual 4D way. E^M_A is the inverse vielbein defined through

$$g^{MN} = E^M_A E^N_B \eta^{AB}\,, \tag{A.11}$$

i. e. it connects the warped space to the flat tangent space. In the case of the RS metric (2.5), we have

$$E^M_A = \begin{cases} 1 & \text{for } A = M = 5\,, \\ e^{ky} & \text{for } A = M = \mu\,, \\ 0 & \text{else}\,, \end{cases} \tag{A.12}$$

and the vielbein e^A_M is given by

$$e^A_M = \begin{cases} 1 & \text{for } A = M = 5\,, \\ e^{-ky} & \text{for } A = M = \mu\,, \\ 0 & \text{else}\,. \end{cases} \tag{A.13}$$

The spin connection ω_M is needed to define the covariant derivative

$$D_M = \partial_M + \omega_M \tag{A.14}$$

acting on free spinor fields. It is defined through

$$\omega_M = e_N^A(\partial_M E_B^N + \Gamma_{MK}^N E_B^K)\frac{\sigma_A{}^B}{2}\,, \tag{A.15}$$

with $\sigma_{AB} = \frac{1}{4}[\gamma_A, \gamma_B]$ and Γ_{MK}^N the Christoffel symbols introduced in (A.3). In case of the RS metric (2.5) ω_M is simply given by

$$\omega_M = \begin{cases} \frac{i}{2}ke^{-ky}\gamma_\mu\gamma^5 & \text{for } M = \mu\,, \\ 0 & \text{for } M = 5\,. \end{cases} \tag{A.16}$$

A.2 Explicit formulae for quark masses and flavour mixings

In section 3.4.1 we have seen that the effective 4D Yukawa couplings $Y^{u,d}$ can be written in terms of the fundamental 5D Yukawa couplings $\lambda^{u,d}$ and the fermion shape functions f_i^Q, f_i^u, f_i^d $(i = 1, 2, 3)$ as given in (3.73), where the hierarchies in the 4D Yukawas arises through the hierarchies in $f^{Q,u,d}$.

Making use of the similarity to the FN scenario [13], as discussed in section 3.4.2, we can derive explicit expressions for the quark masses and flavour mixing matrices [35, 76]. Keeping only the leading terms in the hierarchies $f_i^{Q,u,d}/f_j^{Q,u,d}$ $(i < j)$, we obtain for the quark masses

$$m_b = \frac{v}{\sqrt{2}}\lambda_{33}^d\frac{e^{kL}}{L}f_3^Q f_3^d\,, \tag{A.17}$$

$$m_s = \frac{v}{\sqrt{2}}\frac{\lambda_{33}^d\lambda_{22}^d - \lambda_{23}^d\lambda_{32}^d}{\lambda_{33}^d}\frac{e^{kL}}{L}f_2^Q f_2^d\,, \tag{A.18}$$

$$m_d = \frac{v}{\sqrt{2}}\frac{\det(\lambda^d)}{\lambda_{33}^d\lambda_{22}^d - \lambda_{23}^d\lambda_{32}^d}\frac{e^{kL}}{L}f_1^Q f_1^d\,, \tag{A.19}$$

and analogous expressions for the up-type quark masses $m_{t,c,u}$, with only replacing "λ^d" by "λ^u" and "f^d" by "f^u".

Similarly, for the flavour mixing matrices $\mathcal{D}_{L,R}$ defined in (3.75) we find

$$(\mathcal{D}_L)_{ij} = \begin{cases} \omega_{ij}^d\frac{f_i^Q}{f_j^Q} & (i < j) \\ 1 & (i = j) \\ \omega_{ij}^d\frac{f_j^Q}{f_i^Q} & (i > j) \end{cases}\,, \qquad (\mathcal{D}_R)_{ij} = \begin{cases} \rho_{ij}^d\frac{f_i^d}{f_j^d} & (i < j) \\ 1 & (i = j) \\ \rho_{ij}^d\frac{f_j^d}{f_i^d} & (i > j) \end{cases}\,. \tag{A.20}$$

Analogous expressions hold for $\mathcal{U}_{L,R}$ in (3.74) with replacing "d" by "u". Here we introduced the notation

$$\omega_{ii}^d = 1\,, \qquad \omega_{12}^d = \frac{\lambda_{33}^d\lambda_{12}^d - \lambda_{13}^d\lambda_{32}^d}{\lambda_{22}^d\lambda_{33}^d - \lambda_{23}^d\lambda_{32}^d}\,, \qquad \omega_{13}^d = \frac{\lambda_{13}^d}{\lambda_{33}^d}\,, \qquad \omega_{23}^d = \frac{\lambda_{23}^d}{\lambda_{33}^d}\,, \tag{A.21}$$

$$\omega_{21}^d = -\left(\omega_{12}^d\right)^*\,, \qquad \omega_{31}^d = -\left(\omega_{13}^d\right)^* - \left(\omega_{23}^d\right)^*\omega_{21}^d\,, \qquad \omega_{32}^d = -\left(\omega_{23}^d\right)^*\,. \tag{A.22}$$

$$\rho_{ii}^d = 1\,, \qquad \rho_{12}^d = \left(\frac{\lambda_{33}^d\lambda_{21}^d - \lambda_{31}^d\lambda_{23}^d}{\lambda_{22}^d\lambda_{33}^d - \lambda_{23}^d\lambda_{32}^d}\right)^*\,, \qquad \rho_{13}^d = \left(\frac{\lambda_{31}^d}{\lambda_{33}^d}\right)^*\,, \qquad \rho_{23}^d = \left(\frac{\lambda_{32}^d}{\lambda_{33}^d}\right)^*\,, \tag{A.23}$$

$$\rho_{21}^d = -\left(\rho_{12}^d\right)^*\,, \qquad \rho_{31}^d = -\left(\rho_{13}^d\right)^* - \left(\rho_{23}^d\right)^*\rho_{21}^d\,, \qquad \rho_{32}^d = -\left(\rho_{23}^d\right)^*\,. \tag{A.24}$$

The expressions for ω_{ij}^u and ρ_{ij}^u, that enter the formulae for $\mathcal{U}_{L,R}$, are obtained by replacing "d" by "u".

Finally, making use of $V_{\rm CKM} = \mathcal{U}_L^\dagger\mathcal{D}_L$, we obtain

$$V_{us} = \alpha_{12}\frac{f_1^Q}{f_2^Q}\,, \qquad V_{ub} = \alpha_{13}\frac{f_1^Q}{f_3^Q}\,, \qquad V_{cb} = \alpha_{23}\frac{f_2^Q}{f_3^Q}\,, \tag{A.25}$$

with

$$\alpha_{ij} = \sum_{k=i}^{j}\left(\omega_{ki}^u\right)^*\omega_{kj}^d\,. \tag{A.26}$$

We would like to stress that the formulae given above are valid at leading order in $f_i^{Q,u,d}/f_j^{Q,u,d}$ $(i<j)$, but are exact in the entries of the 5D Yukawa couplings $\lambda^{u,d}$.

Finally, we comment on the complex phases in the above formulae. It can straightforwardly be seen that in general the quark masses, as given in (A.17)–(A.19), are complex quantities. In order to obtain positive and real values for the quark masses, the unphysical phases in (A.17)–(A.19) have to be removed by suitable phase redefinitions, which will then also affect the phases of the flavour mixing matrices $\mathcal{U}_{L,R}, \mathcal{D}_{L,R}$. Similarly, suitable phase redefinitions have to be performed in order to work with the standard phase convention for the CKM matrix [1].

A.3 Leptonic couplings of Z, Z_H, Z' and $A^{(1)}$

In this appendix we collect the couplings of the gauge bosons Z, Z_H, Z' and $A^{(1)}$ to the leptonic zero modes which are relevant for the study of rare K and B decays evaluated in section 4.4. To this end we neglect lepton flavour violating effects as

	T_L^3	T_R^3	Q_X	$Q_{\rm em}$
ν_L	$1/2$	$-1/2$	0	0
ν_R	0	0	0	0
ℓ_L	$-1/2$	$-1/2$	0	-1
ℓ_R	0	-1	0	-1

Table A.1: *Electroweak quantum numbers of lepton zero modes. $T^3_{L,R}$ are the third component weak isospins of $SU(2)_{L,R}$ and Q_X is the $U(1)_X$ charge. The electric charge is defined as $Q_{em} = T^3_L + T^3_R + Q_X$.*

these are irrelevant for the present analysis. The flavour violating quark couplings of Z, Z_H, Z', $A^{(1)}$ and $G^{(1)A}$ have already been collected in section 4.2. A complete set of Feynman rules including all gauge couplings of the zero and first KK modes has been derived in [40], to which we refer the reader for further details.

The couplings of Z to $\nu\bar{\nu}$ and $\ell^+\ell^-$are given by

$$Z_\mu \nu\bar{\nu} \quad : \quad -i\gamma_\mu \Delta_L^{\nu\nu}(Z) P_L \,, \tag{A.27}$$

$$Z_\mu \ell\bar{\ell} \quad : \quad -i\gamma_\mu \left(\Delta_L^{\ell\ell}(Z) P_L + \Delta_R^{\ell\ell}(Z) P_R\right) \,, \tag{A.28}$$

where $P_{L,R} = (1 \mp \gamma^5)/2$ are the chirality projectors, and we have introduced

$$\Delta_L^{\nu\nu}(Z) = \frac{1}{2} \frac{g}{\sqrt{L}\cos\psi} \,, \tag{A.29}$$

$$\Delta_L^{\ell\ell}(Z) = \frac{g}{\sqrt{L}\cos\psi}\left(-\frac{1}{2} + \sin^2\psi\right) \,, \qquad \Delta_R^{\ell\ell}(Z) = \frac{g}{\sqrt{L}\cos\psi}\sin^2\psi \,. \tag{A.30}$$

Using the matching relation $g^{\rm 4D} = g/\sqrt{L}$ and $\psi \simeq \theta_W$ they can be reduced to the known SM expressions.

The couplings of Z_H, Z' and $A^{(1)}$ can be obtained from (4.16), (4.17) and (4.11) by using the quantum numbers collected in table A.1. Note that the right-handed neutrinos are introduced as gauge singlets, so that all their gauge couplings vanish. Further for $\bar{\Delta}^{ij\pm}_{L,R}$ one has to insert

$$\bar{\Delta}^{\ell\ell+}_{L,R}, \bar{\Delta}^{\nu\nu+}_{L} \longrightarrow \frac{1}{L}\int_0^L dy\, f^{(0)}_{L,R}(y,c_\psi)^2 g(y) \simeq \frac{1}{\sqrt{kL}} \,, \tag{A.31}$$

$$\bar{\Delta}^{\ell\ell-}_{L,R}, \bar{\Delta}^{\nu\nu-}_{L} \longrightarrow \frac{1}{L}\int_0^L dy\, f^{(0)}_{L,R}(y,c_\psi)^2 \tilde{g}(y) \simeq 0 \,, \tag{A.32}$$

where in our numerical analysis we use $c_\psi = \pm 0.7$ for all left-/right-handed leptons collectively. Note that for $c_\psi > 0.5$ ($c_\psi < -0.5$ for right-handed leptons) the overlap integrals in (A.31), (A.32) depend only very weakly on the actual choice of c_ψ.

Bibliography

[1] **Particle Data Group** Collaboration, C. Amsler *et. al.*, *Review of particle physics*, *Phys. Lett.* **B667** (2008) 1. Updates available on `http://pdg.lbl.gov`.

[2] **UTfit** Collaboration, M. Bona *et. al.*, *The UTfit collaboration report on the unitarity triangle beyond the standard model: Spring 2006*, *Phys. Rev. Lett.* **97** (2006) 151803, [`hep-ph/0605213`]. Updates available on `http://www.utfit.org`.

[3] S. P. Martin, *A Supersymmetry Primer*, `hep-ph/9709356`.

[4] M. E. Peskin, *Supersymmetry in Elementary Particle Physics*, `arXiv:0801.1928`.

[5] M. M. Nojiri *et. al.*, *Physics Beyond the Standard Model: Supersymmetry*, `arXiv:0802.3672`.

[6] E. Farhi and L. Susskind, *Technicolor*, *Phys. Rept.* **74** (1981) 277.

[7] N. Arkani-Hamed, S. Dimopoulos, and G. R. Dvali, *The hierarchy problem and new dimensions at a millimeter*, *Phys. Lett.* **B429** (1998) 263–272, [`hep-ph/9803315`].

[8] G. D'Ambrosio, G. F. Giudice, G. Isidori, and A. Strumia, *Minimal flavour violation: An effective field theory approach*, *Nucl. Phys.* **B645** (2002) 155–187, [`hep-ph/0207036`].

[9] R. S. Chivukula and H. Georgi, *Composite Technicolor Standard Model*, *Phys. Lett.* **B188** (1987) 99.

[10] L. J. Hall and L. Randall, *Weak scale effective supersymmetry*, *Phys. Rev. Lett.* **65** (1990) 2939–2942.

[11] A. J. Buras, P. Gambino, M. Gorbahn, S. Jager, and L. Silvestrini, *Universal unitarity triangle and physics beyond the standard model*, *Phys. Lett.* **B500** (2001) 161–167, [`hep-ph/0007085`].

[12] A. J. Buras, *Minimal flavor violation*, *Acta Phys. Polon.* **B34** (2003) 5615–5668, [`hep-ph/0310208`].

[13] C. D. Froggatt and H. B. Nielsen, *Hierarchy of quark masses, Cabibbo angles and CP violation*, *Nucl. Phys.* **B147** (1979) 277.

[14] R. Barbieri, L. J. Hall, S. Raby, and A. Romanino, *Unified theories with U(2) flavor symmetry*, *Nucl. Phys.* **B493** (1997) 3–26, [hep-ph/9610449].

[15] J. L. Chkareuli, C. D. Froggatt, and H. B. Nielsen, *Minimal mixing of quarks and leptons in the SU(3) theory of flavour*, *Nucl. Phys.* **B626** (2002) 307–343, [hep-ph/0109156].

[16] J. Kubo, A. Mondragon, M. Mondragon, and E. Rodriguez-Jauregui, *The flavor symmetry*, *Prog. Theor. Phys.* **109** (2003) 795–807, [hep-ph/0302196].

[17] G. L. Kane, S. F. King, I. N. R. Peddie, and L. Velasco-Sevilla, *Study of theory and phenomenology of some classes of family symmetry and unification models*, *JHEP* **08** (2005) 083, [hep-ph/0504038].

[18] S. F. King and G. G. Ross, *Fermion masses and mixing angles from SU(3) family symmetry*, *Phys. Lett.* **B520** (2001) 243–253, [hep-ph/0108112].

[19] M.-C. Chen and K. T. Mahanthappa, *From CKM matrix to MNS matrix: A model based on supersymmetric $SO(10) \times U(2)_F$ symmetry*, *Phys. Rev.* **D62** (2000) 113007, [hep-ph/0005292].

[20] G. Altarelli, F. Feruglio, and I. Masina, *From minimal to realistic supersymmetric SU(5) grand unification*, *JHEP* **11** (2000) 040, [hep-ph/0007254].

[21] R. Dermisek and S. Raby, *Bi-large neutrino mixing and CP violation in an SO(10) SUSY GUT for fermion masses*, *Phys. Lett.* **B622** (2005) 327–338, [hep-ph/0507045].

[22] G. G. Ross, L. Velasco-Sevilla, and O. Vives, *Spontaneous CP violation and non-Abelian family symmetry in SUSY*, *Nucl. Phys.* **B692** (2004) 50–82, [hep-ph/0401064].

[23] M. Albrecht, W. Altmannshofer, A. J. Buras, D. Guadagnoli, and D. M. Straub, *Challenging $SO(10)$ SUSY GUTs with family symmetries through FCNC processes*, *JHEP* **10** (2007) 055, [arXiv:0707.3954].

[24] W. Altmannshofer, D. Guadagnoli, S. Raby, and D. M. Straub, *SUSY GUTs with Yukawa unification: A Go/no-go study using FCNC processes*, *Phys. Lett.* **B668** (2008) 385–391, [arXiv:0801.4363].

[25] L. Randall and R. Sundrum, *A large mass hierarchy from a small extra dimension*, *Phys. Rev. Lett.* **83** (1999) 3370–3373, [hep-ph/9905221].

[26] H. Davoudiasl, J. L. Hewett, and T. G. Rizzo, *Bulk gauge fields in the Randall-Sundrum model*, *Phys. Lett.* **B473** (2000) 43–49, [hep-ph/9911262].

[27] A. Pomarol, *Gauge bosons in a five-dimensional theory with localized gravity*, *Phys. Lett.* **B486** (2000) 153–157, [hep-ph/9911294].

[28] S. Chang, J. Hisano, H. Nakano, N. Okada, and M. Yamaguchi, *Bulk standard model in the Randall-Sundrum background*, *Phys. Rev.* **D62** (2000) 084025, [hep-ph/9912498].

[29] Y. Grossman and M. Neubert, *Neutrino masses and mixings in non-factorizable geometry*, *Phys. Lett.* **B474** (2000) 361–371, [hep-ph/9912408].

[30] T. Gherghetta and A. Pomarol, *Bulk fields and supersymmetry in a slice of AdS*, *Nucl. Phys.* **B586** (2000) 141–162, [hep-ph/0003129].

[31] K. Agashe, A. Delgado, M. J. May, and R. Sundrum, *RS1, custodial isospin and precision tests*, *JHEP* **08** (2003) 050, [hep-ph/0308036].

[32] C. Csaki, C. Grojean, L. Pilo, and J. Terning, *Towards a realistic model of Higgsless electroweak symmetry breaking*, *Phys. Rev. Lett.* **92** (2004) 101802, [hep-ph/0308038].

[33] K. Agashe, R. Contino, and A. Pomarol, *The minimal composite Higgs model*, *Nucl. Phys.* **B719** (2005) 165–187, [hep-ph/0412089].

[34] K. Agashe, R. Contino, L. Da Rold, and A. Pomarol, *A custodial symmetry for $Zb\bar{b}$*, *Phys. Lett.* **B641** (2006) 62–66, [hep-ph/0605341].

[35] M. Blanke, A. J. Buras, B. Duling, S. Gori, and A. Weiler, $\Delta F = 2$ *Observables and Fine-Tuning in a Warped Extra Dimension with Custodial Protection*, *JHEP* **03** (2009) 001, [arXiv:0809.1073].

[36] M. Blanke, A. J. Buras, B. Duling, K. Gemmler, and S. Gori, *Rare K and B Decays in a Warped Extra Dimension with Custodial Protection*, *JHEP* **03** (2009) 108, [arXiv:0812.3803].

[37] A. J. Buras, B. Duling, and S. Gori, *The Impact of Kaluza-Klein Fermions on Standard Model Fermion Couplings in a RS Model with Custodial Protection*, arXiv:0905.2318.

[38] S. J. Huber, *Flavor violation and warped geometry*, *Nucl. Phys.* **B666** (2003) 269–288, [hep-ph/0303183].

[39] K. Agashe, G. Perez, and A. Soni, *Flavor structure of warped extra dimension models*, *Phys. Rev.* **D71** (2005) 016002, [hep-ph/0408134].

[40] M. E. Albrecht, M. Blanke, A. J. Buras, B. Duling, and K. Gemmler, *Electroweak and Flavour Structure of a Warped Extra Dimension with Custodial Protection*, arXiv:0903.2415.

[41] N. Arkani-Hamed, A. G. Cohen, and H. Georgi, *(De)constructing dimensions*, *Phys. Rev. Lett.* **86** (2001) 4757–4761, [hep-th/0104005].

[42] N. Arkani-Hamed, A. G. Cohen, and H. Georgi, *Electroweak symmetry breaking from dimensional deconstruction*, *Phys. Lett.* **B513** (2001) 232–240, [hep-ph/0105239].

[43] M. Schmaltz and D. Tucker-Smith, *Little Higgs review*, *Ann. Rev. Nucl. Part. Sci.* **55** (2005) 229–270, [hep-ph/0502182].

[44] M. Perelstein, *Little Higgs models and their phenomenology*, *Prog. Part. Nucl. Phys.* **58** (2007) 247–291, [hep-ph/0512128].

[45] N. Arkani-Hamed, A. G. Cohen, E. Katz, and A. E. Nelson, *The Littlest Higgs*, *JHEP* **07** (2002) 034, [hep-ph/0206021].

[46] H.-C. Cheng and I. Low, *TeV symmetry and the little hierarchy problem*, *JHEP* **09** (2003) 051, [hep-ph/0308199].

[47] H.-C. Cheng and I. Low, *Little hierarchy, little Higgses, and a little symmetry*, *JHEP* **08** (2004) 061, [hep-ph/0405243].

[48] I. Low, *T parity and the Littlest Higgs*, *JHEP* **10** (2004) 067, [hep-ph/0409025].

[49] C. S. Chan, P. L. Paul, and H. L. Verlinde, *A note on warped string compactification*, *Nucl. Phys.* **B581** (2000) 156–164, [hep-th/0003236].

[50] B. L. Altshuler, *String theory provides landmarks fixing RS branes' positions: Possibility to deduce large mass hierarchy from small numbers*, hep-th/0511271.

[51] B. S. Acharya, F. Benini, and R. Valandro, *Warped models in string theory*, hep-th/0612192.

[52] L. Randall and R. Sundrum, *An alternative to compactification*, *Phys. Rev. Lett.* **83** (1999) 4690–4693, [hep-th/9906064].

[53] A. J. Buras and D. Guadagnoli, *Correlations among new CP violating effects in $\Delta F = 2$ observables*, *Phys. Rev.* **D78** (2008) 033005, [arXiv:0805.3887].

[54] A. J. Buras and D. Guadagnoli, *On the consistency between the observed amount of CP violation in the K- and B_d-systems within minimal flavor violation*, arXiv:0901.2056.

[55] E. Lunghi and A. Soni, *Possible Indications of New Physics in B_d-mixing and in $\sin(2\beta)$ Determinations*, *Phys. Lett.* **B666** (2008) 162–165, [arXiv:0803.4340].

[56] **UTfit** Collaboration, M. Bona *et. al.*, *Model-independent constraints on $\Delta F = 2$ operators and the scale of new physics*, *JHEP* **03** (2008) 049, [arXiv:0707.0636].

[57] N. Arkani-Hamed and M. Schmaltz, *Hierarchies without symmetries from extra dimensions*, *Phys. Rev.* **D61** (2000) 033005, [hep-ph/9903417].

[58] C. Csaki, C. Grojean, H. Murayama, L. Pilo, and J. Terning, *Gauge theories on an interval: Unitarity without a Higgs*, *Phys. Rev.* **D69** (2004) 055006, [hep-ph/0305237].

[59] C. Csaki, C. Grojean, J. Hubisz, Y. Shirman, and J. Terning, *Fermions on an interval: Quark and lepton masses without a Higgs*, *Phys. Rev.* **D70** (2004) 015012, [hep-ph/0310355].

[60] C. Csaki, J. Hubisz, and P. Meade, *Electroweak symmetry breaking from extra dimensions*, hep-ph/0510275.

[61] M. E. Peskin and T. Takeuchi, *Estimation of oblique electroweak corrections*, *Phys. Rev.* **D46** (1992) 381–409.

[62] I. Maksymyk, C. P. Burgess, and D. London, *Beyond S, T and U*, *Phys. Rev.* **D50** (1994) 529–535, [hep-ph/9306267].

[63] G. Altarelli, R. Barbieri, and F. Caravaglios, *Nonstandard analysis of electroweak precision data*, *Nucl. Phys.* **B405** (1993) 3–23.

[64] C. P. Burgess, S. Godfrey, H. Konig, D. London, and I. Maksymyk, *A Global fit to extended oblique parameters*, *Phys. Lett.* **B326** (1994) 276–281, [hep-ph/9307337].

[65] C. P. Burgess, S. Godfrey, H. Konig, D. London, and I. Maksymyk, *Model independent global constraints on new physics*, *Phys. Rev.* **D49** (1994) 6115–6147, [hep-ph/9312291].

[66] Z. Han and W. Skiba, *Effective theory analysis of precision electroweak data*, *Phys. Rev.* **D71** (2005) 075009, [hep-ph/0412166].

[67] R. Barbieri, A. Pomarol, R. Rattazzi, and A. Strumia, *Electroweak symmetry breaking after LEP1 and LEP2*, *Nucl. Phys.* **B703** (2004) 127–146, [hep-ph/0405040].

[68] Z. Han, *Electroweak constraints on effective theories with $U(2) \times U(1)$ flavor symmetry*, *Phys. Rev.* **D73** (2006) 015005, [hep-ph/0510125].

[69] G. Cacciapaglia, C. Csaki, G. Marandella, and A. Strumia, *The minimal set of electroweak precision parameters*, *Phys. Rev.* **D74** (2006) 033011, [hep-ph/0604111].

[70] H. Flacher *et. al.*, *Gfitter - Revisiting the Global Electroweak Fit of the Standard Model and Beyond*, *Eur. Phys. J.* **C60** (2009) 543–583, [arXiv:0811.0009]. Updates available on http://gfitter.desy.de/.

[71] S. J. Huber, C.-A. Lee, and Q. Shafi, *Kaluza-Klein excitations of W and Z at the LHC?*, *Phys. Lett.* **B531** (2002) 112–118, [hep-ph/0111465].

[72] J. L. Hewett, F. J. Petriello, and T. G. Rizzo, *Precision measurements and fermion geography in the Randall-Sundrum model revisited*, *JHEP* **09** (2002) 030, [hep-ph/0203091].

[73] C. Csaki, J. Erlich, and J. Terning, *The effective Lagrangian in the Randall-Sundrum model and electroweak physics*, *Phys. Rev.* **D66** (2002) 064021, [hep-ph/0203034].

[74] G. Burdman, *Constraints on the bulk standard model in the Randall-Sundrum scenario*, *Phys. Rev.* **D66** (2002) 076003, [hep-ph/0205329].

[75] M. S. Carena, A. Delgado, E. Ponton, T. M. P. Tait, and C. E. M. Wagner, *Precision electroweak data and unification of couplings in warped extra dimensions*, *Phys. Rev.* **D68** (2003) 035010, [hep-ph/0305188].

[76] S. Casagrande, F. Goertz, U. Haisch, M. Neubert, and T. Pfoh, *Flavor Physics in the Randall-Sundrum Model: I. Theoretical Setup and Electroweak Precision Tests*, *JHEP* **10** (2008) 094, [arXiv:0807.4937].

[77] K. Agashe, C. Csaki, C. Grojean, and M. Reece, *The S-parameter in holographic technicolor models*, *JHEP* **12** (2007) 003, [arXiv:0704.1821].

[78] J. M. Maldacena, *The large N limit of superconformal field theories and supergravity*, *Adv. Theor. Math. Phys.* **2** (1998) 231–252, [hep-th/9711200].

[79] M. S. Carena, A. Delgado, E. Ponton, T. M. P. Tait, and C. E. M. Wagner, *Warped fermions and precision tests*, *Phys. Rev.* **D71** (2005) 015010, [hep-ph/0410344].

[80] C. Bouchart and G. Moreau, *The precision electroweak data in warped extra-dimension models*, *Nucl. Phys.* **B810** (2009) 66–96, [arXiv:0807.4461].

[81] A. Djouadi, G. Moreau, and F. Richard, *Resolving the A_{FB}^b puzzle in an extra dimensional model with an extended gauge structure*, *Nucl. Phys.* **B773** (2007) 43–64, [hep-ph/0610173].

[82] R. Contino, L. Da Rold, and A. Pomarol, *Light custodians in natural composite Higgs models*, *Phys. Rev.* **D75** (2007) 055014, [hep-ph/0612048].

[83] G. Cacciapaglia, C. Csaki, G. Marandella, and J. Terning, *A new custodian for a realistic Higgsless model*, *Phys. Rev.* **D75** (2007) 015003, [hep-ph/0607146].

[84] M. S. Carena, E. Ponton, J. Santiago, and C. E. M. Wagner, *Light Kaluza-Klein states in Randall-Sundrum models with custodial $SU(2)$*, *Nucl. Phys.* **B759** (2006) 202–227, [hep-ph/0607106].

[85] C. Csaki, A. Falkowski, and A. Weiler, *The Flavor of the Composite Pseudo-Goldstone Higgs*, *JHEP* **09** (2008) 008, [arXiv:0804.1954].

[86] M. S. Carena, E. Ponton, J. Santiago, and C. E. M. Wagner, *Electroweak constraints on warped models with custodial symmetry*, *Phys. Rev.* **D76** (2007) 035006, [hep-ph/0701055].

[87] K. Gemmler, *A Realistic Model of Electroweak Symmetry Breaking in Warped Extra Dimensions*. Diploma thesis, Universität Ulm and Technische Universität München, April 2008.

[88] K. Agashe *et. al.*, *LHC Signals for Warped Electroweak Neutral Gauge Bosons*, *Phys. Rev.* **D76** (2007) 115015, [arXiv:0709.0007].

[89] K. Agashe, S. Gopalakrishna, T. Han, G.-Y. Huang, and A. Soni, *LHC Signals for Warped Electroweak Charged Gauge Bosons*, arXiv:0810.1497.

[90] J. Hirn and V. Sanz, *(Not) summing over Kaluza-Kleins*, *Phys. Rev.* **D76** (2007) 044022, [hep-ph/0702005].

[91] A. Muck, A. Pilaftsis, and R. Ruckl, *Minimal higher-dimensional extensions of the standard model and electroweak observables*, *Phys. Rev.* **D65** (2002) 085037, [hep-ph/0110391].

[92] S. J. Huber and Q. Shafi, *Higgs mechanism and bulk gauge boson masses in the Randall-Sundrum model*, *Phys. Rev.* **D63** (2001) 045010, [hep-ph/0005286].

[93] F. Goertz and T. Pfoh, *On the Perturbative Approach in the Randall-Sundrum Model*, *JHEP* **10** (2008) 035, [arXiv:0809.1378].

[94] G. Burdman, *Flavor violation in warped extra dimensions and CP asymmetries in B decays*, *Phys. Lett.* **B590** (2004) 86–94, [hep-ph/0310144].

[95] K. Agashe, G. Perez, and A. Soni, *B-factory signals for a warped extra dimension*, *Phys. Rev. Lett.* **93** (2004) 201804, [hep-ph/0406101].

[96] G. Moreau and J. I. Silva-Marcos, *Flavour physics of the RS model with KK masses reachable at LHC*, *JHEP* **03** (2006) 090, [hep-ph/0602155].

[97] S. Chang, C. S. Kim, and J. Song, *Constraint of $B^0_{d,s} - \bar{B}^0_{d,s}$ mixing on warped extra-dimension model*, *JHEP* **02** (2007) 087, [hep-ph/0607313].

[98] K. Agashe, A. Azatov, and L. Zhu, *Flavor Violation Tests of Warped/Composite SM in the Two-Site Approach*, *Phys. Rev.* **D79** (2009) 056006, [arXiv:0810.1016].

[99] U. Haisch, *Quark flavor in RS: Overtime*. Talk given at the Brookhaven Forum 2008, "Terra Incognita: From LHC to Cosmology", Nov 6–8, 2008, http://www.bnl.gov/BF08/.

[100] H. Davoudiasl, G. Perez, and A. Soni, *The Little Randall-Sundrum Model at the Large Hadron Collider*, *Phys. Lett.* **B665** (2008) 67–71, [arXiv:0802.0203].

[101] M. Bauer, S. Casagrande, L. Gruender, U. Haisch, and M. Neubert, *Little Randall-Sundrum models: ε_K strikes again*, arXiv:0811.3678.

[102] M. Byrd, *The Geometry of SU(3)*, physics/9708015.

[103] A. J. Buras, *Weak Hamiltonian, CP violation and rare decays*, hep-ph/9806471.

[104] S. Herrlich and U. Nierste, *Enhancement of the $K_L - K_S$ mass difference by short distance QCD corrections beyond leading logarithms*, *Nucl. Phys.* **B419** (1994) 292–322, [hep-ph/9310311].

[105] S. Herrlich and U. Nierste, *Indirect CP violation in the neutral kaon system beyond leading logarithms*, *Phys. Rev.* **D52** (1995) 6505–6518, [hep-ph/9507262].

[106] S. Herrlich and U. Nierste, *The Complete $|\Delta S| = 2$ Hamiltonian in the Next-To-Leading Order*, *Nucl. Phys.* **B476** (1996) 27–88, [hep-ph/9604330].

[107] A. J. Buras, M. Jamin, and P. H. Weisz, *Leading and next-to-leading QCD corrections to ϵ parameter and $B^0 - \bar{B}^0$ mixing in the presence of a heavy top quark*, *Nucl. Phys.* **B347** (1990) 491–536.

[108] J. Urban, F. Krauss, U. Jentschura, and G. Soff, *Next-to-leading order QCD corrections for the $B^0 - \bar{B}^0$ mixing with an extended Higgs sector*, *Nucl. Phys.* **B523** (1998) 40–58, [hep-ph/9710245].

[109] M. Blanke *et. al.*, *Particle antiparticle mixing, ε_K, $\Delta\Gamma_q$, A^q_{SL}, $A_{CP}(B_d \to \psi K_S)$, $A_{CP}(B_s \to \psi\phi)$ and $B \to X_{s,d}\gamma$ in the Littlest Higgs model with T- parity*, *JHEP* **12** (2006) 003, [hep-ph/0605214].

[110] J. Hubisz, S. J. Lee, and G. Paz, *The flavor of a little Higgs with T-parity*, *JHEP* **06** (2006) 041, [hep-ph/0512169].

[111] M. Blanke, A. J. Buras, S. Recksiegel, and C. Tarantino, *The Littlest Higgs Model with T-Parity Facing CP-Violation in $B_s - \bar{B}_s$ Mixing*, arXiv:0805.4393.

[112] A. J. Buras, S. Jager, and J. Urban, *Master formulae for $\Delta F = 2$ NLO-QCD factors in the standard model and beyond*, *Nucl. Phys.* **B605** (2001) 600–624, [hep-ph/0102316].

[113] R. Babich *et. al.*, *$K^0 - \bar{K}^0$ mixing beyond the standard model and CP-violating electroweak penguins in quenched QCD with exact chiral symmetry*, *Phys. Rev.* **D74** (2006) 073009, [hep-lat/0605016].

[114] D. Becirevic, V. Gimenez, G. Martinelli, M. Papinutto, and J. Reyes, *B-parameters of the complete set of matrix elements of $\Delta B = 2$ operators from the lattice*, *JHEP* **04** (2002) 025, [hep-lat/0110091].

[115] **UTfit** Collaboration, M. Bona *et. al.*, *The UTfit collaboration report on the status of the unitarity triangle beyond the standard model. I: Model-independent analysis and minimal flavour violation*, *JHEP* **03** (2006) 080, [hep-ph/0509219].

[116] M. Ciuchini, E. Franco, V. Lubicz, F. Mescia, and C. Tarantino, *Lifetime differences and CP violation parameters of neutral B mesons at the next-to-leading order in QCD*, *JHEP* **08** (2003) 031, [hep-ph/0308029].

[117] M. Beneke, G. Buchalla, C. Greub, A. Lenz, and U. Nierste, *Next-to-leading order QCD corrections to the lifetime difference of B_s mesons*, *Phys. Lett.* **B459** (1999) 631–640, [hep-ph/9808385].

[118] Y. Grossman, Y. Nir, and G. Perez, *Testing New Indirect CP Violation*, arXiv:0904.0305.

[119] I. I. Bigi, M. Blanke, A. J. Buras, and S. Recksiegel, *CP Violation in $D^0 - \bar{D}^0$ Oscillations: General Considerations and Applications to the Littlest Higgs Model with T-Parity*, arXiv:0904.1545.

[120] Z. Ligeti, M. Papucci, and G. Perez, *Implications of the measurement of the $B_s^0 - \bar{B}_s^0$ mass difference*, *Phys. Rev. Lett* **97** (2006) 101801, [hep-ph/0604112].

[121] M. Blanke, A. J. Buras, D. Guadagnoli, and C. Tarantino, *Minimal Flavour Violation Waiting for Precise Measurements of ΔM_s, $S_{\psi\phi}$, A_{SL}^s, $|V_{ub}|$, γ and $B_{s,d}^0 \to \mu^+\mu^-$*, *JHEP* **10** (2006) 003, [hep-ph/0604057].

[122] M. Blanke, A. J. Buras, B. Duling, S. Recksiegel, and C. Tarantino, *FCNC Processes in the Littlest Higgs Model with T-Parity: a 2009 Look*, arXiv:0906.5454.

[123] M. Blanke *et. al.*, *Rare and CP-violating K and B decays in the Littlest Higgs model with T-parity*, *JHEP* **01** (2007) 066, [hep-ph/0610298].

[124] A. J. Buras, F. Schwab, and S. Uhlig, *Waiting for precise measurements of $K^+ \to \pi^+\nu\bar{\nu}$ and $K_L \to \pi^0\nu\bar{\nu}$*, *Rev. Mod. Phys.* **80** (2008) 965–1007, [hep-ph/0405132].

[125] M. Artuso *et. al.*, *B, D and K decays*, *Eur. Phys. J.* **C57** (2008) 309–492, [arXiv:0801.1833].

[126] A. J. Buras, M. Gorbahn, U. Haisch, and U. Nierste, *The rare decay $K^+ \to \pi^+\nu\bar{\nu}$ at the next-to-next-to-leading order in QCD*, *Phys. Rev. Lett.* **95** (2005) 261805, [hep-ph/0508165].

[127] A. J. Buras, M. Gorbahn, U. Haisch, and U. Nierste, *Charm quark contribution to $K^+ \to \pi^+\nu\bar{\nu}$ at next-to-next-to-leading order*, *JHEP* **11** (2006) 002, [hep-ph/0603079].

[128] J. Brod and M. Gorbahn, *Electroweak Corrections to the Charm Quark Contribution to $K^+ \to \pi^+\nu\bar{\nu}$*, *Phys. Rev.* **D78** (2008) 034006, [arXiv:0805.4119].

[129] **E391a** Collaboration, J. K. Ahn *et. al.*, *Search for the Decay $K_L^0 \to \pi^0\nu\bar{\nu}$*, *Phys. Rev. Lett.* **100** (2008) 201802, [arXiv:0712.4164].

[130] **E949** Collaboration, A. V. Artamonov *et. al.*, *New measurement of the $K^+ \to \pi^+\nu\bar{\nu}$ branching ratio*, *Phys. Rev. Lett.* **101** (2008) 191802, [arXiv:0808.2459].

[131] M. Blanke, *Insights from the Interplay of $K \to \pi\nu\bar{\nu}$ and ε_K on the New Physics Flavour Structure*, arXiv:0904.2528.

[132] C. Promberger, S. Schatt, and F. Schwab, *Flavor changing neutral current effects and CP violation in the minimal 3-3-1 model*, *Phys. Rev.* **D75** (2007) 115007, [hep-ph/0702169].

[133] G. Buchalla and A. J. Buras, *The rare decays $K \to \pi\nu\bar{\nu}$, $B \to X\nu\bar{\nu}$ and $B \to \ell^+\ell^-$: An update*, *Nucl. Phys.* **B548** (1999) 309–327, [hep-ph/9901288].

[134] F. Mescia and C. Smith, *Improved estimates of rare K decay matrix-elements from $K_{\ell 3}$ decays*, *Phys. Rev.* **D76** (2007) 034017, [arXiv:0705.2025].

[135] G. Isidori, F. Mescia, and C. Smith, *Light-quark loops in $K \to \pi\nu\bar{\nu}$*, *Nucl. Phys.* **B718** (2005) 319–338, [hep-ph/0503107].

[136] W. Altmannshofer, A. J. Buras, D. M. Straub, and M. Wick, *New strategies for New Physics search in $B \to K^*\nu\bar{\nu}$, $B \to K\nu\bar{\nu}$ and $B \to X_s\nu\bar{\nu}$ decays*, *JHEP* **04** (2009) 022, [arXiv:0902.0160].

[137] G. D'Ambrosio, G. Ecker, G. Isidori, and J. Portoles, *The decays $K \to \pi\ell^+\ell^-$ beyond leading order in the chiral expansion*, *JHEP* **08** (1998) 004, [hep-ph/9808289].

[138] G. Buchalla, G. D'Ambrosio, and G. Isidori, *Extracting short-distance physics from $K_{L,S} \to \pi^0 e^+ e^-$ decays*, *Nucl. Phys.* **B672** (2003) 387–408, [hep-ph/0308008].

[139] G. Isidori, C. Smith, and R. Unterdorfer, *The rare decay $K_L \to \pi^0\mu^+\mu^-$ within the SM*, *Eur. Phys. J.* **C36** (2004) 57–66, [hep-ph/0404127].

[140] A. J. Buras, R. Fleischer, S. Recksiegel, and F. Schwab, *Anatomy of prominent B and K decays and signatures of CP-violating new physics in the electroweak penguin sector*, *Nucl. Phys.* **B697** (2004) 133–206, [hep-ph/0402112].

[141] S. Friot, D. Greynat, and E. De Rafael, *Rare kaon decays revisited*, *Phys. Lett.* **B595** (2004) 301–308, [hep-ph/0404136].

[142] F. Mescia, C. Smith, and S. Trine, *$K_L \to \pi^0 e^+ e^-$ and $K_L \to \pi^0\mu^+\mu^-$: A binary star on the stage of flavor physics*, *JHEP* **08** (2006) 088, [hep-ph/0606081].

[143] A. J. Buras, M. E. Lautenbacher, M. Misiak, and M. Munz, *Direct CP violation in $K_L \to \pi^0 e^+ e^-$ beyond leading logarithms*, *Nucl. Phys.* **B423** (1994) 349–383, [hep-ph/9402347].

[144] **KTeV** Collaboration, A. Alavi-Harati *et. al.*, *Search for the Rare Decay $K_L \to \pi^0 e^+ e^-$*, *Phys. Rev. Lett.* **93** (2004) 021805, [hep-ex/0309072].

[145] **KTEV** Collaboration, A. Alavi-Harati *et. al.*, *Search for the Decay $K_L \to \pi^0\mu^+\mu^-$*, *Phys. Rev. Lett.* **84** (2000) 5279–5282, [hep-ex/0001006].

[146] J. Prades, *ChPT Progress on Non-Leptonic and Radiative Kaon Decays*, *PoS* **KAON** (2008) 022, [arXiv:0707.1789].

[147] C. Bruno and J. Prades, *Rare Kaon Decays in the $1/N_c$-Expansion*, *Z. Phys.* **C57** (1993) 585–594, [hep-ph/9209231].

[148] G. Isidori and R. Unterdorfer, *On the short-distance constraints from $K_{L,S} \to \mu^+\mu^-$ *, *JHEP* **01** (2004) 009, [hep-ph/0311084].

[149] M. Gorbahn and U. Haisch, *Charm quark contribution to $K_L \to \mu^+\mu^-$ at next-to-next-to-leading order*, *Phys. Rev. Lett.* **97** (2006) 122002, [hep-ph/0605203].

[150] **Heavy Flavor Averaging Group** Collaboration, E. Barberio *et. al.*, *Averages of b−hadron and c−hadron Properties at the End of 2007*, arXiv:0808.1297. Updates available on http://www.slac.stanford.edu/xorg/hfag.

[151] **FlaviaNet Working Group on Kaon Decays** Collaboration, M. Antonelli *et. al.*, *Precision tests of the Standard Model with leptonic and semileptonic kaon decays*, arXiv:0801.1817. Updates available on http://www.lnf.infn.it/wg/vus/.

[152] V. Lubicz and C. Tarantino, *Flavour physics and Lattice QCD: averages of lattice inputs for the Unitarity Triangle Analysis*, *Nuovo Cim.* **123B** (2008) 674–688, [arXiv:0807.4605].

[153] R. Barbieri and G. F. Giudice, *Upper Bounds on Supersymmetric Particle Masses*, *Nucl. Phys.* **B306** (1988) 63.

[154] **CDF** Collaboration, T. Aaltonen *et. al.*, *First Flavor-Tagged Determination of Bounds on Mixing-Induced CP Violation in $B_s \to J/\psi\phi$ Decays*, *Phys. Rev. Lett.* **100** (2008) 161802, [arXiv:0712.2397].

[155] **D0** Collaboration, V. M. Abazov *et. al.*, *Measurement of B_s^0 mixing parameters from the flavor-tagged decay $B_s^0 \to J/\psi\phi$*, *Phys. Rev. Lett.* **101** (2008) 241801, [arXiv:0802.2255].

[156] **CDF** Collaboration, G. Brooijmans, *Mixing and CP Violation at the Tevatron*, arXiv:0808.0726.

[157] A. Lenz and U. Nierste, *Theoretical update of $B_s - \bar{B}_s$ mixing*, *JHEP* **06** (2007) 072, [hep-ph/0612167].

[158] **UTfit** Collaboration, M. Bona *et. al.*, *First Evidence of New Physics in $b \leftrightarrow s$ Transitions*, arXiv:0803.0659.

[159] M. Blanke, A. J. Buras, S. Recksiegel, C. Tarantino, and S. Uhlig, *Correlations between ε'/ε and Rare K Decays in the Littlest Higgs Model with T-Parity*, *JHEP* **06** (2007) 082, [0704.3329].

[160] M. Blanke and A. J. Buras, *A guide to flavour changing neutral currents in the Littlest Higgs Model with T-Parity*, *Acta Phys. Polon.* **B38** (2007) 2923, [hep-ph/0703117].

[161] T. Goto, Y. Okada, and Y. Yamamoto, *Ultraviolet divergences of flavor changing amplitudes in the Littlest Higgs model with T-parity*, *Phys. Lett.* **B670** (2009) 378–382, [arXiv:0809.4753].

[162] Y. Grossman and Y. Nir, *$K_L \to \pi^0 \nu\bar{\nu}$ beyond the standard model*, *Phys. Lett.* **B398** (1997) 163–168, [hep-ph/9701313].

[163] T. Hurth, G. Isidori, J. F. Kamenik, and F. Mescia, *Constraints on New Physics in MFV models: A Model-independent analysis of $\Delta F = 1$ processes*, *Nucl. Phys.* **B808** (2009) 326–346, [arXiv:0807.5039].

[164] G. Buchalla and A. J. Buras, *$\sin 2\beta$ from $K \to \pi\nu\bar{\nu}$*, *Phys. Lett.* **B333** (1994) 221–227, [hep-ph/9405259].

[165] A. J. Buras and R. Fleischer, *Bounds on the unitarity triangle, $\sin 2\beta$ and $K \to \pi\nu\bar{\nu}$ decays in models with minimal flavor violation*, *Phys. Rev.* **D64** (2001) 115010, [hep-ph/0104238].

[166] A. J. Buras, *Relations between $\Delta M_{s,d}$ and $B_{s,d} \to \mu^+\mu^-$ in models with minimal flavour violation*, *Phys. Lett.* **B566** (2003) 115–119, [hep-ph/0303060].

[167] C. Bobeth *et. al.*, *Upper bounds on rare K and B decays from minimal flavor violation*, *Nucl. Phys.* **B726** (2005) 252–274, [hep-ph/0505110].

[168] U. Haisch and A. Weiler, *Determining the Sign of the Z Penguin Amplitude*, *Phys. Rev.* **D76** (2007) 074027, [arXiv:0706.2054].

[169] M. Blanke and A. J. Buras, *Lower Bounds on $\Delta M_{s,d}$ from Constrained Minimal Flavour Violation*, *JHEP* **05** (2007) 061, [hep-ph/0610037].

[170] F. del Aguila, J. I. Illana, and M. D. Jenkins, *Precise limits from lepton flavour violating processes on the Littlest Higgs model with T-parity*, *JHEP* **01** (2009) 080, [arXiv:0811.2891].

[171] A. J. Buras, A. Poschenrieder, and S. Uhlig, *Particle antiparticle mixing, ε_K and the unitarity triangle in the Littlest Higgs model*, *Nucl. Phys.* **B716** (2005) 173–198, [hep-ph/0410309].

[172] A. J. Buras, A. Poschenrieder, S. Uhlig, and W. A. Bardeen, *Rare K and B decays in the Littlest Higgs model without T-parity*, *JHEP* **11** (2006) 062, [hep-ph/0607189].

[173] M. Blanke *et. al.*, *Another look at the flavour structure of the Littlest Higgs model with T-parity*, *Phys. Lett.* **B646** (2007) 253–257, [hep-ph/0609284].

[174] M. Blanke, A. J. Buras, B. Duling, A. Poschenrieder, and C. Tarantino, *Charged Lepton Flavour Violation and $(g-2)_\mu$ in the Littlest Higgs Model with T-Parity: a clear Distinction from Supersymmetry*, *JHEP* **05** (2007) 013, [hep-ph/0702136].

[175] M. Blanke, A. J. Buras, S. Recksiegel, C. Tarantino, and S. Uhlig, *Littlest Higgs Model with T-Parity Confronting the New Data on $D^0 - \bar{D}^0$ Mixing*, *Phys. Lett.* **B657** (2007) 81–86, [hep-ph/0703254].